School of Doctoral Studies in Biological Sciences
University of South Bohemia in České Budějovice
Faculty of Science

Study of Cancer Immunotherapy Mechanisms in Pancreatic Adenocarcinoma and Pheochromocytoma Murine Models

Ph.D. Thesis

Mgr. Ondřej Uher

Supervisor: RNDr. Jindřich Chmelař, PhD
Co-supervisor: RNDr. Jan Ženka, CSc.
Co-supervisor: Karel Pacak, MD, PhD, DSc, FACE

Department of Medical Biology, Faculty of Science, University of South Bohemia in České Budějovice, Czech Republic
&
Section of Medical Neuroendocrinology, *Eunice Kennedy Shriver* National Institute of Child Health and Human Development, National Institutes of Health, Bethesda, Maryland, USA

České Budějovice 2022

This thesis should be cited as:

Uher, O., 2022: Study of cancer immunotherapy mechanisms in pancreatic adenocarcinoma and pheochromocytoma murine models. PhD. Thesis Series, No. 4. University of South Bohemia, Faculty of Science, School of Doctoral Studies in Biological Sciences, České Budějovice, Czech Republic, 109p.

Annotation

This dissertation examines the study of intratumoral cancer immunotherapy using a combination of phagocytosis-stimulating ligands and Toll-like receptor ligands (TLR) in murine pancreatic adenocarcinoma and pheochromocytoma murine models. In this study, we show that intratumoral application of the phagocytosis-stimulating ligand Mannan-BAM and three TLR ligands, referred to as MBT therapy, efficiently suppresses tumor growth in more than 83% of mice bearing murine melanoma. However, in aggressive pancreatic adenocarcinoma and pheochromocytoma murine models, such a combination is inefficient and must be combined with an agonistic anti-CD40 antibody, referred to as MBTA therapy, to achieve complete eradication of the tumor. We show that complex intratumoral MBTA therapy can systemically increase the recruitment of innate immune cells followed by activation of adaptive immune cells not only in treated tumors but also in distal non-treated lesions, resulting in the reduction of tumor growth and prolonged survival of treated mice. Taken together, these findings highlight the effect of MBTA therapy and the potential to optimize this therapeutic approach for future use in clinical trials as a treatment for metastatic cancers.

Declaration

I hereby declare that I am the author of this dissertation and that I have used only those sources and literature detailed in the list of references

České Budějovice, 28.3.2022

Mgr. Ondřej Uher

This thesis originates from a partnership of Faculty of Science, University of South Bohemia and *Eunice Kennedy Shriver* National Institute of Child Health and Human Development, National Institutes of Health.

List of papers and author's contribution

The thesis is based on the following papers (listed chronologically):

I. Caisová, V., **Uher, O.**, Nedbalová, P., Jochmanová, I., Kvardová, K., Masáková, K., Krejčová, G., Paďouková, L., Chmelař, J., Kopecký, J., & Ženka, J. (2018). Effective cancer immunotherapy based on combination of TLR agonists with stimulation of phagocytosis. *International immunopharmacology, 59*, 86–96. DOI: 10.1016/j.intimp.2018.03.038
IF (2018): 3.361
OU performed the experiments and analyzed the data. His contribution was 35%.

II. Caisova, V., Li, L., Gupta, G., Jochmanova, I., Jha, A., **Uher, O.**, Huynh, T. T., Miettinen, M., Pang, Y., Abunimer, L., Niu, G., Chen, X., Ghayee, H. K., Taïeb, D., Zhuang, Z., Zenka, J., & Pacak, K. (2019). The Significant Reduction or Complete Eradication of Subcutaneous and Metastatic Lesions in a Pheochromocytoma Mouse Model after Immunotherapy Using Mannan-BAM, TLR Ligands, and Anti-CD40. *Cancers, 11*(5), 654. DOI: 10.3390/cancers11050654
IF (2019): 6.126
OU helped with the writing of the manuscript – review and editing. His contribution was 10%.

III. **Uher, O.**, Caisova, V., Hansen, P., Kopecky, J., Chmelar, J., Zhuang, Z., Zenka, J., & Pacak, K. (2019). Coley's immunotherapy revived: Innate immunity as a link in priming cancer cells for an attack by adaptive immunity. *Seminars in oncology, 46*(4-5), 385–392. DOI: 10.1053/j.seminoncol.2019.10.004 – review.
IF (2019): 4.213
OU conceptualized, wrote, reviewed, and edited the manuscript. OU designed and visualized the figures. His contribution was 40%.

IV. **Uher, O.**, Caisova, V., Padoukova, L., Kvardova, K., Masakova, K., Lencova, R., Frejlachova, A., Skalickova, M., Venhauerova, A., Chlastakova, A., Hansen, P., Chmelar, J., Kopecky, J., Zhuang, Z., Pacak,

K., & Zenka, J. (2021). Mannan-BAM, TLR ligands, and anti-CD40 immunotherapy in established murine pancreatic adenocarcinoma: understanding therapeutic potentials and limitations. *Cancer immunology, immunotherapy: CII, 70*(11), 3303–3312. DOI: 10.1007/s00262-021-02920-9

IF (2020): 6.968

OU performed the experiments and analyzed the data. OU designed and visualized the figures. OU wrote the manuscript. His contribution was 40%.

V.   **Uher, O.**, Huynh, T. T., Zhu, B., Horn, L. A., Caisova, V., Hadrava Vanova, K., Medina, R., Wang, H., Palena, C., Chmelar, J., Zhuang, Z., Zenka, J., & Pacak, K. (2021). Identification of Immune Cell Infiltration in Murine Pheochromocytoma during Combined Mannan-BAM, TLR Ligand, and Anti-CD40 Antibody-Based Immunotherapy. *Cancers, 13* (16), 3942. DOI: 10.3390/cancers13163942

IF (2020): 6.639

OU conceptualized the study, performed the experiments, and analyzed the data. OU designed and visualized the figures. OU wrote, reviewed, and edited the manuscript. His contribution was 70%.

VI.   **Uher, O.**, Hadrava Vanova, K., Wang, H., Zhuang, Z., Zenka, J., & Pacak, K. Intratumoral Immunotherapy of Murine Pheochromocytoma Shows No Age-Dependent Differences in Its Efficacy. [Manuscript]
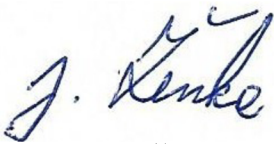
OU conceptualized the study, performed the experiments, and analyzed the data. OU designed and visualized the figures. OU wrote, reviewed, and edited the manuscript. His contribution was 60%.

Co-author agreement

Jan Ženka, the co-supervisor of this thesis and corresponding author of Chapter I and IV, fully acknowledges the contribution of Ondřej Uher as stated above.

RNDr. Jan Ženka, CSc.

Karel Pacak, the co-supervisor of this thesis and corresponding author of Chapter II, III, V, and VI, fully acknowledges the contribution of Ondřej Uher as stated above.

Karel Pacak, MD, PhD, DSc, FACE

Table of content

Introduction

Worldwide, immunotherapy has been considered the fourth cancer treatment modality, following standard therapeutic options such as surgery, chemotherapy, and radiotherapy. Undoubtedly, immunotherapy is currently in the spotlight of cancer research and clinical trials. Immunotherapy has revolutionized cancer treatment because of its ability to produce durable responses in patients with advanced cancers [1].

The oldest immunotherapeutic concept is found in the late nineteenth century and is based on the use of pyogenic bacteria by William Bradley Coley, who is also recognized as the "Father of Cancer Immunotherapy." Coley stimulated the immune system using an intratumoral injection of inactivated *Streptococcus pyogenes* and *Serratia marcescens* bacteria, also known as "Coley's Toxins", which resulted in tumor regression in his patients [2]. Coley's published papers on this phenomenon encouraged others to explore the underlying mechanisms of tumor eradication. Despite his excellent therapeutic results, the later development of well-defined radiotherapy and chemotherapy resulted in the gradual disappearance of "Coley's Toxins" from clinical practice.

In the past few decades, our knowledge of the relationship between tumors and the immune system has increased considerably. Previously, people were skeptical regarding the ability of the immune system to fight cancer. Currently, we know that the immune system can recognize, control, and eliminate tumor cells using the same cells and molecules employed for protection against pathogens. This newfound knowledge has allowed for major breakthroughs in cancer immunotherapy, including the discovery of immune checkpoint inhibitors such as cytotoxic T-lymphocyte-associated protein 4 (CTLA-4), programmed cell death 1 (PD-1), and programmed death-ligand 1 (PD-L1). Despite the overall success of checkpoint inhibitors, many patients remain resistant to the use of this particular immunotherapy treatment [3]. Moreover, other approaches to cancer immunotherapy, including use of monoclonal antibodies, cytokines, adoptive T cell therapies, and cancer vaccines, are heavily oriented toward the adaptive immune system. These one-way oriented approaches could be ineffective against many types of solid tumors, especially those with strong escape mechanisms. Additionally, these popular immunotherapies often require intravenous application and subsequent systemic distribution to the tumors through the circulatory system, which may result in decreased penetration of drugs into the tumors or systemic toxicity [4, 5]. These limitations can be overcome by prodrugs with selective

accumulation in tumors or intratumoral applications that enable the delivery of a therapy directly into a tumor lesion [4, 6]. We believe that the best approach for effective cancer immunotherapy is intratumoral immunotherapy, which activates both the immune system and innate and adaptive immunity.

In 2016, our team demonstrated a strong synergy between a therapeutic mixture containing the ligands of receptors responsible for the recognition of specific molecules of pathogens, such as Toll-like receptors (TLRs) and phagocytosis ligands artificially anchored to tumor cells. The combination of TLR ligand resiquimod (R-848), polyinosinic-polycytidylic acid (poly(I:C)), heat-killed *Listeria monocytogenes*, and mannan (both *L. monocytogenes* and mannan covalently bound to tumor cells through an SMCC anchor) resulted in the eradication of advanced murine B16-F10 melanoma [7]. The imidazoquinoline compound R-848 is an agonist of TLR7/TLR8 in humans and TLR7 in mice and activates innate immune cells, such as monocytes, macrophages, and dendritic cells, with the subsequent production of inflammatory cytokines, such as interferon gamma and interleukin 12 [8]. Poly(I:C) is a synthetic analog of dsRNA that activates immune cells via TLR3 through multiple inflammatory pathways [9]. Heat-killed *L. monocytogenes* is recognized by TLR2. Mannan, a phagocytosis-stimulating ligand, is a simple polysaccharide derived from *Saccharomyces cerevisiae*. Anchored mannan is recognized by the mannose receptor and mannan-binding lectin. Their interaction initiates activation of the complement lectin pathway [10] resulting in opsonization of tumor cells by inactive form of C3b complement protein (iC3b), activation of innate immune cells (e.g., macrophages, dendritic cells, and granulocytes), and subsequent phagocytosis of tumor cells [11].

However, this combination has two main disadvantages. First, the use of the whole *L. monocytogenes* bacterium is unsuitable for clinical application in humans. Second, the SMCC anchor, a heterobifunctional protein crosslinker, requires a two-step application in mice, and consequently increases required injections. Therefore, we have focused on optimizing this therapy by replacing *L. monocytogenes* with another TLR2 agonist, lipoteichoic acid (LTA), and the SMCC anchor with a biocompatible cell membrane anchor (BAM) to make this a one-step application.

In this study, the optimized combination of mannan-BAM + R-848 + poly(I:C) + LTA (MBT therapy) was tested and studied in different tumor models, including murine B16-F10 melanoma [12], pancreatic adenocarcinoma (Panc02) [13], and pheochromocytoma (PHEO) [14] to confirm its efficacy in other tumor types.

Melanoma is a highly aggressive skin tumor that arises from melanocytes that produce melanin. At the beginning of the 21st century, the worldwide incidence of melanoma rapidly increased. While most patients who are diagnosed with localized melanoma can have it surgically removed, a high percentage of these patients already have established micrometastases at the time of diagnosis [15]. In our study, a mouse B16-F10 melanoma model was selected because of the aggressiveness of this melanoma and its ability to spread into the lungs, liver, and spleen [16], therefore allowing us to study metastasis during therapy.

In humans, pancreatic adenocarcinoma is the most common cancer with a lethal prognosis. The biggest challenge with this disease is the limited diagnostic options in combination with high resistance to conventional therapies. The murine ductal adenocarcinoma Panc02 model closely mimics that of human pancreatic cancer. Panc02 cells are aggressive and resistant to every known class of clinically active anti-tumor agents [17].

Pheochromocytomas (PHEOs) and paragangliomas (PGLs) are rare neuroendocrine tumors that arise from adrenal and extra-adrenal chromaffin tissues, respectively. They are characterized by the overproduction of catecholamines such as epinephrine and norepinephrine. Most PHEOs/PGLs are benign and can be easily surgically removed. However, patients with these benign tumors have relatively high morbidity and mortality rates due to increased catecholamine production, which can result in hypertension, arrhythmia, and stroke [18]. Up to 25% of PHEOs/PGLs are malignant, with distant metastases in nonchromaffin tissues. These malignant tumors represent the biggest challenge due to the lack of effective therapies. PHEOs/PGLs are characterized by a pseudo-hypoxic signature (i.e., a situation in which oxygen is present but cannot be processed because of alterations in the oxygen-sensing pathways). Pseudohypoxia has been shown to promote tumor progression and resistance to therapy [19]. In this study, we used an aggressive mouse tumor tissue derived (MTT) PHEO cell line.

We found that MBT therapy in the Panc02 and PHEO tumor models resulted in lower inhibition of tumor growth compared with that seen in the B16-F10 melanoma model. Therefore, we focused on improving the therapy and combined MBT therapy with an anti-CD40 antibody that mimics CD40 ligands on helper T cells, which results in the activation and licensing of antigen-presenting cells and the induction of an effective T cell-based antitumor response [20]. We coined the term 'MBTA therapy' for this.

MBTA therapy was used to treat tumors with high tumor burden, such as the metastatic PHEO [14], bilateral PHEO [21], and bilateral Panc02 [22] models, which also enabled us to study the systemic response to this therapy. We examined numerous combinations of MBTA therapy with other therapeutic approaches, such as checkpoint inhibitors, chemotherapy, and radiotherapy, to effectively treat these aggressive tumor models [22]. Moreover, we describe the composition of innate and adaptive immune cells and cytokines in treated and distal non-treated tumors, as well as in the spleen to study systemic effect of MBTA therapy [21]. We also focused on long-term immune memory after therapy and described which immune cells are involved. Finally, to ensure the absence of age-dependent differences in MBTA therapy, we compared the efficacy of MBTA therapy in young and aged mice.

Chapter I

Effective Cancer Immunotherapy Based on Combination of TLR Agonists
With Stimulation of Phagocytosis

Effective cancer immunotherapy based on combination of TLR agonists with stimulation of phagocytosis

Veronika Caisová[a], Ondřej Uher[a], Pavla Nedbalová[a], Ivana Jochmanová[b], Karolína Kvardová[a], Kamila Masáková[a], Gabriela Krejčová[a], Lucie Paďouková[a], Jindřich Chmelař[a], Jan Kopecký[a,c], Jan Ženka[a,*]

[a] Department of Medical Biology, Faculty of Science, University of South Bohemia, České Budějovice, Czech Republic
[b] 1st Department of Internal Medicine, Medical Faculty of P. J. Šafárik University in Košice, Košice, Slovakia
[c] Institute of Parasitology, Biology Centre of the Czech Academy of Sciences, v.v.i., České Budějovice, Czech Republic

ARTICLE INFO

ABSTRACT

Immunotherapy emerges as a fundamental approach in cancer treatment. Up to date, the efficacy of numerous different immunotherapies has been evaluated. The use of microorganisms or their parts for immune cell activation, referred to as Pathogen-Associated Molecular Patterns (PAMPs), represents highly promising concept. The therapeutic effect of PAMPs can be further amplified by suitable combination of different types of PAMPs such as Toll like receptor (TLR) agonists and phagocytosis activating ligands. Previously, we used the combination of phagocytosis activating ligand (mannan) and mixture of TLR agonists (resiquimod (R-848), poly(I:C), inactivated *Listeria monocytogenes*) for successful treatment of melanoma in murine B16-F10 model. In the present study, we optimized the composition and timing of previously used mixture. Therapeutic mixture based on well-defined chemical compounds consisted of mannan anchoring to tumor cell surface by biocompatible anchor for membranes (BAM) and TLR agonists resiquimod, poly(I:C), and lipoteichoic acid (LTA). The optimization resulted in (1) eradication of advanced stage progressive melanoma in 83% of mice, (2) acquisition of resistance to tumor re-transplantation, and (3) potential anti-metastatic effect. After further investigation of mechanisms, underlying anti-tumor responses, we concluded that both innate and adaptive immunity are activated and involved in these processes.

We tested the efficacy of our treatment in Panc02 murine model of aggressive pancreatic tumor as well. Simultaneous application of agonistic anti-CD40 antibody was necessary to achieve effective therapeutic response (80% recovery) in this model.

Our results suggest that herein presented immunotherapeutic approach is a promising cancer treatment strategy with the ability to eradicate not only primary tumors but also metastases.

1. Introduction

Immunotherapy has a long history in cancer treatment. Many different approaches focusing on immune cells activation and (subsequent) tumor eradication have been evaluated. The oldest immunotherapeutic concept is based on the use of pyogenic bacteria. This concept was described in the late 19th century by William Coley [1] and it is based on the ability of innate immunity to recognize pathogens through germline-encoded pattern-recognition receptors (PRRs) resulting in immune system activation and pathogen elimination [2]. This mechanism can simultaneously increase the effectivity of tumor cell recognition by immune system and, thus, it designates pathogens as a potential tool for cancer treatment [3]. Subsequently, isolation and synthesis of PAMPs opened new perspectives for this therapeutic approach. This research has primarily been focused on a specific group of PAMPs, so-called agonists of Toll-like receptors (TLR) [4]. TLR agonists are very effective in activation of immune cells and their attraction into the tumor [5]. Recently, we have shown that application of TLR agonists along with simultaneous labelling of tumor cells with ligands activating phagocytosis can significantly increase the ability of immune cells to recognize tumor cells [6,7]. The combination of resiquimod (TLR7 and TLR8 agonist, in case of mice TLR7 agonist only) and mannan (ligand activating phagocytosis) was shown to be the most effective formula. Moreover, the effect of therapy was significantly improved by addition of other TLR agonists, specifically poly(I:C) (TLR3) and *L. monocytogenes* (TLR2) [8].

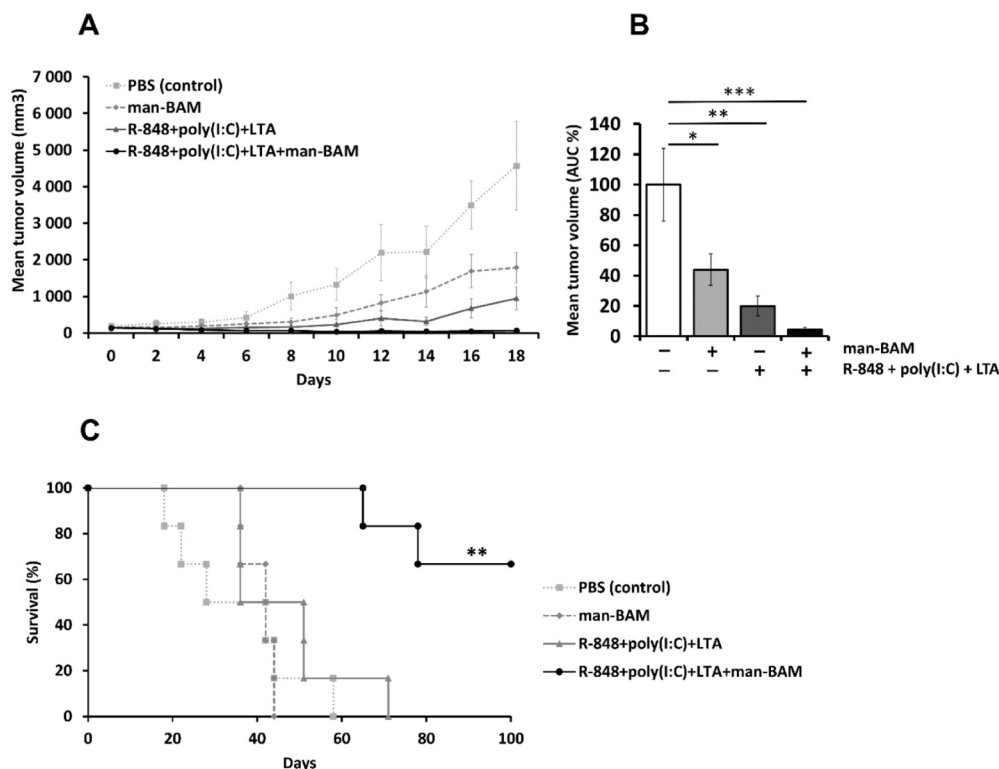**Fig. 1.** Cancer immunotherapy based on the combination of TLR agonists and phagocytosis stimulation. Murine B16-F10 model. Therapeutics were applied in pulse regime (days 0, 1, 2, ... 8, 9, 10). Tumor growth is presented by curves (A) with corresponding area under curve (AUC) analysis for each group (B). PBS treated control was considered as 100%. Statistical analysis was performed on AUC values by one-way ANOVA with Tukey's *post hoc* test. (C) Survival analysis, Long rank test, compared to PBS (control). * = $p < 0.05$, ** = $p < 0.01$, *** = $p < 0.001$.

In the present study we aimed to enhance the efficacy of this therapy. We focused on (1) the optimization of the therapeutic mixture composition and therapeutic timing, (2) analysis of mechanisms involved in anti-tumor responses in B16-F10 melanoma model, and (3) the possibility to combine this therapy with the use of checkpoint inhibitors and immune activators. Furthermore, we investigated the effectiveness of the present therapy in murine model of pancreatic adenocarcinoma (Panc02).

2. Materials and methods

2.1. Ethics statement

All experimental procedures with mice were performed in accordance with the laws of the Czech Republic. The experimental project was approved by the Ministry of Education, Youth and Sports (protocol no. 28842/2014-3).

2.2. Materials

Tissue culture media, media supplements, laminarin from *Laminaria digitata*, mannan from *Saccharomyces cerevisiae*, GM-CSF, TNF-α, lipoteichoic acid (LTA) from *Bacillus subtilis*, and polyinosinic: polycytidylic acid, sodium salt (poly(I:C)) were purchased from Sigma-Aldrich (St. Louis, MO, USA). Resiquimod (R-848) was obtained from Tocris Bioscience (Bristol, UK). Biocompatible Anchor for cell Membrane (BAM, Mw 4000) was purchased from NOF EUROPE (Grobbendonk, Belgium). Mannan-BAM synthesis was performed as previously described [8]. Monoclonal antibodies anti-PD-1 (rat IgG2a, clone RMP1-

14), anti-CTLA-4 (hamster IgG, clone 9H10), and anti-CD40 (rat IgG2a, clone FGK4.5/FGK45) were purchased from BioXCell (West Lebanon, NH, USA).

2.3. Cell lines and mice

The murine melanoma B16-F10 cells were obtained from the American Type Culture Collection (Manassas, VA, USA). Melanoma cells were cultivated in RPMI 1640 supplemented with 10% fetal calf serum and antibiotics (PAA, Pasching, Austria). Cultivation was performed at 37 °C in a humidified atmosphere with 5% carbon dioxide.

The murine pancreatic adenocarcinoma cell line Panc02 was obtained from Prof. Lars Ivo Partecke (Greifswald, Germany). These cells were cultivated in DMEM supplemented with 10% fetal calf serum and antibiotics under the same conditions as melanoma cells.

SPF C57BL/6 mice were purchased from Charles River Laboratories (Sulzfeld, Germany). All mice (weight 18–20 g) were housed in barrier facilities with free access to sterile food and water; the photoperiod was 12/12.

2.4. Tumor transplantation

C57BL/6 mice (females) were subcutaneously injected with 4×10^5 B16-F10/Panc02 cells (suspended in 0.1 ml serum free of RPMI 1640/ DMEM) into the previously shaved right flank. For the melanoma B16-F10 metastasis model, mice were injected with 1×10^5 B16-F10 cells (suspended in 50 μL PBS) into the lateral tail vein.

- 9 -
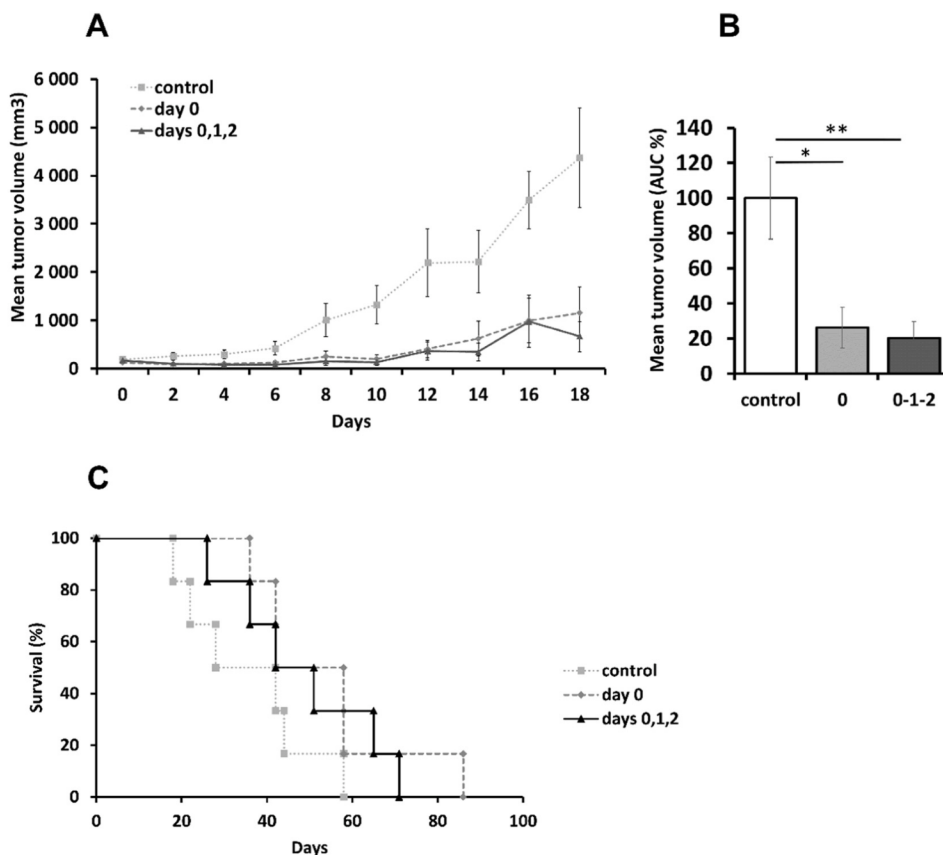
Fig. 2. Shortened cancer immunotherapy, B16-F10 model. Therapeutic mixture (R-848 + poly (I:C) + LTA + mannan-BAM) was applied in two different application regimes (day 0 and days 0, 1, 2). Control group did not receive any treatment. Tumor growth is presented by curves (A) with corresponding area under curve (AUC) analysis for each group (B). Control group was considered as 100%. Statistical analysis was performed on AUC values by one-way ANOVA with Tukey's *post hoc* test. (C) Survival analysis, Log rank test, compared to control. * = p < 0.05, ** = p < 0.01.

2.5. Treatment and evaluation

Twelve days after tumor cell transplantation mice were randomly divided into groups of six (unless otherwise indicated). Immediately after randomization the therapy was started (day 0). Therapeutic substances were applied intratumorally (50 μl/mouse) in particular regime. During the treatment, all animals were housed individually. Tumor size was measured every other day by a caliper. A formula $V = \pi/6 \ AB^2$ (A = largest dimension of tumor, B = smallest dimension) was used for tumor volume calculation [9].

Therapeutic mixtures used for immunotherapy consisted of active compounds – 0.5 mg R-848, HCl form, 0.5 mg poly(I:C), 0.5 mg LTA/ ml, and 0.2 mM mannan-BAM – dissolved in PBS. Plain PBS was used as a control in each experiment.

2.6. Evaluation of metastases

In the B16-F10 mouse model, lungs of experimental animals were carefully removed and fixed with 4% neutral solution of formaldehyde. The presence of metastases was evaluated using dissection microscope as previously described [6].

In the Panc02 mouse model, the examination of all inner organs (lung, heart, liver, stomach, intestine, kidney, spleen) was performed.

2.7. Flow cytometry analysis of tumor-infiltrating leukocytes

Analysis of tumor-infiltrating leukocytes was performed as described previously [8]. Briefly, tumors were digested with Liberase DL and DNase I (both Roche Diagnostics, Mannheim, Germany). Subsequently, particular leukocyte subtypes were determined using BD FACSCanto II flow cytometer (BD Biosciences, San Jose, CA, USA) and following monoclonal antibodies (eBioscience, San Diego, CA, USA) were used in this experiment: a) Total leukocytes - anti-mouse CD45 PerCP-Cy5.5; clone 30-F11, b) T cells - anti-mouse CD3e FITC; clone 145-2C11, c) CD4+ T cells - anti-mouse CD4 APC; clone GK1.5, d) CD8+ T cells - anti-mouse CD8a; clone 53-6.7, e) B cells - anti-mouse CD19 APC; clone eBio1D3, f) NK cells - anti-mouse NK1.1 PE; clone PK136, g) granulocytes (anti-mouse Gr-1 Alexa Fluor 700; clone RB6-8C5, and h) macrophages - anti-mouse F4/80 Antigen PE-Cy7; clone BM8. BD FACSDiva software 6.1.3. (BD Biosciences, San Jose, CA, USA) was used for the flow cytometry data analysis.

2.8. Preparation and priming of neutrophils

Suspension of murine bone marrow cells was prepared as described by Stassen et al. [10]. This suspension was used for preparation of neutrophils purified by magnetic-activated cell sorting (MACS) technique (Miltenyi Biotec, Bergisch Gladbach, Germany). The purity of neutrophils was evaluated by BD FACSCanto II flow cytometer (BD Biosciences, San Jose, CA, USA) using anti-mouse CD45 APC, clone 30-
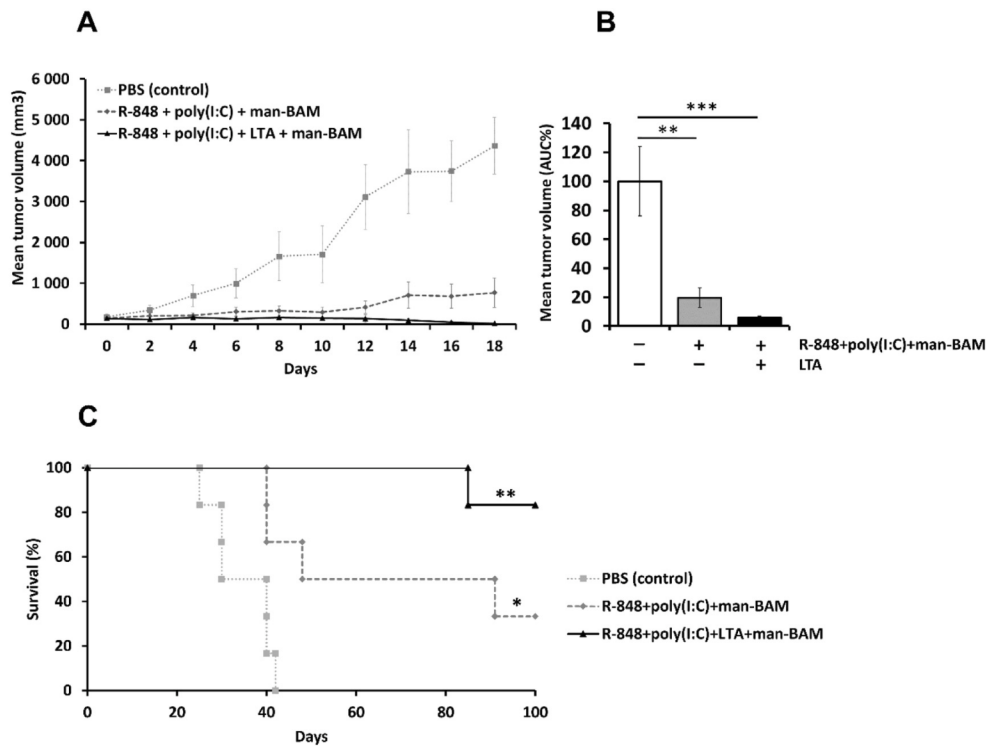
Fig. 3. Efficacy of cancer immunotherapy based on four therapeutic pulses, B16-F10 model. Therapeutic preparations were applied in pulse regime (days 0, 1, 2… 8, 9, 10… 16, 17, 18… 24, 25, 26). Tumor growth is presented by curves (A) with corresponding area under curve (AUC) analysis for each group (B). PBS treated control was considered as 100%. Statistical analysis was performed on AUC values by one-way ANOVA with Tukey's *post hoc* test. (C) Survival analysis, Log rank test, compared to PBS (control). * = p < 0.05, ** = p < 0.01, *** = p < 0.001.
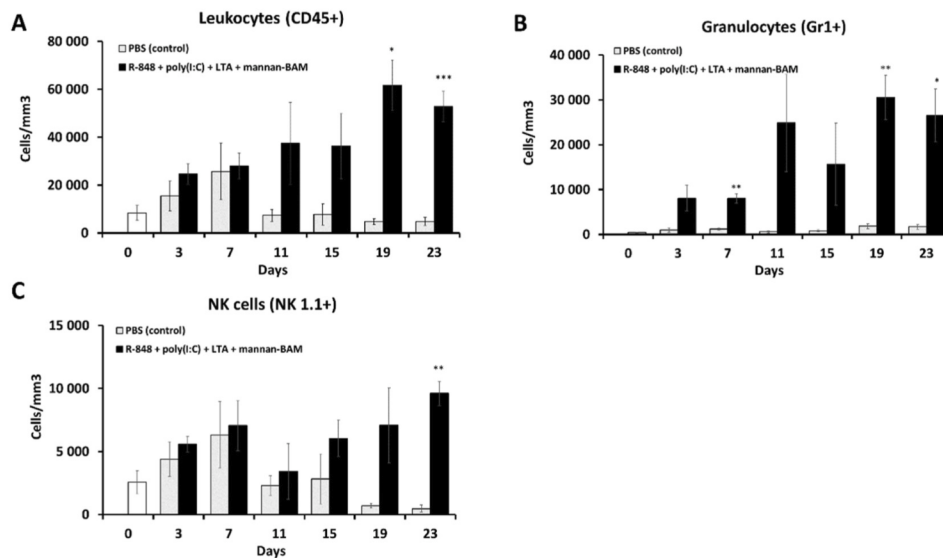
Fig. 4. Changes in tumor-infiltrating lymphocytes during the immunotherapy of murine melanoma (B16-F10). Twelve days following tumor cell transplantation, mice were randomly divided into two groups of 24. The therapeutic mixture (50 μL/mouse) was administered in four pulses on days 0, 1, 2…8, 9, 10…16, 17, 18… 24, 25, 26. Three mice from each group were euthanized on the 3rd, 7th, 11th, 15th, 19th, and 23rd day of the therapy. Another 3 mice were euthanized on day 0 without any treatment. Tumors were excised and analyzed for immune cell infiltrate using flow cytometry. Cell infiltration is expressed as number of cells per mm^3 of tumor mass. Following populations were analyzed: (A) leukocytes (CD45+), (B) Neutrophils (CD45 + Gr-1+), and (C) NK cells (CD45 + NK1.1+). Statistical analysis was performed using one-way ANOVA with Tukey's *post hoc* test, * = p < 0.05, ** = p < 0.01, *** = p < 0.005 compared to PBS (control).

- 11 -
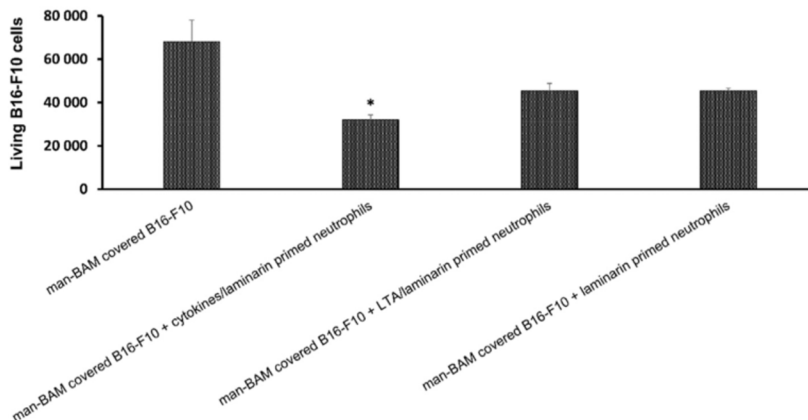
Fig. 5. In vitro analysis of cytotoxic effect of neutrophils on melanoma cells covered by anchored mannan. B16-F10 melanoma cells were incubated (30 min, 37 °C) with 0.02 mM mannan-BAM in culture medium and subsequently they were washed. Suspension of bone marrow neutrophils (90% purity) primed with cytokines (GM-CSF + TNF-alpha) or with LTA in culture medium was added to B16-F10 cells in 5:1 ratio. All mixtures were incubated at 37 °C for 2 h. Afterwards, trypan blue exclusion staining was performed, and viable melanoma cells were counted with a hemocytometer. Statistical analysis was performed using one-way ANOVA with Tukey's *post hoc* test,* = p < 0.05 compared to man-BAM covered B16-F10 cells.
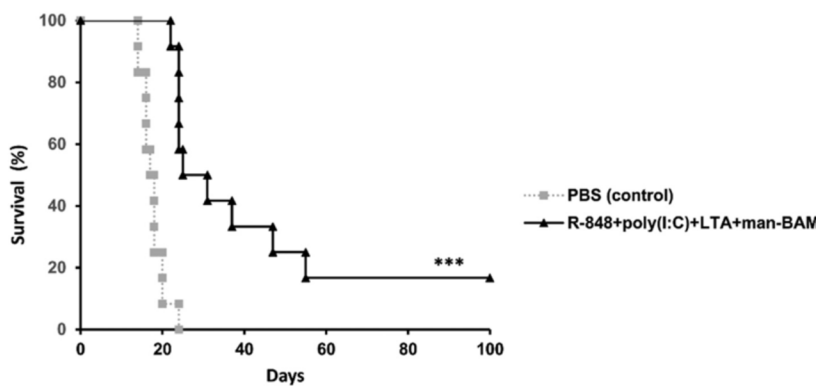
Fig. 6. Potential anti-metastatic effect of cancer immunotherapy. Survival analysis. Subcutaneous transplantation of 4×10^5 of melanoma B16-F10 cells along with intravenous administration of 1×10^5 of the same cells (per mouse) was performed. On day 12 after tumor transplantation, mice were randomized in two groups of 12, and therapy based on intratumoral application of corresponding preparations (50 μL/mouse) was started. Four therapeutic pulses were applied on days 0, 1, 2…8, 9, 10…16, 17, 18…24, 25, 26. Survival analysis and Log rank test were performed. *** = p < 0.001 compared to PBS (control).
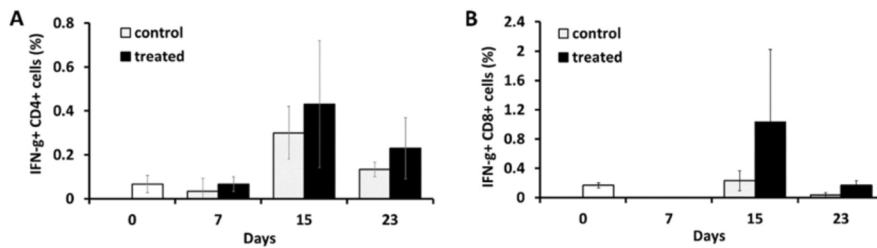
Fig. 7. Activation of adaptive immunity during the course of therapy. The transplantation of melanoma B16-F10 was performed as described in Fig. 1. Twelve days after tumor transplantation, mice were randomized in two groups of 9. Three more mice were euthanized for analysis before onset of treatment. Intratumoral application of the PBS (grey bars, 50 μl/mouse) or therapeutic mixture (R-848 + poly (I:C) + LTA + mannan-BAM, black bars, 50 μl/mouse) was performed in three pulses on days 0, 1, 2… 8, 9, 10… 16, 17, 18. Three mice from each group were euthanized on days 7, 15, and 23. Splenocytes were isolated and cultivated in the presence (or not) of UV killed melanoma cells. The production of intracellular IFN-γ was measured by flow cytometry. Control values (without antigen) were subtracted. (A) Intracellular IFN-γ production in CD4 + cells, (B) intracellular IFN-γ production in CD8 + cells.

F11 and anti-mouse Ly-6G (Gr-1) Alexa Fluor 700, clone RB6-8C5 antibodies (eBioscience, San Diego, CA, USA). Neutrophils were primed with a mixture of GM-CSF and TNF-α (12 ng and 2.5 ng/ml media, respectively) as reported by Dewas et al. [11], or by lipoteichoic acid (LTA, 0.05 mg/ml) for 20 min. Additionally, the priming solution was supplemented with 2 μM solution of soluble beta glucan (laminarin). Non-heat inactivated FBS was used as a source of complement proteins during the procedure.

2.9. Analysis of the cytotoxic effect of neutrophils on B16-F10/Panc02 cells labelled with mannan-BAM

B16-F10/Panc02 tumor cells were incubated with 0.02 mM mannan-BAM for 30 min at 37 °C. After incubation, non-bound mannan-BAM was washed away by centrifugation. Neutrophils

obtained from murine bone marrow were prepared and primed as described above. Subsequently, neutrophils were co-cultured with tumor cells (5:1 ratio) for 2 h in 37 °C. Following the incubation, cells were mixed with trypan blue and the live/dead cell counts were calculated using hemocytometer. Non-heat inactivated FBS was used as a source of complement proteins during the procedure.

2.10. IFN-γ intracellular staining in T cells

Mice were euthanized by cervical dislocation. Single cell suspension of splenocytes was prepared using a plastic strainer (70 μm, BD Biosciences, San Jose, CA, USA). Red blood cells were eliminated by lysis buffer (TRIS buffered 0.84% NH₄Cl solution). Splenocytes were co-cultured with UV-killed-B16-F10 cells (6:1 ratio) for 6 h at 37 °C and 5% CO_2. For each spleen, a sample prepared without UV-killed-B16-F10

- 12 -
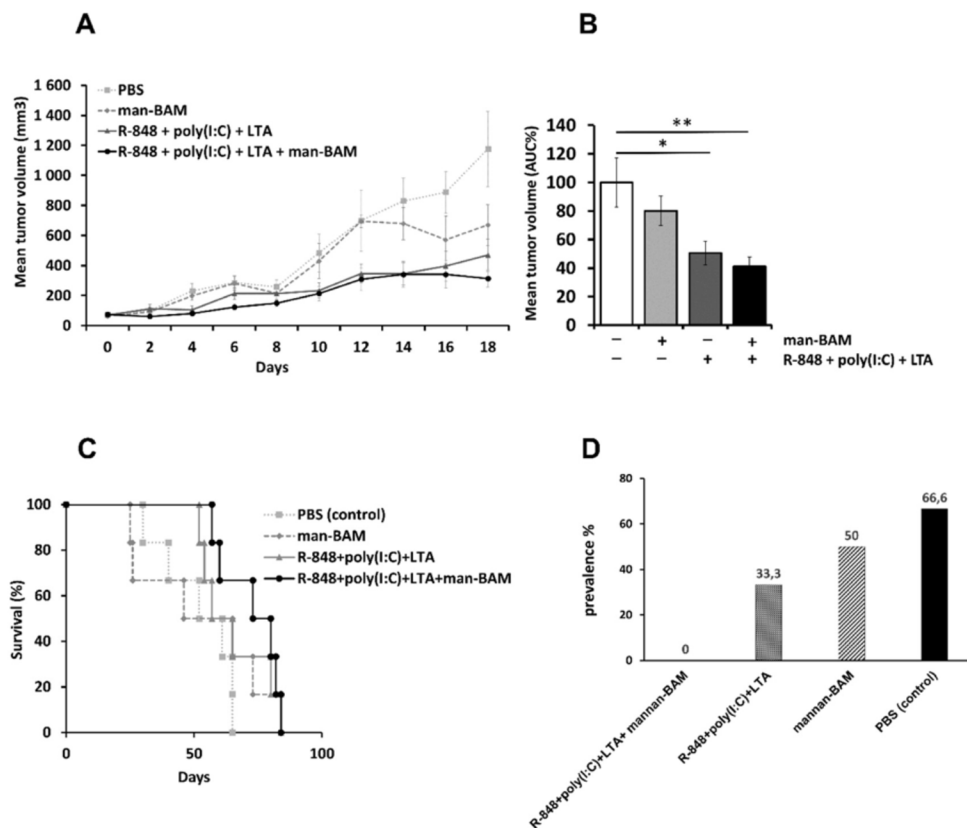
Fig. 8. Immunotherapy of pancreatic adenocarcinoma. Therapeutic preparations were applied in pulse regime (days 0, 1, 2… 8, 9, 10… 16, 17, 18… 24, 25, 26). Growth of tumors is presented as growth curves (A) with corresponding area under curve (AUC) analysis for each group (B), PBS treated control was considered as 100%. Statistical analysis was performed on AUC values by one-way ANOVA with Tukey's *post hoc* test, * = p < 0.05, ** = p < 0.01. (C) Survival analysis, Long rank test. R-848 + poly(I:C) + LTA + mannan-BAM compared to PBS (control) was near to statistical significance, p = 0.063. (D) Prevalence of metastases.

cells was used as a control.

Monensin (1 μl/ml, eBioscience, San Diego, CA, USA) was added to splenocytes for the last 5 h of co-cultivation. Afterwards, surface staining of CD markers was performed with anti-mouse CD3e FITC, anti-mouse CD4 APC, and anti-mouse CD8 PECy7 (eBioscience, San Diego, CA, USA). Cells were washed, fixed, and cell membranes were permeabilized (Foxp3/Transcription Factor Staining Buffer Set, eBioscience, San Diego, CA, USA). Intracellular staining of IFN-γ was performed using anti-mouse IFN-gamma PE (eBioscience, San Diego, CA, USA). Cells were analyzed using BD FACSCanto II flow cytometer (BD Biosciences, San Jose, CA, USA) and results were evaluated using BD FACSDiva software 6.1.3. (BD Biosciences, San Jose, CA, USA).

2.11. Statistical analysis

Area under curve (AUC) was calculated and statistical analysis was performed on AUC values by one-way ANOVA with Tukey's *post hoc* test. For survival analysis Log-rank test was used (STATISTICA 12, StatSoft, Inc., Tulsa, OK, USA). Error bars indicate SEM.

3. Results

3.1. The synergy between TLR agonists and phagocytosis stimulating ligand in cancer immunotherapy

The use of either mixture of three TLR agonists (R-848, poly(I:C), LTA) or anchored phagocytosis stimulating mannan-BAM resulted in

significant reduction of tumor growth without any effect on the survival of treated mice. However, when used in combination (TLR agonists + mannan-BAM), the treatment led to tumor shrinkage and elimination (Fig. 1A, B) along with 66% survival rate of treated mice (Fig. 1C). Mice, surviving for 100 days, did not show any pathological signs. The site of healed tumor was covered by hair and no metastases were found in lungs.

3.2. Design and optimization of dosage regimen

As described in Section 2.1, therapeutic mixture applied in two 3-day pulses separated by five-day gap, resulted in significant reduction of tumor growth with survival time prolongation. Despite that promising results, it was necessary to establish the optimal number of applications. First, we tested the effects of shortening of the duration of therapy. Not only one therapeutic 3-day pulse (0,1,2), but single injection of therapeutic mixture significantly suppressed tumor growth (Fig. 2A, B). Nevertheless, the shortened therapy was not sufficient to prolong survival of the mice (Fig. 2C). This indicates that at least two therapeutic pulses of the complete mixture R-848 + poly (I:C) + LTA + mannan-BAM are necessary to achieve prolonged survival.

Subsequently, we tested the efficacy of four therapeutic pulses. The use of mixture of three TLR agonists (R-848, poly(I:C), LTA) with anchored mannan (mannan-BAM) resulted in the elimination of tumors (Fig. 3A, B) and led to 83% survival in the treated group of mice (Fig. 3C). Moreover, the therapy induced resistance against re-

- 13 -
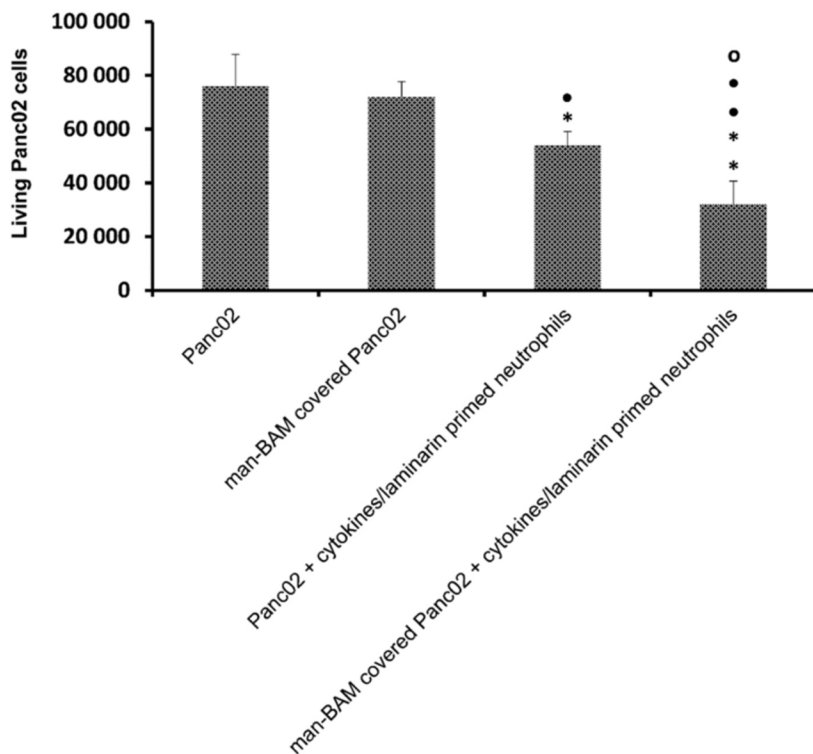
Fig. 9. In vitro analysis of cytotoxic effect of neutrophils on Panc02 cells covered by anchored mannan. The suspension of primed bone marrow neutrophils (90% purity) was added to Panc02 cells (both free and mannan-BAM covered) in a 5:1 ratio. After subsequent incubation, living cells were counted using hemocytometer and trypan blue exclusion staining. Statistical analysis was performed using one-way ANOVA with Tukey's *post hoc* test,* = p < 0.05 compared to Panc02, ** = p < 0.001 compared to Panc02, • = p < 0.05 compared to man-BAM covered Panc02, •• = p < 0.001 compared to man-BAM covered Panc02, o = p < 0.05 compared to Panc02 + neutrophils.

transplantation of cancer cells. Using scheme identical to the primary transplantation, re-transplantation of melanoma cells was performed on day 120 after therapy initiation (4×10^5 melanoma B16-F10 cells/mouse, subcutaneous application). None of the mice regrew the tumor.

Furthermore, this experiment proved the necessity of using the complex TLR agonists mixture. Omission of TLR2 agonist (LTA) decreased the therapeutic effect.

3.3. Tumor leukocyte infiltration changes in the course of immunotherapy

Flow cytometry analysis of tumor infiltrate during the therapy (as described in Fig. 3) showed strong leukocytic infiltration (Fig. 4A) with predominantly granulocytic content (Fig. 4B). Increased counts of NK cells were detected as well (Fig. 4C). The counts of CD4+ and CD8+ T-lymphocytes, B-lymphocytes, and macrophages were low, and no changes in their quantity were observed during the treatment (data not shown).

Evaluation of leukocyte infiltration was terminated on 23rd day of the therapy due to disappearance of all tumors in the treated group. Surviving mice (6 in treated group, 5 controls) were euthanized on day 31 by cervical dislocation and the evaluation of lung metastases was performed. No metastases were found in the treated group, while in the control group (PBS), metastases were present in 80% of mice with average of 4 metastases per mouse.

3.4. Cytotoxic effect of neutrophils on melanoma cells covered by anchored mannan in vitro

Substantial enhancement of the immunotherapy efficacy by LTA (Fig. 3) led us to investigate whether it was caused by direct priming of neutrophils by LTA. Our results (Fig. 5) did not support this presumption. To prime neutrophils, it was necessary to use cytokines (GM-CSF + TNF-alpha), which mimic the natural way of activation.

3.5. Combination of TLR agonists with stimulation of phagocytosis revealed potential anti-metastatic effect

We also evaluated the effect of our therapeutic mixture on metastases. Simultaneous subcutaneous transplantation of melanoma B16-F10 cells (4×10^5 cells per mouse) along with their intravenous administration (1×10^5 cells per mouse) was performed. After 12 days, subcutaneous tumors were treated by intratumoral application of the therapeutic mixture in treated group or by PBS application in control group. The therapy significantly prolonged survival of treated mice and two out of twelve mice were completely cured (Fig. 6). All surviving mice were euthanized 100 days after initiation of the therapy. No metastases were found in lungs of these mice. In contrast, there was a massive occurrence of lung metastases in the control group (78.9 ± 36.4/mouse), resulting in shortened survival (compare to control group in Fig. 3C).

3.6. Onset of innate immunity effectors was followed by activation of adaptive immunity

We consider the activation of innate immunity to be central mechanism of action in the herein presented cancer immunotherapy based on the combination of TLR agonists (R-848, poly(I:C), LTA) and phagocytosis stimulating ligand (mannan). Moreover, stimulation of phagocytosis, support of dendritic cells maturation, and establishment of proinflammatory Th1 millieu [8] create optimal conditions for subsequent activation of adaptive immunity.

In order to investigate the stimulation of adaptive immunity, we analyzed antigen specific activation of splenic T lymphocytes by measuring of IFN-γ intracellular production of in response to melanoma antigens exposure. Adaptive immunity response culminated on day 15 of the therapy at the level of both CD4+ (Fig. 7A) and CD8+ (Fig. 7B) splenocytes. The contribution of adaptive immunity to therapeutic effect was further supported by experiments involving SCID mice, which

- 14 -
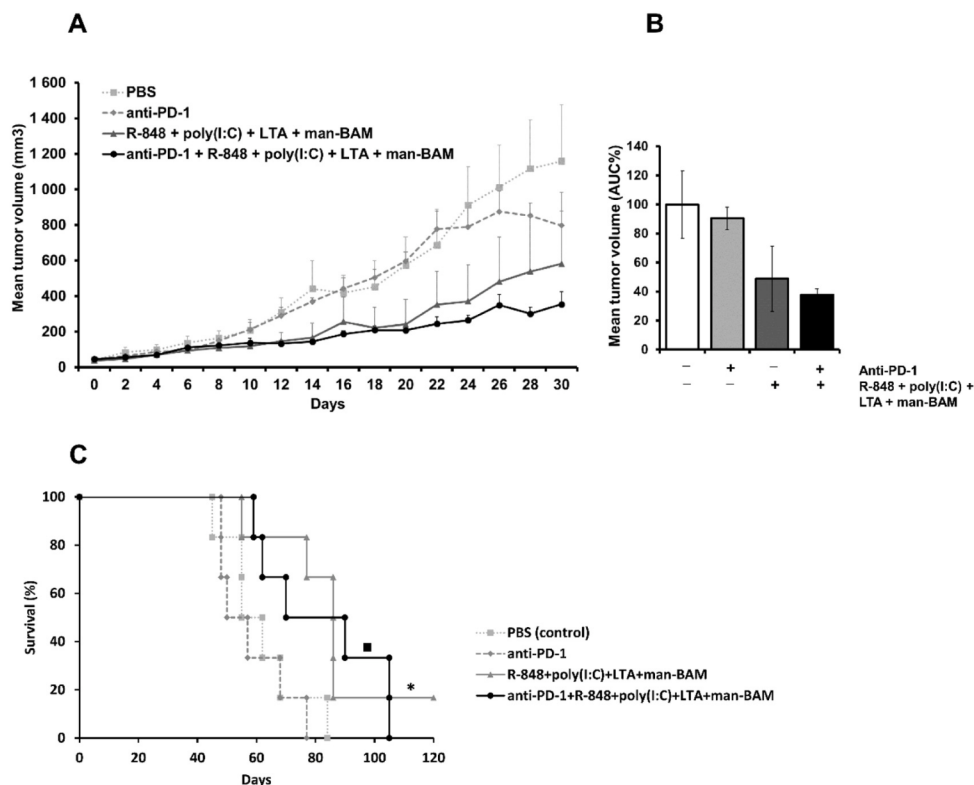
Fig. 10. Combination of TLRs/man-BAM therapy with anti-PD-1. Experimental design was the same as described in the Fig. 8. Where indicated, anti-PD-1 antibody was used in final concentration of 0.4 mg/ml of PBS or therapeutic mixture, respectively. Growth of tumors is presented as curves (A) with corresponding area under curve (AUC) analysis for each group (B). PBS treated control was considered as 100%. Statistical analysis was performed on AUC values by one-way ANOVA with Tukey's *post hoc* test. (C) Survival analysis, Long rank test, * = p < 0.05 compared to PBS (control) and anti-PD-1, ■ = p < 0.05 compared to anti-PD-1.

revealed partial inhibition of tumor growth but not survival prolongation (data not shown).

3.7. Immunotherapy of pancreatic adenocarcinoma

Therapy of pancreatic adenocarcinoma poses one of the greatest challenges in oncology. Thus, we examined the effect of our therapy based on intratumoral application of R-848, poly(I:C), LTA, and mannan-BAM in the Panc02/mouse model. We evaluated the effects of the TLR agonists alone (R-848, poly(I:C), LTA), the phagocytosis stimulating compound (mannan-BAM), and the complete therapeutic mixture (R-848, poly(I:C), LTA, mannan-BAM). The use of the complete therapeutic mixture exhibited the highest efficacy, as indicated by reduction of tumor growth (Fig. 8A, B), survival prolongation (Fig. 8C), and suppression of metastases (Fig. 8D).

As demonstrated above (Fig. 4), therapy based on the combination of R-848, poly(I:C), LTA, and mannan-BAM significantly stimulates granulocytic inflammatory infiltration. Therefore, we studied the cytotoxic effect of neutrophils on Panc02 cells covered by mannan-BAM *in vitro*. This effect (Fig. 9) was comparable to the effect of neutrophils on B16-F10 cells described above and previously [7]. Thus, the lower efficacy of the therapeutic mixture in the Panc02/mouse model compared to the B16-F10/mouse model cannot be explained by higher resistance of Panc02 cells to neutrophil attack. Furthermore, we examined the cytotoxic effect of NK cells on Panc02 cells covered by mannan-BAM. Killing of 32% of Panc02 cells correspond well to effects of NK cells on melanoma B16-F10 cells (29%) described previously [7].

3.8. Simultaneous administration of checkpoint inhibitors/agonist enhanced antitumoral activity of therapeutic mixture

To achieve higher efficacy of our immunotherapy, we decided to involve checkpoint inhibitors (anti-PD-1 and anti-CTLA-4 antibodies, respectively) and one activator (agonistic anti-CD40 antibody). Anti-PD-1 antibody itself had only negligible effect on the growth of Panc02 tumors (Fig. 10A, B). Combination of anti-PD-1 with mixture of R-848, poly(I:C), LTA, and mannan-BAM resulted in additive effects on reduction of tumor growth (Fig. 10A, B), although not statistically significant.

The combination of our immunotherapeutic mixture with anti-CTLA-4 antibody showed strong synergy leading to reduction of tumor growth (Fig. 11A, B) and prolongation of survival (Fig. 11C).

The strongest synergy was achieved by combination of R-848 + poly(I:C) + LTA + mannan-BAM mixture with agonistic anti-CD40 antibody (Fig. 12A, B, C). Anti-CD40 antibody itself showed an inhibiting effect (though not significant) on the tumor growth, but the synergy with R-848 + poly(I:C) + LTA + mannan-BAM dramatically affected both tumor growth (Fig. 12A, B) and mice survival (Fig. 12C). Importantly, the addition of anti-CD40 antibody significantly prolonged the survival of mice, when compared with R-848 + poly(I:C) + LTA + mannan-BAM mixture alone (Fig. 12C). Mice remained resistant to this type of tumor, as assessed by re-transplantation of Panc02 cells (s.c. application of 4×10^5 cells/mouse) on day 120 after the therapy initiation.
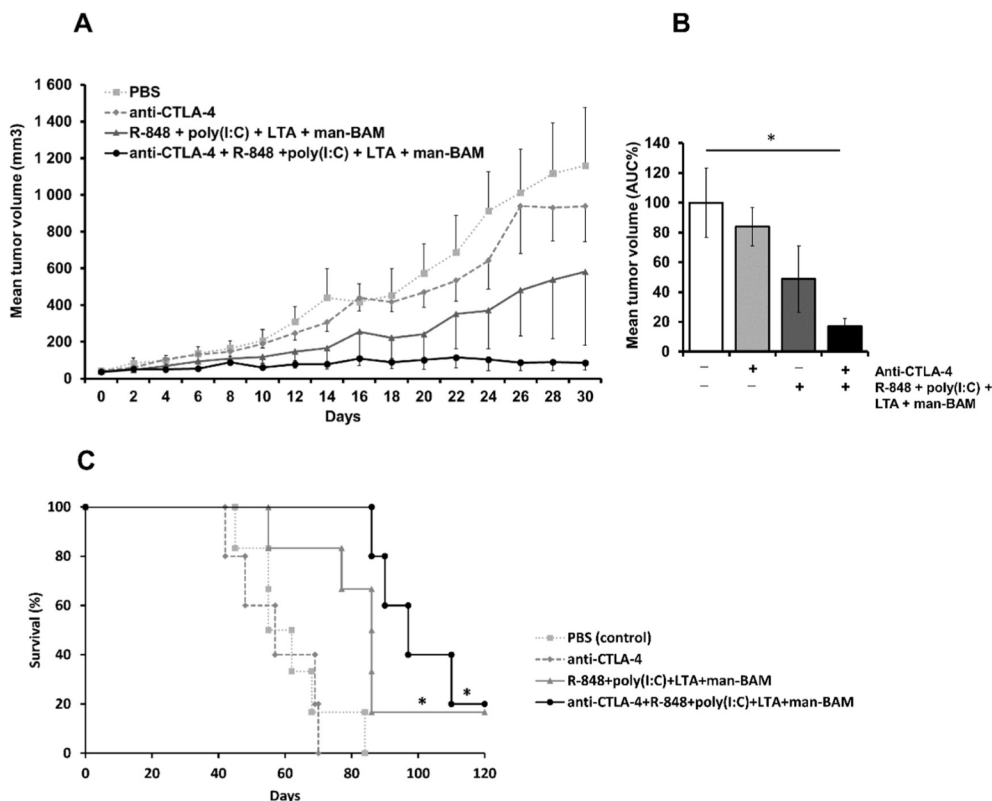
Fig. 11. Combination of TLRs/man-BAM therapy with anti-CTLA-4 therapy. Experimental design was the same as described in the Fig. 8. Where indicated, anti-CTLA-4 antibody was used in final concentration of 0.4 mg/ml of PBS or therapeutic mixture, respectively. Growth of tumors is presented as curves (A) with corresponding area under curve (AUC) analysis for each group (B). PBS treated control was considered as 100%. Statistical analysis was performed on AUC values by one-way ANOVA with Tukey's *post hoc* test, * = p < 0.05. (C) Survival analysis, Long rank test, * = p < 0.05 compared to PBS (control) and anti-CTLA-4.

4. Discussion

Recently, we demonstrated a strong synergy between the therapeutic mixture containing three TLR agonists (R-848 + poly(I:C) + heat-killed *L. monocytogenes*-SMCC) and anchored phagocytosis stimulating mannan (mannan-SMCC), which resulted in eradication of advanced melanoma [8]. *L. monocytogenes* significantly increased the efficacy of the treatment; however, the use of whole microorganisms is inconvenient for pertinent clinical applications. Thus, we replaced *L. monocytogenes* by another TLR2 agonist, lipoteichoic acid (LTA). Furthermore, an effective, but complicated anchoring of mannan to tumor cells with SMCC was replaced by BAM anchor (mannan-BAM, one-step application). Our new cancer immunotherapeutic mixture was highly effective, even if applied in only two therapeutic pulses. Four pulses resulted in 83% cure rate, which is the same efficacy as described previously [8]. The advantage of this improved treatment is the simple one-step anchoring of mannan and the use of well-defined chemical compounds including LTA. Moreover, LTA is not only TLR2 agonist; it is important ligand of scavenger receptors. LTA is able to interact with cell membranes [12] so its binding to tumor cells and fragments of tumor cell membranes can support scavenger receptors-mediated recognition of tumor antigens by dendritic cells. If significant contribution of LTA to efficacy of treatment is based on mentioned mechanisms will be matter of further studies.

We found four pulses regime as an optimal timing schedule. Separation of treatment pulses by treatment free intervals is necessary for recovery of sensitivity of TLR receptors to their agonists [8,13]. Moreover, as will be discussed below, our treatment initiated by innate

immunity attack is followed by activation of adaptive immunity. So four pulses lasting treatment resembling vaccination scheme creates better conditions for activation of adaptive immunity than shorter one.

Investigation of mechanisms underlying the action of present experimental immunotherapy confirmed our previous observations and conclusions [6–8]. The major effects of the treatment seem to be massive inflammatory infiltration with dominant granulocytic fraction and immune destruction of tumor cells covered by anchored mannan. Mannan activates complement with a subsequent stimulation of phagocytosis (iC3b formation) [6,7]. Granulocytes most likely stand in the centre of cytotoxic anti-cancer effect of the treatment. Based on their counts, we consider neutrophils to be key phagocytic cells involved in the tumor eradication. Higher amount of NK cells, especially in the later phase of the treatment, may contribute to the general effect of experimental immunotherapy, as previously described [7]. Contribution of macrophages should be considered as well [6].

We presume that the attack of innate immunity cells on tumor cells is followed by activation of adaptive immunity. Presented experimental immunotherapy stimulates phagocytosis and thus supports subsequent antigen presentation by phagocytes. The function of dendritic cells, the main antigen presenting cells, is dependent on their proper maturation and presence of costimulatory molecules. This maturation is significantly supported by our therapeutic mixture, specifically by R-848 and poly(I:C) [14,15]. Activation of adaptive immunity is proved by long lasting resistance to re-transplantation of melanoma cells and antigen specific response of CD4+ and CD8+ T-cells.

Herein presented immunotherapeutic approach was effective also in the treatment of murine model of pancreatic adenocarcinoma. Similarly

- 16 -
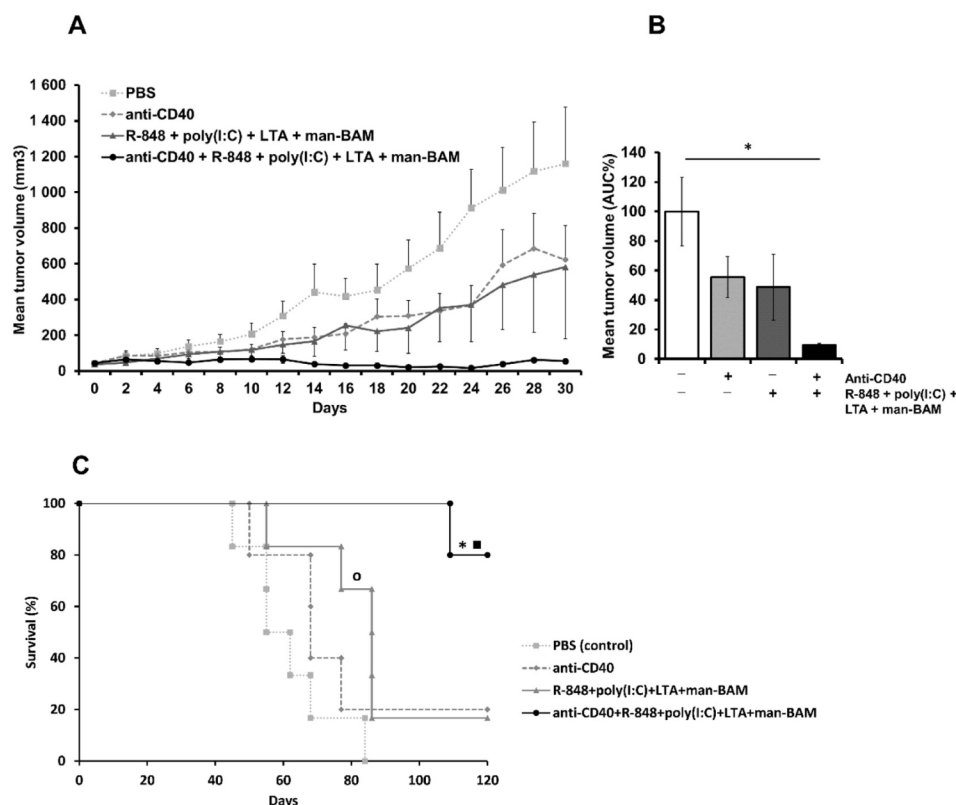
Fig. 12. Combination of TLRs/man-BAM therapy with anti-CD40 therapy. Experimental design was the same as described in the Fig. 8. Where indicated, anti-CD40 antibody was used in final concentration of 0.4 mg/ml of PBS or therapeutic mixture, respectively. Growth of tumors is presented as curves (A) with corresponding area under curve (AUC) analysis for each group (B). PBS treated control was considered as 100%. Statistical analysis was performed on AUC values by one-way ANOVA with Tukey's *post hoc* test, * = p < 0.05. (C) Survival analysis, Long rank test, * = p < 0.05 compared to anti-CD40 and R-848 + poly(I:C) + LTA + man-BAM groups, ■ = p < 0.005 compared to PBS (control), o = p < 0.05 compared to PBS (control).

to the melanoma model, synergy between TLR agonists and stimulation of phagocytosis was observed during the treatment of pancreatic adenocarcinoma as well as the suppression of metastasis. However, the outcomes of the treatment were not as significant as in melanoma. Since there is no evidence of resistance of pancreatic adenocarcinoma cells against attack of innate immune cells (based on our *in vitro* results), there has to be another mechanism responsible for lower efficacy of our experimental immunotherapy. The lower efficacy of our experimental immunotherapy can be partially explained by low infiltration of effector T- cells and simultaneous massive infiltration by immunosuppressive leukocytes in pancreatic adenocarcinoma. Dense desmoplastic stroma supports angiogenesis while evading from immune cells. Stroma is not only a passive barrier for the immune system; it also interacts with tumor cells stimulating their progression and invasiveness [16]. In effort to improve effect of our experimental immunotherapy in pancreatic adenocarcinoma, we combined the TLRs/mannan-BAM treatment with anti-CTLA-4 and anti-CD40 antibodies, respectively. Depletion of T-regulatory lymphocytes (Tregs) is considered to be the major outcome of anti-CTLA-4 therapy. Synergy between anti-CTLA-4 and TLRs/mannan-BAM therapy indicates the role of adaptive immunity in our immunotherapeutic approach, as in pancreatic adenocarcinoma Tregs play important role in suppression of adaptive immunity [16]. The synergy of anti-CD40 antibody with our treatment was expected since TLR agonists/mannan-BAM therapy is based on the primary stimulation of phagocytosis. Agonistic anti-CD40 antibody mimics CD40L on Th cells, resulting in activation of phagocytes and licensing of APC to induce anti-tumor T cell response.

Our treatment joins innate immunity based attack with activation of adaptive immunity. As own tumor is utilized for vaccination, we suppose that this treatment corresponds to the new paradigm for cancer therapy, *intratumoral immunization* [17]. Successful intratumoral immunization has to combine release of tumor antigens with support of antigen presentation, reduction of immune suppression and activation of cytotoxic cells [17–22]. Our treatment fulfils main criterions of this approach. The primary innate immunity based attack of tumors mimics natural elimination of pathogens and leads to both tumor shrinkage and release of tumor antigens. Moreover, the maturation of dendritic cells and the antigen presentation is supported by TLR agonists and can be further amplified by agonistic anti-CD40 antibody [23]. Anti-CTLA-4 can be used for Tregs depletion, if desirable [21,22].

5. Conclusion

The presented immunotherapeutic approach uses mechanisms of innate immunity for direct elimination of tumors by application of therapeutic mixture directly into the tumor. Consequently, due to support of T-cells by antigen presentation, the whole organism is vaccinated against the tumor. This is demonstrated by suppression of metastasis and acquisition of resistance to cancer recurrence.

Conflict of interests

The authors declare that there is no conflict of interests regarding the publication of this article.

Acknowledgements

References

[1] W.B. Coley, The treatment of malignant tumors by repeated inoculations of erysipelas: with a report of ten original cases, Am. J. Med. Sci. 10 (5) (1893) 487–511.

[2] S. Akira, S. Uematsu, O. Takeushi, Pathogen recognition and innate immunity, Cell 124 (2006) 783–801.

[3] G. D'Errico, H.L. Machado, B. Sainz Jr., A current perspective on cancer immune therapy: step-by-step approach to constructing the magic bullet, Clin. Transl. Med. 6 (2017) 3, http://dx.doi.org/10.1186/s40169-016-0130-5.

[4] H. Kanzler, F.J. Barrat, E.M. Hessel, R.L. Coffman, Therapeutic targeting of innate immunity with Toll-like receptor agonists and antagonists, Nat. Med. 13 (2007) 552–559.

[5] S. Adams, Toll-like receptor agonists in cancer therapy, Immunotherapy 1 (6) (2009) 949–964.

[6] T. Janotová, M. Jalovecká, M. Auerová, et al., The use of anchored agonists of phagocytic receptors for cancer immunotherapy: B16-F10 murine melanoma model, PLoS ONE 9 (1) (2014) e85222.

[7] E. Waldmannová, V. Caisová, J. Fáberová, et al., The use of Zymosan A and bacteria anchored to tumor cells for effective cancer immunotherapy: B16-F10 murine melanoma model, Int. Immunopharmacol. 39 (2016) 295–306.

[8] V. Caisová, A. Vieru, Z. Kumžáková, et al., Innate immunity based cancer immunotherapy: B16-F10 murine melanoma model, BMC Cancer 16 (2016) 940, http://dx.doi.org/10.1186/s12885-016-2982-x.

[9] J. Li, Y.F. Piao, Z. Jiang, L. Chen, H.B. Sun, Silencing of signal transducer and activator of transcription 3 expression by RNA interference suppresses growth of human hepatocellular carcinoma in tumor-bearing nude mice, World J. Gastroenterol. 15 (21) (2009) 2602–2608.

[10] M. Stassen, A. Valeva, I. Walev, E. Schmitt, Activation of mast cells by streptolysin O and lipopolysaccharide, Methods Mol. Biol. 315 (2006) 393–403.

[11] C. Dewas, P.M. Dang, M.A. Gougerot-Pocidalo, J. El-Benna, TNF-α induces phosphorylation of p47^{phox} in human neutrophils: partial phosphorylation of p47^{phox} is a common event of priming of human neutrophils by TNF-α and granulocyte-macrophage colony-stimulating factor, J. Immunol. 171 (8) (2003) 4392–4398.

[12] E.H. Beachey, T.M. Chiang, I. Ofek, A.H. Kang, Interaction of lipoteichoic acid of group A *Streptococci* with human platelets, Infect. Immun. 16 (2) (1977) 649–654.

[13] C. Bourquin, C. Hotz, D. Noerenberg, et al., Systemic cancer therapy with a small molecule agonist of Toll-like receptor 7 can be improved by circumventing TLR tolerance, Cancer Res. 71 (15) (2011) 5123–5133.

[14] S.J. Gibson, J.M. Lindh, T.R. Riter, et al., Plasmacytoid dendritic cells produce cytokines and mature in response to the TLR7 agonists, imiquimod and resiquimod, Cell. Immunol. 218 (2002) 74–86.

[15] H. Tsujimoto, P.A. Efron, T. Matsumoto, et al., Maturation of murine bone marrow-derived dendritic cells with poly(I:C) produces altered TLR-9 expression and response to CpG DNA, Immunol. Lett. 107 (2006) 155–162.

[16] P.R. Kunk, T.W. Bauer, C.L. Slingluff, O.E. Rahma, From bench to bedside a comprehensive review of pancreatic cancer immunotherapy, Journal for ImmunoTherapy of Cancer 4 (14) (2016).

[17] A. Marabelle, H. Kohrt, C. Caux, R. Levy, Intratumoral immunization: a new paradigm for cancer therapy, Clin. Cancer Res. 20 (7) (2014) 1747–1756.

[18] J.G. van den Boorn, G. Hartmann, Turning tumors into vaccines: co-opting the innate immune system, Immunity 39 (2013) 27–37.

[19] D. Nelson, S. Fisher, B. Robinson, The "Trojan horse" approach to tumor immunotherapy: targeting the tumor microenvironment, J Immunol Res 2014 (2014).

[20] L. Hammerich, N. Bhardwaj, H. Kohrt, et al., *In situ* vaccination for the treatment of cancer, Immunotherapy 8 (3) (2016) 315–330.

[21] R.H. Pierce, J.S. Cambell, S.I. Pai, et al., In-situ tumor vaccination: bringing the fight to the tumor, Hum. Vaccin. Immunother. 11 (8) (2015) 1901–1909.

[22] A. Marabelle, L. Tselikas, T. de Baere, R. Houot, Intratumoral immunotherapy: using the tumor as the remedy, Ann. Oncol. 28 (Suppl. 12) (2017) xii33–xii43.

[23] C.L. Ahonen, C.L. Doxsee, S.M. McGurran, et al., Combined TLR and CD40 triggering induces potent CD8^{+} T cell expansion with variable dependence on type I IFN, J. Exp. Med. 199 (6) (2004) 775–784.

- 18 -

Chapter II

The Significant Reduction or Complete Eradication of Subcutaneous and Metastatic Lesions in a Pheochromocytoma Mouse Model After Immunotherapy Using Mannan-BAM, TLR Ligands, and Anti-CD40

Article

The Significant Reduction or Complete Eradication of Subcutaneous and Metastatic Lesions in a Pheochromocytoma Mouse Model after Immunotherapy Using Mannan-BAM, TLR Ligands, and Anti-CD40

Veronika Caisova [1,2], Liping Li [1] , Garima Gupta [1], Ivana Jochmanova [1], Abhishek Jha [1], Ondrej Uher [1,2], Thanh-Truc Huynh [1], Markku Miettinen [3], Ying Pang [1], Luma Abunimer [1], Gang Niu [4], Xiaoyuan Chen [4] , Hans Kumar Ghayee [5], David Taïeb [6], Zhengping Zhuang [7], Jan Zenka [2] and Karel Pacak [1,*]

[1] Section on Medical Neuroendocrinology, *Eunice Kennedy Shriver* National Institute of Child Health and Human Development, National Institutes of Health, Bethesda, MD 20814, USA; veronika.caisova@nih.gov (V.C.); bat.150@hotmail.com (L.L.); garima.gupta83@gmail.com (G.G.); ivana.jochmanova@gmail.com (I.J.); abhishek.jha@nih.gov (A.J.); ondrej.uher@nih.gov (O.U.); huynht@mail.nih.gov (T.-T.H.); ying.pang@nih.gov (Y.P.); luma.abunimer@nih.gov (L.A.)

[2] Department of Medical Biology, Faculty of Science, University of South Bohemia, Ceske Budejovice 37005, Czech Republic; jzenka@gmail.com

[3] Laboratory of Pathology, National Cancer Institute, National Institutes of Health, Bethesda, MD 20814, USA; markku.miettinen@nih.gov

[4] Laboratory of Molecular Imaging and Nanomedicine, National Institute of Biomedical Imaging and Bioengineering, National Institutes of Health, Bethesda, MD 20814, USA; gang.niu@nih.gov (G.N.); shawn.chen@nih.gov (X.C.)

[5] Biological Molecular Imaging Section, University of Florida College of Medicine, Gainesville, FL 32603, USA; Hans.Ghayee@medicine.ufl.edu

[6] Department of Nuclear Medicine, La Timone University Hospital, CERIMED, Aix-Marseille University, 13385 Marseille, France; David.TAIEB@ap-hm.fr

[7] Surgical Neurology Branch, National Institute of Neurological Disorders and Stroke, National Institutes of Health, Bethesda, MD 20814, USA; zhengping.zhuang@nih.gov

* Correspondence: karel@mail.nih.gov; Tel.: +1-301-402-4594

check for updates

Abstract: Therapeutic options for metastatic pheochromocytoma/paraganglioma (PHEO/PGL) are limited. Here, we tested an immunotherapeutic approach based on intratumoral injections of mannan-BAM with toll-like receptor ligands into subcutaneous PHEO in a mouse model. This therapy elicited a strong innate immunity-mediated antitumor response and resulted in a significantly lower PHEO volume compared to the phosphate buffered saline (PBS)-treated group and in a significant improvement in mice survival. The cytotoxic effect of neutrophils, as innate immune cells predominantly infiltrating treated tumors, was verified in vitro. Moreover, the combination of mannan-BAM and toll-like receptor ligands with agonistic anti-CD40 was associated with increased mice survival. Subsequent tumor re-challenge also supported adaptive immunity activation, reflected primarily by long-term tumor-specific memory. These results were further verified in metastatic PHEO, where the intratumoral injections of mannan-BAM, toll-like receptor ligands, and anti-CD40 into subcutaneous tumors resulted in significantly less intense bioluminescence signals of liver metastatic lesions induced by tail vein injection compared to the PBS-treated group. Subsequent experiments focusing on the depletion of T cell subpopulations confirmed the crucial role of CD8^{+} T cells in inhibition of bioluminescence signal intensity of liver metastatic lesions. These data call for a

new therapeutic approach in patients with metastatic PHEO/PGL using immunotherapy that initially activates innate immunity followed by an adaptive immune response.

Keywords: pheochromocytoma; paraganglioma; metastatic; immunotherapy; innate immunity; adaptive immunity; toll-like receptor; pathogen-associated molecular patterns; neutrophil; T cell

---

1. Introduction

Pheochromocytomas (PHEOs) and paragangliomas (PGLs) are rare catecholamine-producing neuroendocrine/neural crest cell tumors arising from the adrenal medulla and extra-adrenal paraganglia, respectively [1]. Approximately 10–30% of all PHEOs/PGLs become metastatic and therapeutic options for treating metastatic disease are limited [2]. Therefore, efforts to find new and more effective therapies are urgently needed for patients with either inoperable or metastatic PHEO/PGL.

Immunotherapy, in which immune cells of a patient are used to attack and subsequently eliminate tumor cells, is currently one of the most extensively studied therapeutic approaches in cancer research [3,4]. Not much is known about the interaction between PHEO/PGL and a patient's immune system. Overall, PHEO/PGL can be considered as immunologically "cold" compared to other cancer types because of their lack of leukocyte fraction, low amount of neoantigens, and low somatic sequence mutation rate [5–7]. To date, only one experimental study proposed the use of immunotherapy in PHEO/PGL, specifically chromogranin A, as a potential treatment target [8]. In this study, immunization with chromogranin A peptides induced the production of cytotoxic T cells with subsequent elimination of chromogranin A expressing PHEO cells. Moreover, chromogranin A peptides were suggested as a potential anti-tumor vaccine in PHEO patients with risk of metastatic disease [8]. Recently, two clinical trials focusing on the application of checkpoint inhibitors (specifically nivolumab, ipilimumab, and pembrolizumab) in rare tumors, including PHEO/PGL, were initiated and are in the stage of patient recruitment (ClinicalTrials.gov Identifier: NCT02834013 and NCT02721732).

Current immunotherapeutic approaches to cancer treatment are based either on the activation of innate or more frequently adaptive immunity [9–11]. The innate immune system is well conserved, and its response is uniform, robust, and short-lasting, but it can well contribute to cancer treatment and the elimination of metastatic lesions [12–14]. Recently, immunotherapy based on the activation of innate immunity via pathogen-associated molecular patterns (PAMPs) has been tested in melanoma, which is also a neural crest tumor. Intratumoral application of PAMPs, particularly ligands stimulating phagocytosis and toll-like receptor (TLR) ligands, resulted in the complete elimination of over 80% of subcutaneous tumors in the B16-F10 melanoma mouse model [15–17].

Ligands stimulating phagocytosis initiate ingestion of pathogens by phagocytic immune cells [18,19]. PAMP-based immunotherapy uses intratumoral administration of mannan, a simple polysaccharide from *Saccharomyces cerevisiae,* as a ligand stimulating phagocytosis [16]. Mannan recognized by mannan-binding lectin (MBL) activates the complement lectin pathway [20]. This activation results in iC3b molecule production, followed by iC3b tumor cell opsonization [21,22], and consequently their elimination by phagocytes, particularly neutrophils, macrophages, and dendritic cells. In this type of immunotherapy, mannan is bound to a tumor cell membrane by the biocompatible anchor for a membrane called BAM (Figure 1).

TLRs are expressed on the surface of various cells, mainly those belonging to the innate immune system. These receptors recognize their specific ligands and initiate immune system mobilization [23–25]. This process is well supported by previous reports showing that the intratumoral application of TLR ligands increased the number of tumor-infiltrating leukocytes in melanoma and renal cell carcinoma mouse models [15–17,26]. Resiquimod (R-848), polyinosinic-polycytidylic acid (poly(I:C)), and lipoteichoic acid (LTA) are TLR ligands used in the present study. R-848 is an imidazoquinoline compound with anti-viral effects that activates immune cells via TLR7/TLR8 in humans and TLR7 in

mice [27]. Poly(I:C) is a synthetic analog of dsRNA that activates immune cells via TLR3 [28]. LTA is a constituent of the cell wall of Gram-positive bacteria that activates immune cells via TLR2 [29].
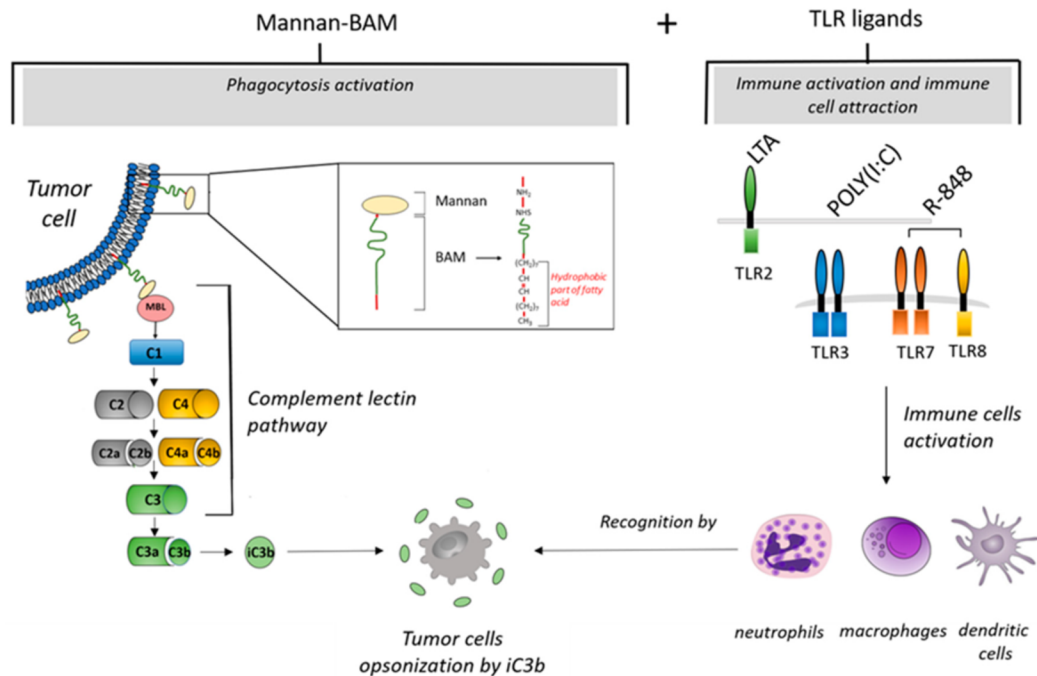
Figure 1. Mechanisms of tumor cell elimination during immunotherapy based on intratumoral application of mannan-BAM+TLR ligands (MBT). After intratumoral application of mannan with a biocompatible anchor for membrane-BAM, the hydrophobic part of BAM is incorporated into the lipid bilayer of tumor cells. Mannan attached to membranes activates innate immunity by the interaction of mannan with mannan binding lectin (MBL). This interaction initiates activation of the complement lectin pathway. This results in iC3b production and opsonization of tumor cells followed by migration of immune cells (macrophages, dendritic cells, or granulocytes) and phagocytosis activation. Further, simultaneous intratumoral application of TLR ligands (resiquimod (R-848), polyinosinic-polycytidylic acid (poly(I:C)), and lipoteichoic acid (LTA)) causes a strong attraction of immune cells (macrophages, dendritic cells, or granulocytes) to the tumor.

Thus, in the present study, we aimed to evaluate the therapeutic effects of intratumorally administered mannan-BAM and TLR ligands (MBT) in a subcutaneous and metastatic mouse PHEO. Specifically, we focused on the initial activation of innate immunity, an assessment of its role in the elimination of PHEO, and the detection of the potential role of subsequent engagement of adaptive immunity in elimination of distant metastatic PHEO organ lesions. This model was established using B6(Cg)-*Tyr^{c-2J}*/J mouse strains with subcutaneously and/or intravenously injected experimental PHEO cells called mouse tumor tissue (MTT)-luciferase cells [30,31]. Subsequently, the intratumoral application of MBT resulted in a significantly lower PHEO volume compared to the phosphate buffered saline (PBS)-treated group and in an improvement in mice survival. As neutrophils infiltrated the treated subcutaneous PHEOs, their role in this therapeutic model was established by measuring neutrophil cytotoxic activity and neutrophil-tumor cell interactions with MTT-luciferase and hPheo1 cell lines. An additional boost of MBT with anti-CD40 (this combination is henceforth referred to as MBTA) significantly improved the effect of the MBT application on the survival of experimental mice. Since re-challenge experiment suggested potential engagement of adaptive immunity, the therapy was tested in metastatic PHEO with a positive effect on the bioluminescence signal intensity of PHEO metastatic organ lesions compared to the PBS-treated group. Finally, the crucial role of CD8+ cells in

the inhibition of bioluminescence signal intensity of metastatic organ lesions was further supported by the antibody-dependent $CD4^+/CD8^+$ cell depletion experiment.

2. Results

2.1. A Syngeneic PHEO Mouse Model for Immunotherapy Evaluation

Since there is a very limited number of animal models for PHEO, we first decided to establish a PHEO mouse model that is appropriate for immunotherapy evaluation. Female B6(Cg)-Tyr^{c-2J}/J mice were subcutaneously injected with 3×10^6 MTT-luciferase cells in 0.2 mL of DMEM without additives in the right lower dorsal site or intravenously with 1.5×10^6 MTT-luciferase cells in 0.1 mL of PBS in a lateral tail vein. Subcutaneous PHEO tumors reached a mean volume of 118 mm^3 (range 8.5–407.2 mm^3) 45 days after tumor cell injection. Mice with intravenously injected tumor cells had detectable metastatic organ lesions 14 days after tumor cell transplantation. These metastatic organ lesions were located predominantly in the liver; small lesions were also detected in bones and lymph nodes (Figure 2A).
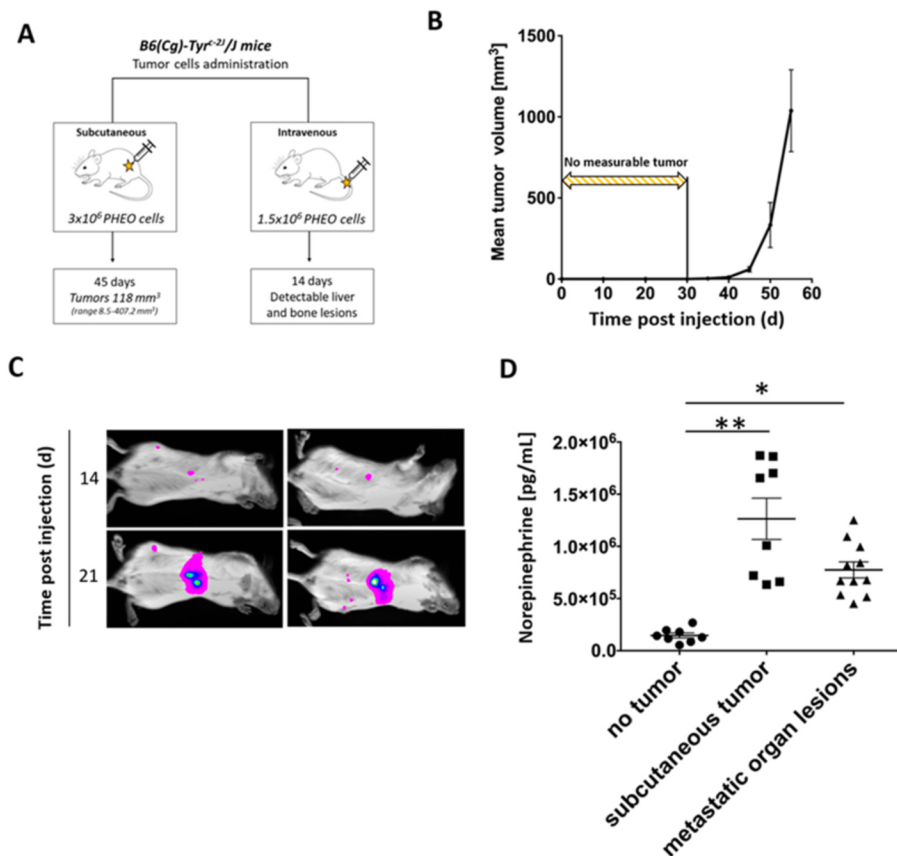
Figure 2. Subcutaneous and metastatic PHEO in mouse model suitable for immunotherapy testing established using MTT-luciferase cells. (**A**) B6(Cg)-Tyr^{c-2J}/J mice were subcutaneously ($n = 24$) or intravenously ($n = 10$) injected with MTT-luciferase cells. (**B**) Subcutaneous MTT-luciferase tumors reached a mean volume of 118 mm^3 45 days after tumor cell injection. No tumors were detected for 30 days after tumor cells injection. (**C**) Metastatic organ lesions were detectable 14 days after intravenous tumor cells injection using bioluminescence imaging. Metastatic organ lesions were predominantly located in the liver; small lesions were also detected in bones and lymph nodes. (**D**) Tumor-bearing mice, either with subcutaneous tumors or metastatic organ lesions, had significantly higher urine norepinephrine levels than those without tumors (* $p < 0.05$; ** $p < 0.01$ against no tumor).

Subcutaneous PHEO tumors were not measurable until 30 days after tumor cell injection. However, 40 days after tumor cell injection, the tumor volume increased significantly (Figure 2B). A diameter size of 2 cm was reached after 57 days (range 49–85 days) in most of the experimental mice. Subcutaneous tumors development was observed in 100% of mice. Metastatic organ lesions, after intravenous PHEO tumor cell injection, were detectable in 65% of mice 14 days after tumor cell injection using bioluminescence imaging. On the 21st day, 95% of mice had detectable metastatic liver lesions (Figure 2C).

To further characterize the established PHEO mouse model, urine catecholamine levels (norepinephrine, dopamine, and epinephrine) were measured in B6(Cg)-*Tyr*$^{c-2J}$/J tumor-bearing mice (subcutaneous tumor and metastatic organ lesions) after the injection of MTT-luciferase cells. Norepinephrine levels were significantly higher in tumor-bearing mice (subcutaneous tumor and metastatic organ lesions) compared to non-tumor-bearing mice (no tumor) (Figure 2D). Dopamine levels did not reveal any significant changes when comparing groups of tumor-bearing mice (subcutaneous tumor and metastatic organ lesions) to non-tumor-bearing mice (no tumor) (Figure S1A). Epinephrine levels were higher in mice with metastatic organ lesions compared to non-tumor-bearing mice (no tumor) and tumor-bearing mice (subcutaneous tumor) (Figure S1B).

2.2. MBT Immunotherapy Stabilize Tumor Volume and Improves Mice Survival

To evaluate the effect of MBT in PHEO, we applied MBT into subcutaneous PHEO tumors (on specific days as described in Materials and Methods). MBT application resulted in a significant stabilization of subcutaneous PHEO volume compared to the PBS-treated group (Figure 3A,B).
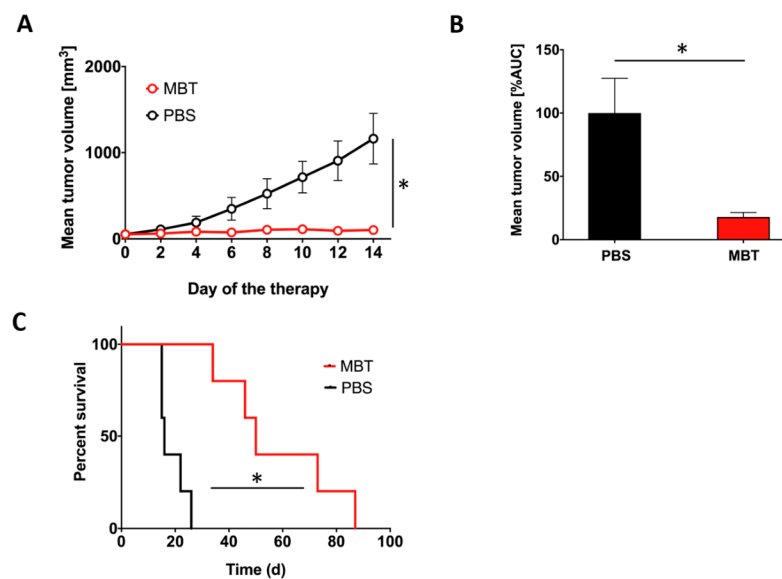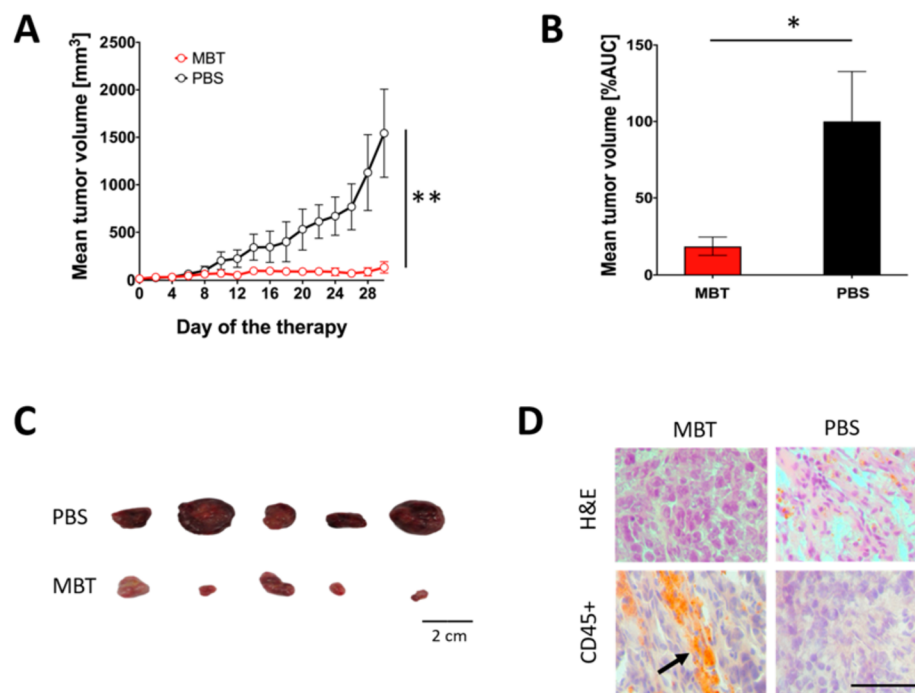

Figure 3. Intratumoral application of MBT in subcutaneous PHEO. B6(Cg)-*Tyr*$^{c-2J}$/J mice were subcutaneously injected with MTT-luciferase cells. After tumors grew to the desired size (about 100 mm^3), mice were randomized into two groups (*n* = 5/group): (i) the group treated with MBT; (ii) the group treated with PBS. MBT and PBS were given intratumorally on days 0, 1, 2, 8, 9, 10, 16, 17, 18, 24, 25, and 26. Tumor volume was measured with a caliper. (**A**) The tumor volume growth is presented as a growth curve (* *p* < 0.05 against PBS) and (**B**) as an area under the curve (AUC) (* *p* < 0.05 against PBS). (**C**) The survival analysis for the two groups are presented as a Kaplan–Meier curve (* *p* < 0.05 against PBS).

In addition, intratumoral application of MBT resulted in significantly longer survival of the treated mice. The median survival increased from 16 days (range 15–26 days) in the PBS-treated group to 50 days (range 34–87 days) in the MBT-treated group (Figure 3C).

2.3. Significant Participation of Innate Immunity in Subcutaneous PHEO Volume Stabilization

In the subsequent experiment, we used B6.CB17-*Prkdc^scid*/SzJ mice lacking functional T and B cells to verify the role of innate and adaptive immunity in the PHEO volume stabilization during MBT therapy. Subcutaneous PHEOs were treated intratumorally with MBT or PBS on specific days as described in Materials and Methods. Intratumoral application of MBT resulted in PHEO volume stabilization compared to the PBS-treated group (Figure 4A,B). Since we started this experiment with a lower tumor volume than in the previous experiment (about 50 mm^3), most of the experimental mice (five of six mice from both the MBT- and PBS-treated groups) survived during the whole course of the therapy (30 days). On the 30th day of therapy, mice from both groups were sacrificed, and subcutaneous tumors were harvested and then analyzed. The MBT-treated tumors were significantly smaller than the PBS-treated tumors (Figure 4C). Additional immunohistochemical analysis showed higher levels of tumor-infiltrating leukocytes (CD45$^+$ cells) in the MBT-treated group compared to the PBS-treated group (Figure 4D).

Figure 4. Significance of innate immunity in MBT immunotherapy in subcutaneous PHEO. B6.CB17-Prkdc^{scid}/SzJ mice were subcutaneously injected with MTT-luciferase cells. After tumors grew to the desired size (about 50 mm^3), mice were randomized into two groups ($n = 6$/group): (i) the group treated with MBT and (ii) the group treated with PBS. MBT and PBS were given intratumorally on days 0, 1, 2, 8, 9, 10, 16, 17, 18, 24, 25, and 26. Tumor volume was measured with a caliper. (**A**) The tumor volume growth is presented as a growth curve (** $p < 0.01$ against PBS) and (**B**) as an area under the curve (AUC) (* $p < 0.05$ against PBS). (**C**) Surviving mice were sacrificed on the 30th day of therapy (five mice from the MBT-treated group and five mice from the PBS-treated group), and tumors were documented. (**D**) Hematoxylin and eosin (H&E) staining and CD45$^+$ immunohistochemistry staining were performed on tumor cryosections (a thickness of 8 μm). Bar = 20 μm.

2.4. Characterization of Tumor-Infiltrating Leukocytes and Tumor Environment during MBT Immunotherapy

2.4.1. Flow Cytometry Analysis of Tumor-Infiltrating Leukocytes in the MBT-Treated Tumors

To identify immune cells infiltrating subcutaneous PHEO tumors during MBT therapy, we performed a flow cytometry analysis of tumor-infiltrating leukocytes. Since we limited the number of mice per group (n = 3/group), we decided to present tumor-infiltrating leukocytes data as individual values for each mouse, with a color legend based on the size of the analyzed tumors. The flow cytometry analysis of tumor-infiltrating leukocytes showed increased levels of CD45$^+$ cells in the MBT-treated group. This trend culminated on the 15th day of therapy (Figure 5A). T cells (CD3$^+$) were the most common leukocytes in the MBT-treated tumors (Figure 5A). The analysis of CD3$^+$ subpopulations revealed increased levels of Th cells (CD4$^+$) (Figure S2A) and Tc cells (CD8$^+$) (Figure S2B) in the MBT-treated group. Furthermore, a significant increase in granulocytes was observed on the 3rd and 19th days of therapy (Figure 5A). No significant changes were observed in B cells (CD19$^+$) (Figure S2C), monocytes/macrophages (F4/80$^+$) (Figure S2D), or natural killer (NK) cells (Figure S2E).

2.4.2. Histological Analysis of Tumor-Infiltrating Leukocytes in the MBT-Treated Tumors

To verify the flow cytometry results of tumor-infiltrating leukocytes, we performed hematoxylin and eosin (H&E) staining and immunohistochemistry staining on the same tumors, which were originally used for the flow cytometry analysis (Figure 5B). Tumors harvested on the 19th day of therapy are presented in Figure 5B as a representative example of infiltrating CD45$^+$ cells and their subpopulations. H&E staining showed extensive necrotic areas in tumor tissues in the MBT-treated group. In contrast, no or very small necrotic areas were detected in the PBS-treated group. CD45$^+$ immunostaining revealed higher levels of tumor-infiltrating leukocytes during the whole course of therapy in the MBT-treated group compared to the PBS-treated group (Figure 5B). CD45$^+$ cells were predominantly localized in necrotic areas of the tumor. Furthermore, CD3$^+$ immunohistochemistry staining revealed higher T cell infiltration in the MBT-treated group during the entire course of therapy compared to the PBS-treated group (Figure 5B). Ly6G/Ly6C immunostaining revealed increased infiltration of neutrophils on the 19th day of therapy in the MBT-treated group (Figure 5B).

2.4.3. Interferon Gamma (IFN-γ) and Interleukin 10 (IL-10) Levels Detection in the MBT-Treated Tumors

The high levels of IFN-γ (Figure 5C), low levels of IL-10 (Figure 5C), and high ratio of IFN-γ/IL-10 (Figure 5C) revealed a Th1 shift in the tumor microenvironment in the MBT-treated tumors.

2.5. In Vitro Analysis of Neutrophil Cytotoxic Effects toward PHEO Cells and Neutrophil-PHEO Cell Interactions Based on Labeling of Tumor Cells with Mannan-BAM

To verify the positive effect of mannan-BAM binding to PHEO cells on their recognition by innate immune cells, we measured (i) cytotoxic activity of neutrophils on PHEO cells with or without mannan-BAM and (ii) neutrophil-PHEO cell interactions. The cytotoxic experiments using PHEO cell lines (MTT-luciferase and hPheo1) revealed an increased cytotoxic effect of neutrophils toward PHEO cells labeled by mannan-BAM compared to the cells without mannan-BAM (Figure 6A,B). Microscopic evaluation of neutrophils and mannan-BAM-labeled PHEO cells showed enhanced frustrated phagocytosis and neutrophil rosette formation in the mannan-BAM group (Figure 6C).
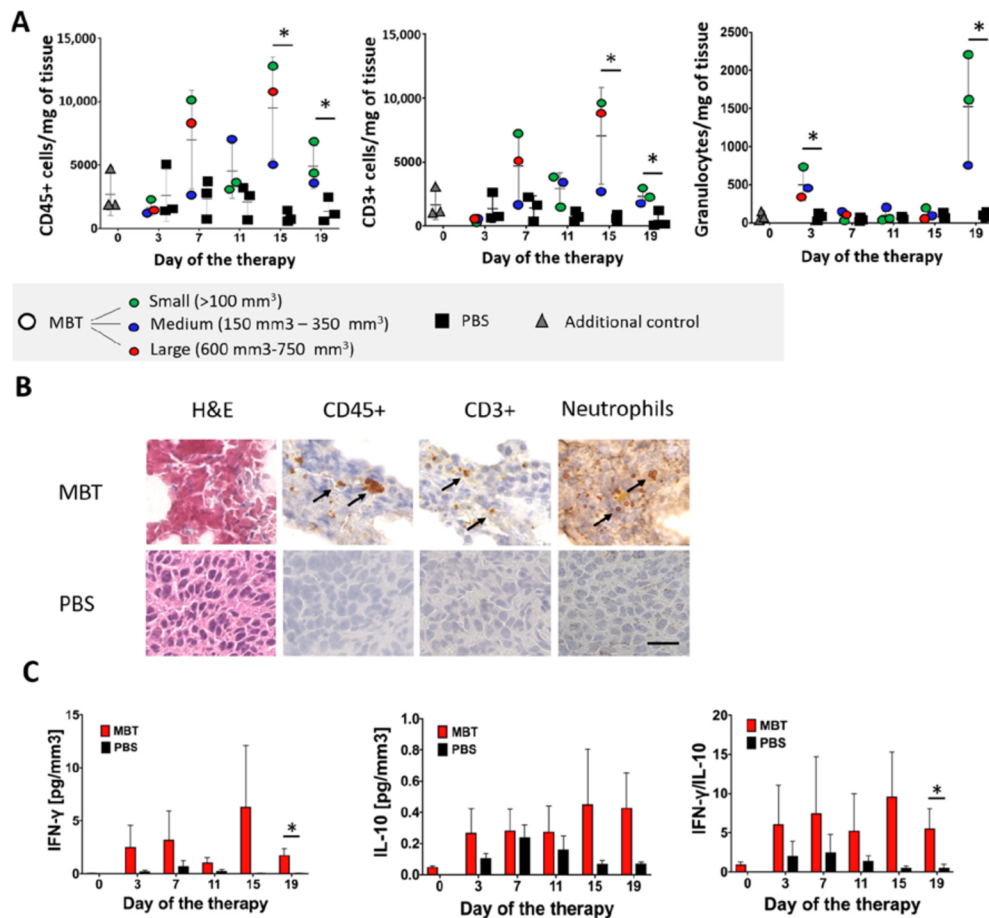
Figure 5. Flow cytometry and immunohistochemistry analysis of tumor-infiltrating leukocytes in the MBT-treated tumors. B6(Cg)-*Tyr*[c-2J]/J mice were subcutaneously injected with MTT-luciferase cells. After tumors grew to the desired size (about 100 mm^3), mice were randomized into two groups ($n = 24$/group): (i) the group treated with MBT and (ii) the group treated with PBS. MBT and PBS were given intratumorally on days 0, 1, 2, 8, 9, 10, 16, 17, 18, 24, 25, and 26. Three mice from both groups were sacrificed on days 3, 7, 11, 15, and 19. One half of the harvested subcutaneous tumors was used for flow cytometry analysis of tumor-infiltrating leukocytes and the second half was used for immunohistochemistry analysis of tumor-infiltrating leukocytes. Three mice were sacrificed on day 0 and used as an additional control—gray triangles (no application of any compounds into the tumor). (**A**) The analysis of tumor-infiltrating CD45$^+$ and CD3$^+$ cells revealed their elevation on the 15th and 19th days of therapy in the MBT-treated group. Granulocytes (Ly6G$^+$ cells) were elevated on the 3rd and 19th days of therapy in the MBT-treated group. The results are presented as individual values for each mouse, with a color legend based on the size of the analyzed tumors. (* $p < 0.05$ against PBS). (**B**) Hematoxylin and eosin (H&E) staining and CD45$^+$, CD3$^+$, and Ly6G/Ly6C immunohistochemistry staining were performed on tumor cryosections (a thickness of 8 μm). Bar = 20 μm. (**C**) IFN-γ levels, measured by ELISA from tumor supernatants collected during tumor-infiltrating leukocyte analysis revealed significantly higher levels in the MBT-treated group compared to the PBS-treated group. The IL-10 analysis revealed low levels in both the MBT-treated group and the PBS-treated group. The IFN-γ/IL-10 ratio was significantly higher in the MBT-treated group compared to the PBS-treated group (* $p < 0.05$ against PBS).
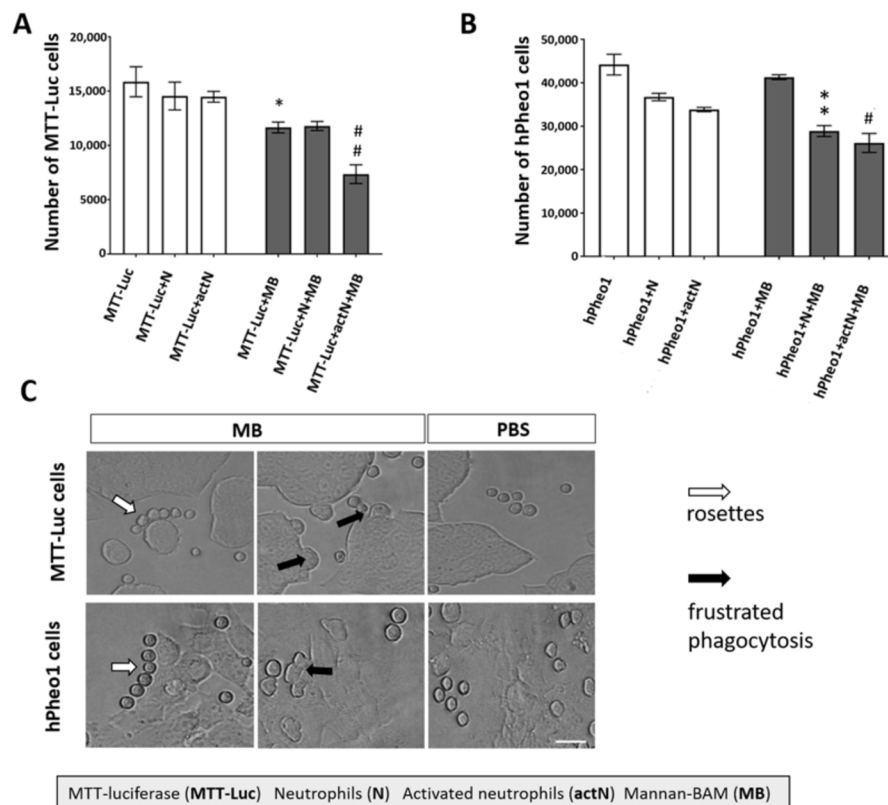
Figure 6. Neutrophil cytotoxicity against PHEO cells labeled with mannan-BAM and neutrophil-PHEO cell interactions. Mouse neutrophils (isolated from bone marrow of B6(Cg)-*Tyr*$^{c-2J}$/J non-tumor-bearing mice) and human neutrophils (isolated from whole blood of healthy donors) were activated by cytokines (granulocyte-macrophages colony-stimulatory factor (GM-CSF), tumor necrosis factor alpha (TNFα), and laminarin) and cultivated with MTT-luciferase and hPheo1 tumor cells with or without mannan-BAM attached to their surface. Mouse neutrophils were mixed with MTT-luciferase cells and human neutrophils were mixed with hPheo1 cells. After two hours of incubation, neutrophils were stained with anti-mouse or anti-human CD45 antibody. One microliter of DAPI was used for the staining of dead cells. Live tumor cells were measured using a BD FACSCanto II analyzer and evaluated using FlowJo software. (**A**) Analysis of mouse neutrophil cytotoxicity against MTT-luciferase cells revealed a statistically significant increase in neutrophil cytotoxicity toward MTT-luciferase cells with mannan-BAM attached to the tumor cell membrane (* $p < 0.05$ against MTT-luciferase (MTT-Luc) group, ## $p < 0.01$ against MTT-luciferase activated neutrophils group (MTT-Luc+actN)). (**B**) Analysis of human neutrophil cytotoxicity against hPheo1 cells revealed a statistically significant increase in neutrophil cytotoxicity toward hPheo1 cells with mannan-BAM attached to the tumor cell membrane (** $p < 0.01$ against hPheo1+neutrophils group (hPheo1+N), # $p < 0.05$ against hPheo1+activated neutrophils group (hPheo+actN)). (**C**) Frustrated phagocytosis (black arrows) and neutrophil rosettes (white arrows) were detected in the group with mannan-BAM attached to the tumor cell membrane. Bar = 100 μm.

2.6. Anti-CD40 Addition Improved Survival in the MBT-Treated Mice

In order to increase the therapeutic effect of MBT in the PHEO mouse model, we decided to combine MBT with an immunostimulatory monoclonal antibody: anti-CD40. Anti-CD40 is an agonist antibody binding to CD40 transmembrane protein expressed on a variety of cells such as macrophages, dendritic cells, and some tumor cells. The interaction of anti-CD40 with CD40 on the surface of immune cells supports their activation and enhances the immune response (Figure 7A).

Interestingly, the beneficial effect of anti-CD40 addition into the MBT therapeutic mixture was not evident during the first 14 days of the therapy (Figure 7B,C). However, the combination of MBT with anti-CD40 (MBTA), in the long term, increased mice survival when compared to the group treated only with MBT (Figure 7D). Moreover, five of eight mice from the MBTA-treated group manifested a complete elimination of subcutaneous tumor, compared to only two of eight mice from the MBT-treated group. A re-challenge experiment, performed with these mice manifested a complete elimination of tumors, revealed resistance against PHEO tumor cell re-injection in both groups, MBT and MBTA (Figure 7E). Interestingly, re-challenged mice initially developed small detectable tumors in the first 14 days; however, after that, all tumors were eradicated with the simultaneous development of skin lesions. These skin lesions were subsequently also eliminated and the whole re-challenged area healed completely.
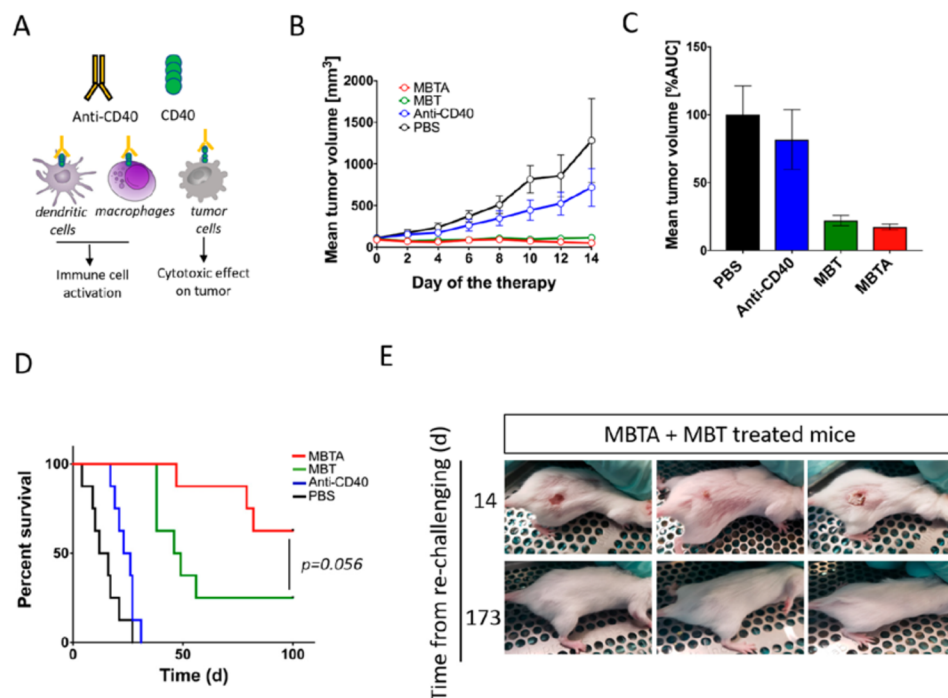

Figure 7. The effect of anti-CD40 addition into MBT therapeutic mixture and re-challenge experiment. B6(Cg)-*Tyr*$^{c-2J}$/J mice were subcutaneously injected with MTT-luciferase cells. After tumors grew to the desired size (about 100 mm^3), mice were randomized into four groups ($n = 8$/group): (i) the group treated with MBTA, (ii) the group treated with MBT, (iii) the group treated with anti-CD40, and (iv) the group treated with PBS. Therapy was given intratumorally on days 0, 1, 2, 8, 9, 10, 16, 17, 18, 24, 25, and 26. (**A**) Anti-CD40 is an agonist antibody binding to transmembrane protein CD40. CD40 is expressed on variety of cells, such as macrophages, dendritic cells, and some tumor cells. (**B**) The tumor volume growth is presented as a growth curve and (**C**) as an area under the curve (AUC). (**D**) The survival analysis is presented as a Kaplan–Meier curve ($p = 0.056$). (**E**) Mice with complete tumor elimination from the groups treated with MBTA ($n = 5$) and with MBT ($n = 2$) were re-challenged on day 120 (since the start of the therapy) by 3×10^6 MTT-luciferase cells. All animals rejected injected tumor cells.

2.7. MBTA Therapy in Metastatic PHEO

Our results from the re-challenge experiment suggested that MBTA therapy activate not only innate immunity but also adaptive immunity. Therefore, we decided to evaluate MBTA therapy in metastatic PHEO. Metastatic PHEO was established by prior subcutaneous injection of MTT cells into the right flank of experimental mice followed by intravenous injection of MTT-luciferase cells into the lateral tail vein (2 weeks after subcutaneous injection). These mice, which developed both

subcutaneous tumors as well as metastatic organ lesions (predominantly in the liver), were selected for the subsequent experiment (Figure 8A).
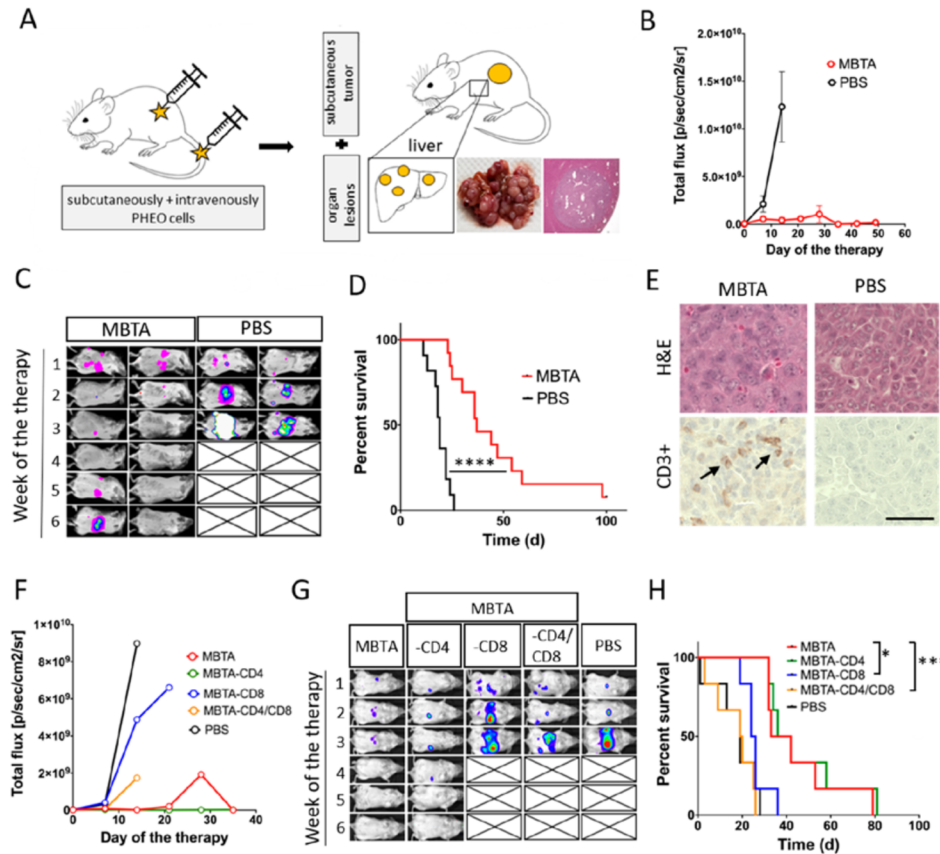
Figure 8. MBTA therapy in metastatic PHEO and the crucial role of CD8$^+$ T cells. (**A**) B6(Cg)-*Tyr*$^{c-2J}$/J mice were subcutaneously injected with MTT cells, with subsequent injection of MTT-luciferase cells into the lateral tail vein (2 weeks after subcutaneous injection). When mice developed subcutaneous tumors (around 250 mm^3) together with metastatic lesions (predominantly in the liver), they were randomized into two groups: (i) the group treated with MBTA ($n = 13$) and (ii) the group treated with PBS ($n = 12$). Therapy was given intratumorally on days 0, 1, 2, 8, 9, 10, 16, 17, 18, 24, 25, and 26. (**B,C**) An in vivo bioluminescence assay showed bioluminescence signal intensity inhibition of metastatic organ lesions in the MBTA-treated group compared to the PBS-treated group (p/sec/cm^2/sr = photons/second/cm^2/steradian). (**D**) The survival analysis is presented as a Kaplan–Meier curve (**** $p < 0.0001$ against PBS). (**E**) Immunohistochemistry analysis of CD3$^+$ cells in metastatic organ lesions in the MBTA- and the PBS-treated group revealed strong infiltration by CD3$^+$ cells in the MBTA-treated group. Bar = 20 μm. For the CD4$^+$ and CD8$^+$ T cell depletion experiment, mice with both subcutaneous PHEO tumor and metastatic organ lesions were randomized equally into five groups ($n = 6$/group): (a) the group treated with MBTA, (b) the group treated with MBTA with intraperitoneal application of anti-CD4, (c) the group treated with MBTA with intraperitoneal application of anti-CD8, (d) the group treated with MBTA with intraperitoneal application of anti-CD4 and anti-CD8, and (e) the group treated with PBS. (**F,G**) An in vivo bioluminescence assay showed the important role of CD8$^+$ cells in bioluminescence signal intensity inhibition of metastatic organ lesions during MBTA therapy. Part F is presented without SEM as a result of extensive overlap of SEM error bars. (**H**) The survival analysis is presented as a Kaplan–Meier curve (* $p < 0.05$, *** $p < 0.001$ against MBTA).

When MBTA therapy was tested in this metastatic PHEO (MBTA was applied intratumorally into subcutaneous tumors), we detected lower bioluminescence signal intensity of metastatic organ lesions

in the MBTA-treated group compared to the PBS-treated group (Figure 8B,C). In addition, the survival in the MBTA-treated group increased significantly (median survival: 37 days) compared to the PBS-treated group (median survival: 19 days, $p < 0.0001$). Moreover, one mouse from the MBTA-treated group survived for more than 100 days since the beginning of the therapy and manifested a complete regression of metastatic organ lesions (Figure 8D). Histologic sections of metastatic liver lesions showed stronger T cell (CD3$^+$) infiltration in the MBTA-treated group compared to the PBS-treated group (Figure 8E).

We further evaluated the role of T cells, specifically CD4$^+$ and CD8$^+$ T cells, in MBTA therapy. The CD4$^+$ and CD8$^+$ T cell depletion in metastatic PHEO revealed the importance of CD8$^+$ T cells in inhibition of bioluminescence signal intensity of metastatic organ lesions (Figure 8F,G). When CD8$^+$ T cells, alone or simultaneously with CD4+ T cells, were depleted in the MBTA-treated group, the bioluminescence signal intensity of metastatic organ lesions was comparable to the PBS-treated group (Figure 8F,G). The same effect was reflected in survival analysis where the depletion of CD8$^+$ T cells alone (MBTA-CD8) or with CD4$^+$ T cells (MBTA-CD4/CD8) significantly decreased the survival of treated mice (Figure 8H).

3. Discussion

In the present study, we showed that the application of mannan anchored to a tumor cell membrane via BAM along with TLR ligands (R-848, poly(I:C), LTA) (a combination referred as MBT) resulted in the stabilization of subcutaneous PHEO volume and significantly improved mice survival. The crucial role of initial activation of innate immunity during MBT therapy was further verified using B6.CB17-*Prkdc^{scid}*/SzJ mice lacking functional T and B cells. Similar to B6(Cg)-*Tyr^{c-2J}*/J mice, in B6.CB17-*Prkdc^{scid}*/SzJ mice, the subcutaneous PHEO volume remained stable in the MBT-treated group compared to the PBS-treated group. Flow cytometry analysis of tumor-infiltrating leukocytes and in vitro experiments in this model showed the potential role of granulocytes (specifically neutrophils) in innate immunity-induced PHEO elimination. An additional combination of MBT with agonistic anti-CD40 antibody (MBTA) resulted in increased mice survival and increased incidence of complete subcutaneous PHEO elimination. Interestingly, a re-challenge experiment in animals with the complete elimination of subcutaneous PHEO showed a generation of an excellent memory immune response with subsequent rejection of MTT-luciferase cells. To verify the activation of specific immunity (which was suggested by the observed immune memory response), we performed an experiment in a metastatic PHEO mouse model, where MBTA therapy resulted in lower bioluminescence signal intensity of metastatic organ lesions compared to the PBS-treated group. The subsequent CD4$^+$ and CD8$^+$ T cell depletion experiment confirmed the role of CD8$^+$ T cells in this bioluminescence signal intensity inhibition of metastatic organ lesions.

As a first step, we developed a mouse model of PHEO for immunotherapy testing with an option to inject PHEO tumor cells subcutaneously or intravenously. We used the B6(Cg)-*Tyr^{c-2J}*/J mouse strain injected with MTT or MTT-luciferase cells. MTT cells were originally developed from liver metastases arising from MPC cells injected intravenously [31]. Moreover, this PHEO mouse model is known to release catecholamines from experimental tumors resembling PHEOs found in patients. However, there are two main limitations arising from the practical use of this PHEO mouse model: (i) a long waiting period from tumor cell injection to tumor formation and (ii) very inconsistent tumor growth, which caused difficulties with the randomization of mice into the groups, resulting in lower numbers of mice per group.

After establishing a subcutaneous PHEO mouse model, we initiated the evaluation of MBT immunotherapy in PHEO. The MBT immunotherapy was previously tested in a melanoma mouse model and a very challenging pancreatic adenocarcinoma mouse model. Specifically, in the melanoma mouse model, MBT immunotherapy resulted in an 83% survival rate of treated mice with a potential anti-metastatic effect [17]. In pancreatic adenocarcinoma, MBT immunotherapy resulted in the suppression of metastases growth, but no increase in the survival rate of treated mice was detected [17].

In a PHEO mouse model, MBT therapy resulted in a subcutaneous PHEO volume stabilization compared to the PBS-treated group. The strategy of promoting an anti-tumor immune response using TLR ligands is well known and was previously successfully tested in many types of tumors [32–34]. However, our concept is unique, because of the specific combination of TLR ligands (particularly TLR2, TLR3, and TLR7/8), which seems to have an extraordinary effect on innate immunity activation and tumor elimination, as previously presented in melanoma and pancreatic adenocarcinoma mouse models [15–17]. Moreover, an additional anti-tumor effect of TLR ligands in this novel concept is provided by a combination with phagocytosis-stimulating ligands, such as mannan, bound to the tumor cell surface [15–17].

To further investigate the role of innate and adaptive immunity in the stabilization of subcutaneous PHEO volume during MBT immunotherapy, we used mice lacking functional T and B cells (B6.CB17-Prkdc^{scid}/SzJ mice) and, therefore, lacking basic adaptive immunity function. The stabilization of PHEO volume in mice lacking adaptive immunity treated with MBT was comparable to the stabilization of PHEO volume in a mouse model with a fully functional immune system. These results clearly suggest that innate immunity is crucial for stabilization of subcutaneous PHEO volume during MBT immunotherapy.

In order to characterize the underlying innate immunity mechanisms and tumor environment during MBT therapy in subcutaneous PHEO, we analyzed tumor-infiltrating leukocytes in the MBT- and the PBS-treated groups. In the MBT-treated group, we observed a higher level of tumor-infiltrating leukocytes compared to the PBS-treated group. Tumor-infiltrating leukocytes were mainly represented by T cells and granulocytes. As demonstrated in previous experiments with mice lacking functional T and B cells, T cells do not seem to have an important role in the initial elimination of subcutaneous PHEO, so we decided to further focus on the role of granulocytes in this model.

The high ratio of IFN-γ and IL-10 in the MBT-treated tumors indicates that the Th1 polarization of the tumor environment. In general, the tumor environment can be characterized by Th1 or Th2 polarization. Th2 polarization is considered to favor tumor growth (e.g., promoting angiogenesis, inhibiting cell-mediated immunity and tumor cell killing), whereas Th1 polarization exerts antitumor effects [35]. It was also described previously that PHEO/PGL tumors present high levels of M2 macrophage fractions, leading to Th2 polarization and the promotion of tumor angiogenesis [6]. TLRs are known to play crucial roles in immune response polarization. The activation of TLR3 and TLR7 triggers Th1 polarization in a tumor through increased IL-12, IL-23, and type I IFN production [36].

In vitro cytotoxicity experiments confirmed the importance of mannan-BAM bound to the PHEO cell membrane. The decision to use neutrophils, as the most abundant granulocytes, for these in vitro experiments was based on our tumor-infiltrating leukocyte analysis results as described previously. The increase in neutrophil cytotoxicity was dependent on the presence of mannan-BAM attached to the PHEO cells. Moreover, the presence of complement proteins in the tumor-neutrophils reaction environment (ensured by non-heat inactivated fetal bovine serum (FBS) addition) was crucial for the recognition of tumor cells with mannan-BAM and subsequent neutrophil cytotoxicity toward them.

Moreover, the participation of frustrated phagocytosis in PHEO cell elimination was fully dependent on the presence of mannan-BAM. The same findings were observed in the melanoma model when mannan-BAM was used [37].

From the aforementioned results, we concluded that MBT immunotherapy is effective for the stabilization of subcutaneous PHEO volume and for improvement in survival in mouse models with a robust initial activation of innate immunity. However, the biggest challenge in PHEO is metastatic disease. Therefore, in the next part of our study, we focused on how to simultaneously boost activation of adaptive immunity in MBT immunotherapy to achieve a systematic anti-tumor response with subsequent metastatic organ lesion elimination.

In the first step, we chose the anti-CD40 antibody to boost activation of adaptive immunity. The Anti-CD40 agonistic antibody supports the activation of antigen presenting cells, such as B and T cells, dendritic cells, and macrophages, and so establishes an effective humoral and cellular immune

response [38]. The combination of anti-CD40 with MBT applied in a pancreatic adenocarcinoma mouse model resulted in an 80% survival rate, which represented significant improvement compared to the MBT therapy without anti-CD40 [17]. In a PHEO mouse model, the combination of the anti-CD40 antibody with MBT increased the incidence of complete elimination of subcutaneous tumors and improved the overall survival of the treated mice. This effect can be explained by the support of tumor antigen presentation and the stronger participation of adaptive immunity via anti-CD40 [39]. A similar effect was previously reported, when the combination of TLR ligands with anti-CD40 significantly stimulated CD8$^+$ T cell responses and induced the migration of activated dendritic cells with a promotion in their capacity to present antigens [40,41]. The activation of adaptive immunity with the subsequent generation of a memory immune response was further verified by a re-challenge experiment in animals with a complete elimination of subcutaneous PHEO from the MBT- and MBTA-treated groups. All re-challenged mice rejected injected PHEO cells, which suggests that the MBT-treated mice also manifest partial activation of adaptive immunity. However, anti-CD40 beneficially boosted adaptive immunity, since 62.5% of mice in the MBTA-treated group completely eliminated subcutaneous PHEO compared to only 25% of mice in the MBT-treated group.

To further support our hypothesis of the adaptive immunity activation during MBTA immunotherapy, we tested MBTA immunotherapy in metastatic PHEO. MBTA immunotherapy resulted in a lower bioluminescence signal intensity of metastatic organ lesions compared to the PBS-treated group and in a significant prolongation of mice survival. Moreover, in this experiment, we observed an interesting phenomenon. Mice with fast initial elimination of subcutaneous tumors (complete elimination in the first week of MBTA therapy) manifested decreased bioluminescence signal intensity inhibition of metastatic organ lesions compared to those where subcutaneous tumors persisted during the first three weeks of MBTA therapy. This observation can be explained by insufficient activation of adaptive immunity caused by short-lasting tumor antigen stimulation since the main source of tumor antigens (the subcutaneous tumor) was eliminated very shortly after MBTA therapy initiation. This is also consistent with principles of tumor vaccines, where repeated applications of these vaccines are usually needed to develop a strong adaptive immune response [42,43]. Since we partially predicted this situation, we decided in advance to enroll mice with higher subcutaneous tumor volume (around 250 mm^3) compared to the previous experiments to provide enough tumor mass for tumor antigen release and adaptive immunity stimulation. The crucial role of T cells in the inhibition of bioluminescence signal intensity of metastatic organ lesions was further verified in the CD4$^+$ and CD8$^+$ T cell depletion experiment. The depletion of CD8$^+$ T cells, alone or both CD4$^+$ and CD8$^+$ T cells resulted in decreased survival and decreased bioluminescence signal intensity inhibition of metastatic organ lesions compared to the group treated by MTBA without depletion. These finding are consistent with several studies, where the importance of CD8$^+$ T cells on visceral disease was also highlighted [44,45].

Although the presented data may be important for future metastatic PHEO/PGL treatment, one important concern must be addressed. This therapy requires a direct application of MBT or MBTA into a tumor. Initially, this could be considered a limitation, particularly for metastatic PHEO/PGL, because metastases are exclusively found in deep organs, lymph nodes, or bones. However, current interventional radiology approaches are capable of treating metastases, even in those problematic locations [46]. Moreover, local therapy offers certain advantages over systemic therapies, such as a delivery of higher concentrations of the drug into the tumor, minimal systemic side effects, no required tumor antigen identification, in situ vaccination by tumor authentic antigens, no pretreatment biopsy, no major histocompatibility complex (MHC) restriction, polyclonal T and B cell stimulation, and low cost [4,47].

We also acknowledge that there are unanswered questions regarding the underlying immune mechanisms during the presented therapy. Therefore, our future directions involve a deeper understanding of adaptive immunity participation during MBTA therapy and its maximal boost for better control of metastatic organ lesion growth. Moreover, a possible combination of MBTA therapy

with other therapies will be considered. There may be great potential in the combination of MBTA with checkpoint inhibitors, as MBTA can support the initial infiltration of leukocytes into the tumor or metastatic organ lesions. This can be especially beneficial, since PHEO/PGL are tumors with a low lymphocyte fraction [6] and the prediction for checkpoint inhibitor therapy, as a single treatment, is thus not favorable [48–50]. Interestingly, certain subsets of PHEO/PGL tumors showed programed cell death 1 (PD-L1) and programed cell death 2 (PD-L2) expression [51]. In these specific PHEO/PGL subsets, the combination of MBTA with checkpoint inhibitor therapy can potentially intensify the therapeutic response. The doors are also open to a possible combination of MBTA therapy with radiotherapy and/or chemotherapy [52].

4. Materials and Methods

4.1. Mannan-BAM Synthesis

Mannan-BAM synthesis was performed as previously reported [15–17]. Mannan was obtained from Sigma-Aldrich, Saint Louis, MO, USA. BAM was obtained from NOF Corporation, White Plains, NY, USA.

4.2. Cell Lines

MTT, MTT-luciferase, and human hPheo1 cell lines were used in this study [30,31]. MTT and MTT-luciferase cells are rapidly growing cells derived from liver metastases of MPC cells, and MTT-luciferase cells are transfected by a luciferase plasmid [30,31]. hPheo1 (obtained from University of Texas, Southwestern Medical Center, Dr. Hans Kumar Ghayee, D.O., MTA# 41611) is a progenitor cell line derived from human PHEO [53].

MTT and MTT-luciferase cells were maintained in Dulbecco's modified eagle media (DMEM) (Sigma-Aldrich) supplemented with 10% heat-inactivated fetal bovine serum (Gemini, West Sacramento, CA, USA) and penicillin/streptomycin (100 U/mL; Gemini). In MTT-luciferase cells, geneticin (750 µg/mL; Thermo Fisher Scientific, Waltham, MA, USA) was used for stable cell line selection. hPheo1 cells were maintained in RPMI (Sigma-Aldrich) supplemented with 10% heat-inactivated fetal bovine serum and penicillin/streptomycin (100 U/mL). Both cell lines were cultured at 37 °C in humidified air with 5% CO_2.

All cell lines used were routinely tested for mycoplasma using the MycoAlert^{TM} detection kit (Lonza, Walkersville, MD, USA). Cell authentication was performed per ATCC guidelines using morphology, growth curves, and mycoplasma testing. After thawing, cells were cultured for no longer than 3 weeks.

4.3. Establishment of a PHEO Mouse Model and Tumor Cell Injection

Female B6(Cg)-*Tyr^{c-2J}*/J and B6.CB17-*Prkdc^{scid}*/SzJ mice were purchased from the Jackson Laboratory, Bar Harbor, ME, USA. B6(Cg)-*Tyr^{c-2J}*/J mice were used for subcutaneous and metastatic PHEO and represent mouse models with fully functional immune systems. B6.CB17-*Prkdc^{scid}*/SzJ mice lacking functional T and B cells were used for subcutaneous PHEO and represent mouse models with dysfunctional adaptive immunity. Mice were housed in specific pathogen-free conditions and all experiments were approved by the *Eunice Kennedy Shriver* National Institute of Child Health and Human Development animal protocol (ASP: 15 028).

For subcutaneous PHEO, B6(Cg)-*Tyr^{c-2J}*/J and B6.CB17-*Prkdc^{scid}*/SzJ mice were subcutaneously injected in the right lower dorsal site with 3×10^6 and 1.5×10^6 MTT-luciferase cells in 0.2 mL of DMEM without additives, respectively. For metastatic PHEO, B6(Cg)-*Tyr^{c-2J}*/J mice were also subcutaneously injected in the right lower dorsal site with 3×10^6 MTT cells in 0.2 mL of DMEM without additives and were simultaneously injected intravenously with 1.5×10^6 MTT-luciferase cells in 0.1 mL of PBS. MTT cells without luciferase where used for the establishment of subcutaneous PHEO to prevent the

possibility that the signal from MTT-luciferase cells in large subcutaneous tumors will cover the signal from small metastatic organ lesions during bioluminescence imaging.

For a re-challenge experiment, 3×10^6 MTT-luciferase cells in 0.2 mL of DMEM without additives were injected subcutaneously on day 120 since the beginning of therapy in the animals manifested a complete elimination of tumors due to used immunotherapy.

4.4. Treatment

Treatment in subcutaneous PHEO was initiated when subcutaneous tumors reached an average volume of 100 mm^3 in B6(Cg)-*Tyr^{c-2J}*/J mice. In B6.CB17-*Prkdc^{scid}*/SzJ mice, lacking functional T and B cells, the treatment was initiated with a lower tumor volume (average volume of 50 mm^3) to prevent the potential early reach of a tumor endpoint size as a result of the rapid growth of subcutaneous PHEO in mice with a specific immunity disfunction. Treatment in metastatic PHEO was initiated when subcutaneous tumors reached an average volume of 250 mm^3 with a simultaneous presence of detectable signal in organs using bioluminescence imaging. This greater starting tumor volume was purposely chosen to ensure enough tumor mass for tumor antigen gradual release during the whole course of the therapy. Mice, with both subcutaneous PHEO and metastatic PHEO, were treated intratumorally (into the subcutaneous tumor) on days 0, 1, 2, 8, 9, 10, 16, 17, 18, 24, 25, and 26 with 50 μL of the following mixtures: (a) 0.5 mg of R-848 hydrogen chloride (HCl) (Tocris, Minneapolis, MN, USA), 0.5 mg of poly(I:C) (Sigma-Aldrich), 0.5 mg of LTA/mL (Sigma-Aldrich), and 0.2 mM mannan-BAM (MBT), and later on in combination with anti-CD40, clone FGK4.5/FGK45 (BioXCell, West Lebanon, NH, USA) (MBTA), in PBS; and (b) PBS.

4.5. Tumor Size Evaluation

Subcutaneous tumor volume was measured every other day with a caliper and calculated as $V = (\pi/6) \ AB^2$ (A and B = the largest and the smallest dimension of the tumor, respectively) [54]. Survival curves are based on the time of death caused by tumor growth or on the time of sacrifice of mice reaching the maximally allowed tumor size of 2 cm in diameter.

In metastatic PHEO, mice were imaged by an IVIS system (Bruker, Billerica, MA, USA) once a week to detect a bioluminescence signal intensity of metastatic organ lesions, and the signal was evaluated using Bruker MI SE software.

4.6. Urine Catecholamine Determination

Urine specimens from B6(Cg)-*Tyr^{c-2J}*/J tumor-bearing mice were collected after subcutaneous or intravenous injection of MTT-luciferase cells. B6(Cg)-*Tyr^{c-2J}*/J mice without tumors were used as controls. All specimens were collected at the same time of the day to prevent any variance in catecholamine levels caused by circadian rhythms. Urine catecholamines (norepinephrine, epinephrine, and dopamine) were analyzed by liquid chromatography with electrochemical detection as described previously [55].

4.7. Analysis of Tumor Infiltrating Leukocytes and Spleen Leukocytes

B6(Cg)-*Tyr^{c-2J}*/J tumor-bearing mice were euthanized by cervical dislocation. Tumors were harvested from the body. Tumors were washed in cold DMEM and cut into small pieces. For tumor cell dissociation, a tumor dissociation kit (Miltenyi Biotech, Auburn, CA, USA) was used. One hour after incubation in 37 °C with constant agitation, samples were centrifuged. Supernatant was collected and used for the detection of cytokines (interferon gamma (IFN-γ) and interleukin 10 (IL-10)) by an enzyme-linked immunosorbent assay (ELISA). The tumor cell pellet was passed through a 70 μm strainer. The red blood cells were removed using ammonium-chloride-potassium (ACK) lysing buffer (Thermo Fisher Scientific). Leukocytes (CD45$^+$ cells) and their subpopulations were stained using the following antibodies: APC anti-mouse CD45, clone: 30-F11 (BioLegend, Dedham, MA, USA); Brilliant Violet 650 anti-mouse CD19, clone: 6D5 (BioLegend); FITC anti-mouse CD3, clone: 17A2

(BioLegend); Brilliant Violet 605 anti-mouse CD4, clone: RM4-5 (BioLegend); APC/Cy7 anti-mouse CD8a, clone: 53-6.7 (BioLegend); PE/Cy7 anti-mouse Ly-6G/Ly-6C (GR-1), clone: RB6-8C5 (BioLegend); PE anti-mouse NK-1.1, clone: PK136 (BioLegend); and Brilliant Violet 421 anti-mouse F4/80, clone: BM8 (BioLegend). LIVE/DEAD® fixable yellow dead cell stain (Invitrogen, Carlsbad, CA, USA) was used to eliminate dead cells. Samples were measured using a BD Fortessa analyzer (San Jose, CA, USA) and evaluated with FlowJo software (Ashland, OR, USA). CountBright absolute counting beads (Invitrogen) were used to count absolute numbers of individual CD45+ cells.

4.8. Cytokine Assay

Supernatant collected during the analysis of tumor infiltrating leukocytes was used to measure INF-γ and IL-10 levels in the tumors during the therapy. The following ELISA kits were used for the detection: IFN-γ Mouse ELISA Kit, Extra Sensitive (Thermo Fisher), and Mouse IL-10 ELISA Kit (LSBio, Seattle, WA, USA).

4.9. Immunohistochemistry

Tumor tissue samples embedded in Tissue-Tek optimum cutting temperature (OCT) were sectioned by a microtome-cryostat (8 μm). Formalin fixed, paraffin-embedded tissue specimen was prepared for 5 μm sections. Frozen sections were fixed in HistoChoice MB tissue Fixative solution (Ambresco, Cleveland, OH, USA). Subsequently in both frozen and paraffin-embedded sections, peroxidase activity was inhibited by 3% hydrogen peroxide. Additionally, samples were blocked using SuperBlock blocking buffer (Thermo Fisher Scientific). Anti-mouse CD45 antibody, anti-mouse Ly6G/Ly6C antibody, and anti-mouse CD3 antibody (Abcam, Cambridge, MA, USA) were used for immunohistochemistry staining. The signal was developed by diaminobenzidine (DAB) substrate (Dako, Santa Clara, CA, USA).

4.10. Neutrophil Cytotoxicity toward PHEO Cells

Bone marrow from B6(Cg)-*Tyr*^{c-2J}/J non-tumor-bearing mice was used as a source of mouse neutrophils. Bone marrow isolation was performed according to Stassen et al. [56]. Untouched mouse neutrophils were isolated by magnetic-activated cell sorting using a neutrophil isolation kit (Miltenyi Biotec). Human neutrophils were isolated from whole blood of healthy donors received from the National Institutes of Health (NIH) Blood Bank using an EasySep Direct Human Neutrophils Isolation kit (Stemcell Technologies, Cambridge, MA, USA). Both human and mouse neutrophils were activated for 20 min by a mixture of GM-CSF (12 ng/mL) (Sigma-Aldrich), TNFα (2.5 ng/mL) (Sigma-Aldrich), and 2 μM laminarin (Sigma) as previously described [57].

MTT-luciferase or hPheo1 cells were incubated with 0.02 mM mannan-BAM in culture medium for 30 min in 37 °C. After incubation and washing by centrifugation, mouse MTT-luciferase cells were co-cultured with activated or non-activated murine neutrophils and human hPheo1 cells with activated or non-inactivated human neutrophils for 2 h in 37 °C. The tumor cell/neutrophil ratio was 1:5 (50,000 tumor cells to 250,000 neutrophils). Dead cells were stained with DAPI (1 μM) (Invitrogen). APC anti-mouse CD45 antibody, clone 30-F11 (BioLegend), and APC anti-human CD45 antibody, clone H130 (BioLegend), were used to stain leukocytes (in this specific case neutrophils). CountBright absolute counting beads (Invitrogen) were used to count absolute numbers of live tumor cells in the samples. Samples were measured by FACSCantoII. FlowJo software was used for analysis.

4.11. Imaging of PHEO Cell–Neutrophil Interactions

Adhered hPheo1 or MTT-luciferase cells were incubated with 0.02 mM mannan-BAM in culture medium for 30 min in 37 °C. Following incubation, unbound mannan-BAM was washed by centrifugation and human neutrophils were added to the hPheo1 cells and mouse neutrophils to the MTT-luciferase cells (the ratio of tumor cells to neutrophils was 1:2 (50,000 tumor cells:100,000

neutrophils). Neutrophils and hPheo1/MTT-luciferase cell interactions were documented after 2 h of co-culturing in 37 °C. A Leica DMRB microscope and Leica LAS AF software were used for analysis.

4.12. Depletions

Cellular subsets were depleted by administering 300 μg of depleting antibody intraperitoneally twice weekly starting one day prior to immunotherapy: CD8$^+$ T-cells with anti-CD8α, clone 2.43 (BioXCell), and CD4$^+$ T-cells with anti-CD4, clone GK1.5 (BioXCell). Cellular depletion of CD8$^+$ and CD4$^+$ T-cells were confirmed by flow cytometry of PBMC blood levels (Figure S3). Samples were measured by FACSCantoII. FlowJo software was used for analysis.

4.13. Statistical Analysis

Data were analyzed using STATISTICA 12 (StatSoft, Tulsa, OK, USA) or Prism 7 (GraphPad Software, San Diego, CA, USA). Individual data sets were compared using a dependent/independent Student's *t*-test. Analyses across multiple groups and times were performed using repeated measures ANOVA (for data with normal distribution) with individual groups assessed using Tukey's multiple comparison. For data without normal distribution, non-parametric ANOVA was used with individual groups were assessed by Kruskal–Wallis test. Kaplan–Meier survival curves were compared using a log-rank test. Error bars indicate the standard error of the mean (SEM). $^* p < 0.05$; $^{**} p < 0.01$; $^{***} p < 0.001$; $^{****} p < 0.0001$. $^\# p < 0.05$; $^{\#\#} p < 0.01$.

5. Conclusions

We demonstrate here promising therapeutic effects of enhanced innate immunity with subsequent activation of adaptive immunity using intratumoral application of ligands stimulating phagocytosis combined with TLR ligands in subcutaneous and metastatic PHEO in mouse models. This effect was verified in vitro in mouse PHEO and human PHEO cell lines. We suggest that this immunotherapeutic approach could potentially become a novel treatment option in patients with metastatic PHEO/PGL.

References

1. Lenders, J.W.; Eisenhofer, G.; Mannelli, M.; Pacak, K. Phaeochromocytoma. *Lancet* **2005**, *366*, 665–675. [CrossRef]
2. Crona, J.; Taieb, D.; Pacak, K. New Perspectives on Pheochromocytoma and Paraganglioma: Toward a Molecular Classification. *Endocr. Rev.* **2017**, *38*, 489–515. [CrossRef]

3. Mellman, I.; Coukos, G.; Dranoff, G. Cancer immunotherapy comes of age. *Nature* **2011**, *480*, 480–489. [CrossRef]

4. Marabelle, A.; Tselikas, L.; de Baere, T.; Houot, R. Intratumoral immunotherapy: Using the tumor as the remedy. *Ann. Oncol.* **2017**, *28*, xii33–xii43. [CrossRef] [PubMed]

5. Fishbein, L.; Leshchiner, I.; Walter, V.; Danilova, L.; Robertson, A.G.; Johnson, A.R.; Lichtenberg, T.M.; Murray, B.A.; Ghayee, H.K.; Else, T.; et al. Comprehensive Molecular Characterization of Pheochromocytoma and Paraganglioma. *Cancer Cell* **2017**, *31*, 181–193. [CrossRef] [PubMed]

6. Thorsson, V.; Gibbs, D.L.; Brown, S.D.; Wolf, D.; Bortone, D.S.; Ou Yang, T.H.; Porta-Pardo, E.; Gao, G.F.; Plaisier, C.L.; Eddy, J.A.; et al. The Immune Landscape of Cancer. *Immunity* **2018**, *48*, 812–830. [CrossRef]

7. Wood, M.A.; Paralkar, M.; Paralkar, M.P.; Nguyen, A.; Struck, A.J.; Ellrott, K.; Margolin, A.; Nellore, A.; Thompson, R.F. Population-level distribution and putative immunogenicity of cancer neoepitopes. *BMC Cancer* **2018**, *18*, 414. [CrossRef] [PubMed]

8. Papewalis, C.; Kouatchoua, C.; Ehlers, M.; Jacobs, B.; Porwol, D.; Schinner, S.; Willenberg, H.S.; Anlauf, M.; Raffel, A.; Eisenhofer, G.; et al. Chromogranin A as potential target for immunotherapy of malignant pheochromocytoma. *Mol. Cell. Endocrinol.* **2011**, *335*, 69–77. [CrossRef]

9. Gubin, M.M.; Zhang, X.; Schuster, H.; Caron, E.; Ward, J.P.; Noguchi, T.; Ivanova, Y.; Hundal, J.; Arthur, C.D.; Krebber, W.J.; et al. Checkpoint blockade cancer immunotherapy targets tumour-specific mutant antigens. *Nature* **2014**, *515*, 577–581. [CrossRef]

10. Rosenberg, S.A.; Restifo, N.P. Adoptive cell transfer as personalized immunotherapy for human cancer. *Science* **2015**, *348*, 62–68. [CrossRef]

11. Corrales, L.; Matson, V.; Flood, B.; Spranger, S.; Gajewski, T.F. Innate immune signaling and regulation in cancer immunotherapy. *Cell Res.* **2017**, *27*, 96–108. [CrossRef] [PubMed]

12. Coley, W.B. The treatment of malignant tumors by repeated inoculations of erysipelas. With a report of ten original cases. 1893. *Clin. Orthop. Relat. Res.* **1991**, 3–11.

13. Akira, S.; Uematsu, S.; Takeuchi, O. Pathogen recognition and innate immunity. *Cell* **2006**, *124*, 783–801. [CrossRef]

14. Herr, H.W.; Morales, A. History of bacillus Calmette-Guerin and bladder cancer: An immunotherapy success story. *J. Urol.* **2008**, *179*, 53–56. [CrossRef]

15. Janotova, T.; Jalovecka, M.; Auerova, M.; Svecova, I.; Bruzlova, P.; Maierova, V.; Kumzakova, Z.; Cunatova, S.; Vlckova, Z.; Caisova, V.; et al. The use of anchored agonists of phagocytic receptors for cancer immunotherapy: B16-F10 murine melanoma model. *PLoS ONE* **2014**, *9*, e85222. [CrossRef]

16. Caisova, V.; Vieru, A.; Kumzakova, Z.; Glaserova, S.; Husnikova, H.; Vacova, N.; Krejcova, G.; Padoukova, L.; Jochmanova, I.; Wolf, K.I.; et al. Innate immunity based cancer immunotherapy: B16-F10 murine melanoma model. *BMC Cancer* **2016**, *16*, 940. [CrossRef]

17. Caisova, V.; Uher, O.; Nedbalova, P.; Jochmanova, I.; Kvardova, K.; Masakova, K.; Krejcova, G.; Padoukova, L.; Chmelar, J.; Kopecky, J.; et al. Effective cancer immunotherapy based on combination of TLR agonists with stimulation of phagocytosis. *Int. Immunopharmacol.* **2018**, *59*, 86–96. [CrossRef]

18. Stahl, P.D.; Ezekowitz, R.A. The mannose receptor is a pattern recognition receptor involved in host defense. *Curr. Opin. Immunol.* **1998**, *10*, 50–55. [CrossRef]

19. Freeman, S.A.; Grinstein, S. Phagocytosis: Receptors, signal integration, and the cytoskeleton. *Immunol. Rev.* **2014**, *262*, 193–215. [CrossRef]

20. Garred, P.; Genster, N.; Pilely, K.; Bayarri-Olmos, R.; Rosbjerg, A.; Ma, Y.J.; Skjoedt, M.O. A journey through the lectin pathway of complement-MBL and beyond. *Immunol. Rev.* **2016**, *274*, 74–97. [CrossRef]

21. Fujita, T.; Matsushita, M.; Endo, Y. The lectin-complement pathway-its role in innate immunity and evolution. *Immunol. Rev.* **2004**, *198*, 185–202. [CrossRef] [PubMed]

22. Reis, E.S.; Mastellos, D.C.; Ricklin, D.; Mantovani, A.; Lambris, J.D. Complement in cancer: Untangling an intricate relationship. *Nat. Rev. Immunol.* **2018**, *18*, 5–18. [CrossRef] [PubMed]

23. Medzhitov, R. Toll-like receptors and innate immunity. *Nat. Rev. Immunol.* **2001**, *1*, 135–145. [CrossRef] [PubMed]

24. Takeda, K.; Akira, S. Toll-like receptors in innate immunity. *Int. Immunol.* **2005**, *17*, 1–14. [CrossRef] [PubMed]

25. Kawasaki, T.; Kawai, T. Toll-like receptor signaling pathways. *Front. Immunol.* **2014**, *5*, 461. [CrossRef] [PubMed]

26. Kauffman, E.C.; Liu, H.; Schwartz, M.J.; Scherr, D.S. Toll-like receptor 7 agonist therapy with imidazoquinoline enhances cancer cell death and increases lymphocytic infiltration and proinflammatory cytokine production in established tumors of a renal cell carcinoma mouse model. *J. Oncol.* **2012**, *2012*, 103298. [CrossRef] [PubMed]

27. Wu, J.J.; Huang, D.B.; Tyring, S.K. Resiquimod: A new immune response modifier with potential as a vaccine adjuvant for Th1 immune responses. *Antiviral. Res.* **2004**, *64*, 79–83. [CrossRef]

28. Matsumoto, M.; Seya, T. TLR3: Interferon induction by double-stranded RNA including poly(I:C). *Adv. Drug Deliv. Rev.* **2008**, *60*, 805–812. [CrossRef]

29. Seo, H.S.; Michalek, S.M.; Nahm, M.H. Lipoteichoic acid is important in innate immune responses to gram-positive bacteria. *Infect. Immun.* **2008**, *76*, 206–213. [CrossRef]

30. Martiniova, L.; Lai, E.W.; Elkahloun, A.G.; Abu-Asab, M.; Wickremasinghe, A.; Solis, D.C.; Perera, S.M.; Huynh, T.T.; Lubensky, I.A.; Tischler, A.S.; et al. Characterization of an animal model of aggressive metastatic pheochromocytoma linked to a specific gene signature. *Clin. Exp. Metastasis* **2009**, *26*, 239–250. [CrossRef]

31. Korpershoek, E.; Pacak, K.; Martiniova, L. Murine models and cell lines for the investigation of pheochromocytoma: Applications for future therapies? *Endocr. Pathol.* **2012**, *23*, 43–54. [CrossRef] [PubMed]

32. Cai, Z.; Sanchez, A.; Shi, Z.; Zhang, T.; Liu, M.; Zhang, D. Activation of Toll-like receptor 5 on breast cancer cells by flagellin suppresses cell proliferation and tumor growth. *Cancer Res.* **2011**, *71*, 2466–2475. [CrossRef] [PubMed]

33. Liu, C.Y.; Xu, J.Y.; Shi, X.Y.; Huang, W.; Ruan, T.Y.; Xie, P.; Ding, J.L. M2-polarized tumor-associated macrophages promoted epithelial-mesenchymal transition in pancreatic cancer cells, partially through TLR4/IL-10 signaling pathway. *Lab. Invest.* **2013**, *93*, 844–854. [CrossRef] [PubMed]

34. Sagiv-Barfi, I.; Czerwinski, D.K.; Levy, S.; Alam, I.S.; Mayer, A.T.; Gambhir, S.S.; Levy, R. Eradication of spontaneous malignancy by local immunotherapy. *Sci. Transl. Med.* **2018**, 10. [CrossRef]

35. Johansson, M.; Denardo, D.G.; Coussens, L.M. Polarized immune responses differentially regulate cancer development. *Immunol Rev.* **2008**, *222*, 145–154. [CrossRef] [PubMed]

36. Napolitani, G.; Rinaldi, A.; Bertoni, F.; Sallusto, F.; Lanzavecchia, A. Selected Toll-like receptor agonist combinations synergistically trigger a T helper type 1-polarizing program in dendritic cells. *Nat. Immunol.* **2005**, *6*, 769–776. [CrossRef]

37. Waldmannova, E.; Caisova, V.; Faberova, J.; Svackova, P.; Kovarova, M.; Svackova, D.; Kumzakova, Z.; Jackova, A.; Vacova, N.; Nedbalova, P.; et al. The use of Zymosan A and bacteria anchored to tumor cells for effective cancer immunotherapy: B16-F10 murine melanoma model. *Int. Immunopharmacol.* **2016**, *39*, 295–306. [CrossRef]

38. Vonderheide, R.H.; Glennie, M.J. Agonistic CD40 antibodies and cancer therapy. *Clin. Cancer Res.* **2013**, *19*, 1035–1043. [CrossRef]

39. Elgueta, R.; Benson, M.J.; de Vries, V.C.; Wasiuk, A.; Guo, Y.; Noelle, R.J. Molecular mechanism and function of CD40/CD40L engagement in the immune system. *Immunol. Rev.* **2009**, *229*, 152–172. [CrossRef]

40. Ahonen, C.L.; Doxsee, C.L.; McGurran, S.M.; Riter, T.R.; Wade, W.F.; Barth, R.J.; Vasilakos, J.P.; Noelle, R.J.; Kedl, R.M. Combined TLR and CD40 triggering induces potent CD8+ T cell expansion with variable dependence on type I IFN. *J. Exp. Med.* **2004**, *199*, 775–784. [CrossRef]

41. Scarlett, U.K.; Cubillos-Ruiz, J.R.; Nesbeth, Y.C.; Martinez, D.G.; Engle, X.; Gewirtz, A.T.; Ahonen, C.L.; Conejo-Garcia, J.R. In situ stimulation of CD40 and Toll-like receptor 3 transforms ovarian cancer-infiltrating dendritic cells from immunosuppressive to immunostimulatory cells. *Cancer Res.* **2009**, *69*, 7329–7337. [CrossRef]

42. Lutz, E.; Yeo, C.J.; Lillemoe, K.D.; Biedrzycki, B.; Kobrin, B.; Herman, J.; Sugar, E.; Piantadosi, S.; Cameron, J.L.; Solt, S.; et al. A lethally irradiated allogeneic granulocyte-macrophage colony stimulating factor-secreting tumor vaccine for pancreatic adenocarcinoma. A Phase II trial of safety, efficacy, and immune activation. *Ann. Surg.* **2011**, *253*, 328–335.

43. Srivatsan, S.; Patel, J.M.; Bozeman, E.N.; Imasuen, I.E.; He, S.; Daniels, D.; Selvaraj, P. Allogeneic tumor cell vaccines: The promise and limitations in clinical trials. *Hum. Vaccin. Immunother.* **2014**, *10*, 52–63. [CrossRef]

44. Yu, P.; Lee, Y.; Wang, Y.; Liu, X.; Auh, S.; Gajewski, T.F.; Schreiber, H.; You, Z.; Kaynor, C.; Wang, X.; et al. Targeting the primary tumor to generate CTL for the effective eradication of spontaneous metastases. *J. Immunol.* **2007**, *179*, 1960–1968. [CrossRef]

45. Lengagne, R.; Graff-Dubois, S.; Garcette, M.; Renia, L.; Kato, M.; Guillet, J.G.; Engelhard, V.H.; Avril, M.F.; Abastado, J.P.; Prevost-Blondel, A. Distinct role for CD8 T cells toward cutaneous tumors and visceral metastases. *J. Immunol.* **2008**, *180*, 130–137. [CrossRef] [PubMed]

46. Lubner, M.G.; Brace, C.L.; Hinshaw, J.L.; Lee, F.T., Jr. Microwave tumor ablation: Mechanism of action, clinical results, and devices. *J. Vasc. Interv. Radiol.* **2010**, *21*, S192–S203. [CrossRef] [PubMed]

47. Brody, J.D.; Ai, W.Z.; Czerwinski, D.K.; Torchia, J.A.; Levy, M.; Advani, R.H.; Kim, Y.H.; Hoppe, R.T.; Knox, S.J.; Shin, L.K.; et al. In situ vaccination with a TLR9 agonist induces systemic lymphoma regression: A phase I/II study. *J. Clin. Oncol.* **2010**, *28*, 4324–4332. [CrossRef]

48. Maleki Vareki, S. High and low mutational burden tumors versus immunologically hot and cold tumors and response to immune checkpoint inhibitors. *J. Immunother. Cancer* **2018**, *6*, 157. [CrossRef]

49. Gujar, S.; Pol, J.G.; Kroemer, G. Heating it up: Oncolytic viruses make tumors 'hot' and suitable for checkpoint blockade immunotherapies. *Oncoimmunology* **2018**, *7*, e1442169. [CrossRef]

50. Vonderheide, R.H. The Immune Revolution: A Case for Priming, Not Checkpoint. *Cancer Cell* **2018**, *33*, 563–569. [CrossRef]

51. Pinato, D.J.; Black, J.R.; Trousil, S.; Dina, R.E.; Trivedi, P.; Mauri, F.A.; Sharma, R. Programmed cell death ligands expression in phaeochromocytomas and paragangliomas: Relationship with the hypoxic response, immune evasion and malignant behavior. *Oncoimmunology* **2017**, *6*, e1358332. [CrossRef] [PubMed]

52. Dwary, A.D.; Master, S.; Patel, A.; Cole, C.; Mansour, R.; Mills, G.; Koshy, N.; Peddi, P.; Burton, G.; Hammoud, D.; et al. Excellent response to chemotherapy post immunotherapy. *Oncotarget* **2017**, *8*, 91795–91802. [CrossRef] [PubMed]

53. Ghayee, H.K.; Bhagwandin, V.J.; Stastny, V.; Click, A.; Ding, L.H.; Mizrachi, D.; Zou, Y.S.; Chari, R.; Lam, W.L.; Bachoo, R.M.; et al. Progenitor cell line (hPheo1) derived from a human pheochromocytoma tumor. *PLoS ONE* **2013**, *8*, e65624. [CrossRef]

54. Li, J.; Piao, Y.F.; Jiang, Z.; Chen, L.; Sun, H.B. Silencing of signal transducer and activator of transcription 3 expression by RNA interference suppresses growth of human hepatocellular carcinoma in tumor-bearing nude mice. *World J. Gastroenterol.* **2009**, *15*, 2602–2608. [CrossRef] [PubMed]

55. Eisenhofer, G.; Goldstein, D.S.; Stull, R.; Keiser, H.R.; Sunderland, T.; Murphy, D.L.; Kopin, I.J. Simultaneous liquid-chromatographic determination of 3,4-dihydroxyphenylglycol, catecholamines, and 3,4-dihydroxyphenylalanine in plasma, and their responses to inhibition of monoamine oxidase. *Clin. Chem.* **1986**, *32*, 2030–2033.

56. Stassen, M.; Valeva, A.; Walev, I.; Schmitt, E. Activation of mast cells by streptolysin O and lipopolysaccharide. *Methods Mol. Biol.* **2006**, *315*, 393–403.

57. Dewas, C.; Dang, P.M.; Gougerot-Pocidalo, M.A.; El-Benna, J. TNF-alpha induces phosphorylation of p47(phox) in human neutrophils: Partial phosphorylation of p47phox is a common event of priming of human neutrophils by TNF-alpha and granulocyte-macrophage colony-stimulating factor. *J. Immunol.* **2003**, *171*, 4392–4398. [CrossRef] [PubMed]
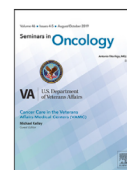
Chapter III

Coley's Immunotherapy Revived: Innate Immunity as a Link in Priming Cancer Cells for an Attack by Adaptive Immunity

Coley's immunotherapy revived: Innate immunity as a link in priming cancer cells for an attack by adaptive immunity

Ondrej Uher[a,b,1], Veronika Caisova[a,1], Per Hansen[c], Jan Kopecky[b], Jindrich Chmelar[b], Zhengping Zhuang[d], Jan Zenka[b], Karel Pacak[a,*]

[a] Section on Medical Neuroendocrinology, Eunice Kennedy Shriver National Institute of Child Health and Human Development, National Institutes of Health, Bethesda, Maryland, MD 20814, USA
[b] Department of Medical Biology, Faculty of Science, University of South Bohemia, Ceske Budejovice 37005, Czech Republic
[c] Immunoaction LLC, Charlotte, Vermont, VT 05445, USA
[d] Neuro-Oncology Branch, National Cancer Institute, National Institutes of Health, Bethesda, Maryland, MD 20814, USA

ARTICLE INFO

ABSTRACT

There is no doubt that immunotherapy lies in the spotlight of current cancer research and clinical trials. However, there are still limitations in the treatment response in certain types of tumors largely due to the presence of the complex network of immunomodulatory and immunosuppressive pathways. These limitations are not likely to be overcome by current immunotherapeutic options, which often target isolated steps in immune pathways preferentially involved in adaptive immunity. Recently, we have developed an innovative anti-cancer immunotherapeutic strategy that initially elicits a strong innate immune response with subsequent activation of adaptive immunity in mouse models. Robust primary innate immune response against tumor cells is induced by toll-like receptor ligands and anti-CD40 agonistic antibodies combined with the phagocytosis-stimulating ligand mannan, anchored to a tumor cell membrane by biocompatible anchor for membrane. This immunotherapeutic approach results in a dramatic therapeutic response in large established murine subcutaneous tumors including melanoma, sarcoma, pancreatic adenocarcinoma, and pheochromocytoma. Additionally, eradication of metastases and/or long-lasting resistance to subsequent re-challenge with tumor cells was also accomplished. Current and future advantages of this immunotherapeutic approach and its possible combinations with other available therapies are discussed in this review.

Published by Elsevier Inc.

Introduction

The history of cancer immunotherapy spans more than 100 years from the earliest forms using bacteria for immune system activation to current, highly sophisticated immune checkpoint inhibitors or monoclonal antibody therapy [1,2]. Despite the potential of modern medicine and science, cancer treatment remains challenging, and no universal approach and solution exists. The first immunotherapy was pioneered by William Coley, who stimulated the immune system by using intratumoral injections of the inactivated gram-positive bacteria *Streptococcus pyogenes* and gram-negative bacteria *Serratia marcescens* – so-called 'Coley's toxins' [3]. Although the underlying mechanism was not understood at that time, Coley achieved an immune response against sarcomas, resulting in a strong tumor burden reduction and even tumor elimination in some patients. Later on, a more clear understanding of this treatment response came through the discovery of pathogen-associated molecular patterns (PAMPs) and their receptors (pattern recognition receptors, PRRs) [4].

Subsequently, the discovery of various new groups of tumor antigens and their matching receptors on immune cells opened another door to cancer immunotherapy and represented a promising avenue for cancer elimination and recurrence prevention [5]. However, some discouraging results from vaccine-based clinical trial studies [6,7] led to the discovery of new immunosuppressive mechanisms by which tumor cells provide unique and strong protection against immune attack [8,9]. Thus, current cancer immunotherapies are heavily focused on the elimination of immunosuppressive mechanisms, specifically on the use of checkpoint inhibitors and activators [10,11]. However, their systemic application is associated with lower efficacy (only about 20% of patients overall respond to these drugs in some cancers [12]) and a simultaneous risk of autoimmunity [13]. In contrast to some current immunotherapy trends heavily oriented towards adaptive immunity, here we present a new immunotherapeutic approach tested in several different types of mouse tumor models, which affects the immune system on several levels with initial activation of innate immunity followed by activation of adaptive immunity. This immunotherapy is predicted to be highly effective in a broad range of tumors, including immunologically "cold" tumors which are challenging for most current immunotherapies.

The immune system in cancer pathogenesis

The immune system is the body's defense system protecting against infection and diseases. It can be categorized into 2 cooperative arms: (1) nonspecific, innate immunity and (2) specific, adaptive immunity [14].

Innate immunity represents the first line of host defense and provides nonspecific protection through several mechanisms, including physical barriers, such as epithelial cells with close cell-cell contact, as in the gastrointestinal tract, respiratory tract and genitourinary tract. Innate immunity also involves proteins and bioactive small molecules either permanently present in biological fluids, like complement proteins and defensins, or secreted upon activation, like cytokines, chemokines, lipids, and enzymes. Complement proteins represent a far-reaching and potent mechanism of innate immune defense. Complement is a hierarchical system of more than 30 plasmatic and surface proteins involved in initial pathogen identification, which results in the release of proinflammatory mediators, pathogen opsonization, and targeted lysis of the pathogen surface [14].

The last and very crucial component of the innate immunity defense involves receptors or cytoplasmic proteins binding specific molecular patterns (ligands) expressed by invading microbes. Recognition of these patterns (PAMPs), by innate immune cell receptors (PRRs), results in the release of inflammatory mediators and subsequent elimination of pathogens by attracted effector immune cells [4].

Adaptive immunity, the second arm of the immune system, is specific for its targeted antigens. The adaptive response is mainly based on the activation of T and B cells. The effector portion of adaptive immunity can be divided into 2 main parts, humoral immunity involving the production of antibodies by B cells and cell-mediated immunity involving the action of T cells. Moreover, adaptive immunity provides immunologic memory, which enables rapid and often long-lasting responses in the case of re-exposure to the same pathogen [14].

The role of the immune system in cancer pathogenesis has been intensively studied for many decades and is usually referred to as cancer immunosurveillance [15]. The relationship between tumors and immunity is based on a delicate balance that controls whether a tumor will progress or will get eliminated. This unique balance is known as immunoediting [15,16]. All immune cells or immune mechanisms interact with a tumor in specific ways, and their role

is mostly ambivalent regarding tumor progression or elimination [17].

Innate immunity can affect tumors on several levels. Various studies have demonstrated that tumor cells are able to activate complement, which can lead to their elimination and to enhancement of T and B cell activation [18]. However, complement can also demonstrate a pro-tumor effect when its activation increases vascular permeability, histamine release, and the generation of radical oxygen species (ROS), thereby promoting a microenvironment favorable for tumor progression [19,20]. Natural killer (NK) cells, another type of innate immune cells, are able to recognize tumors based on their aberrant or reduced major histocompatibility complex class I (MHC I) [21]. However, even here, the potential role of NK cells in tumor progression is questionable, since NK cells can be a source of IFN-gamma and promote resistance to adaptive immunity [22]. Neutrophils, the most abundant innate immunity granulocytes, are known to promote cancer progression through granular proteases supporting tumor growth, invasion, and spread of metastases [23]. Nevertheless, based on studies with neutrophils isolated from human donors, they also possess some unique mechanisms to recognize and eliminate tumor cells [24]. Dendritic cells (DCs) represent an important and unique communication bridge between innate and adaptive immunity. DCs might also be polarized by the tumor microenvironment into cells with pro-tumorigenic and anti-tumorigenic functions. The most obvious anti-tumorigenic function is their ability to present tumor antigens to T cells and so initiate their activation, however, their polarization into an immunosuppressive subset of regulatory DCs may have a significant effect on tumor growth and progression [25]. Typical tumor polarization can also be observed in macrophages. Macrophages infiltrating tumors, so-called tumor-associated macrophages (TAM), can be classified based on their function as M1 and M2 macrophages. M1 macrophages exert an anti-tumor function, whereas M2 macrophages are associated with pro-tumor features [26].

Like innate immunity, adaptive immunity also affects tumor pathogenesis, mainly via tumor neoantigens presented by antigen presenting cells (APCs) to T and B cells. This can result in T cell-mediated lysis of cancer cells or in the formation of tumor-specific antibodies. However, here the tumor microenvironment can also cause polarization of adaptive immune cells. This can lead to the accumulation of suppressive regulatory T and B cells (Tregs, tBregs) in a tumor, where their presence correlates with tumor progression [27,28].

From the examples discussed above, it is clear that the immune system has an important function in tumor pathogenesis. Both arms have an unquestionable ability to recognize and eliminate tumor cells. However, immune cells are constantly challenged by multiple tumor immune escape mechanisms. These mechanisms can establish an immunosuppressive environment in tumors by promoting the production of cytokines such as interleukin 10 (IL-10), transforming growth factor beta (TGF-beta), vascular endothelial growth factor (VEGF), or immunoregulatory molecules such as programmed cell death 1 (PD-1), programmed cell death 1-ligand (PD-L1), and indoleamine-2,3-dioxygenase (IDO) [29]. The effect of an immunosuppressive environment on immune cells with their subsequent polarization towards a pro-tumorigenic function was already discussed previously (M2 macrophages, regulatory DCs, Tregs, and tBregs). Simultaneously, tumor cells can also alter their antigenicity (disable recognition by APCs) [29], release tumor-derived exosomes (leading to downregulation of T cell and NK cell-mediated antitumor immunity) [30], or use specialize tumor stroma to pose an additional immune challenge [31].

Despite all these tumor immunosuppressive mechanisms, there is a strong potential in using the immune system as a tool for cancer treatment. However, we have to fully understand and be aware of this fragile relationship between tumors and the

immune system in order to develop an effective therapeutic strategy.

Activation of innate immunity as an initial step of successful immunotherapy

Innate immunity represents an old and conserved evolutionary mechanism of body protection. Since the tumor environment and tumor cells themselves are very unstable with constant changes in antigenicity, the nonspecific and rapid recognition that innate immunity uniquely offers represents a major advantage compared to the specific and delayed adaptive immune response. Therefore, activation of innate immunity could be the optimal initial therapeutic option for a broad range of tumors.

Our confidence that innate immunity may be a potent tool for initial cancer treatment arises from a study where Cui and his colleagues described a mouse model with a unique mutation, SR/CR, where innate immune cells showed a remarkable ability to recognize and eliminate a broad range of tumors [32]. This brought us to the idea that effective recognition of tumor cells by innate immunity could result in a strong antitumor effect and lead to the elimination of the tumor. Since innate immune cells can demonstrate difficulty in tumor cell recognition, we decided to support this recognition by artificially anchoring PAMPs to the tumor cell surface. Such tumor cell opsonization leads to their effective recognition and elimination by phagocytic cells [33]. After a series of optimization experiments, we determined the critical importance of combining two groups of PAMPs, anchored ligands stimulating phagocytosis and soluble toll-like receptor (TLR) ligands. This combination results in strong tumor infiltration by inflammatory cells [33] with subsequent extensive primary tumor burden reduction and, in most of the experimental animals, even a complete eradication of tumors [33-36].

This therapy is directly targeted via intratumoral application, which significantly decreases any side effects and results in the concentration of administered substances needed for effective activation of immunity. This proposed immunotherapy corresponds well with a new paradigm of intratumoral immunization [37-39]. Detailed steps of our immunotherapy paradigm as well as results related to the treatment of various tumors using this immunotherapy approach are summarized in subsequent sections.

Artificial opsonization of tumor cells by ligands stimulating phagocytosis

The concept of tumor cell artificial opsonization by phagocytosis-stimulating ligands originated from the essential nature of various ligands in the process of pathogen recognition by the innate immune system [40]. Thus, several individual ligands stimulating phagocytosis were tested in an effort to induce a strong anti-cancer innate immune response, namely laminarin, mannan, formyl-methionyl-leucyl phenylalanine (f-MLF), and zymosan A. Simultaneously, heat killed bacteria (*Mycobacterium tuberculosis* and *Stenotrophomonas maltophilia*), representing a complex group of ligands stimulating phagocytosis, were tested as well [34]. Even though whole bacteria present a complex combination of PAMPs (including multiple phagocytosis-stimulating ligands) and should logically result in strong immune system stimulation, the use of individual ligands stimulating phagocytosis was found to yield a more potent immune anti-tumor response. Specifically, with mannan, we achieved the best therapeutic effects.

The identification of the most potent ligand stimulating phagocytosis was just the first step in the successful artificial opsonization of tumors by PAMPs. The mechanism of anchoring phagocytosis-stimulating ligands to tumor cells also played a

key role. We tested various methods of anchoring phagocytosis stimulating-ligands, namely charge interaction, use of the hydrophobic anchors BAM/DOPE (biocompatible anchor for membrane/dioleylphosphatidylethanolamine), and covalent binding based on the heterobifunctional crosslinker SMCC (succinimidyl-4-(N-maleimidomethyl) cyclohexane-1-carboxylate) [33-36]. The best results were achieved with a BAM anchor containing one fatty acid aliphatic chain.

The anti-cancer effect is dependent on the recognition of mannan anchored by BAM (mannan-BAM) (Fig. 1A) via mannan binding lectin (MBL) (Fig. 1B). This recognition process is complement dependent (does not work in heat-inactivated serum); however, it is not the final membrane attack complex that kills the tumor cells. Mannan-BAM triggers lectin complement pathway activation and results in iC3b opsonization of tumor cells. This tumor cell opsonization attracts the attention of phagocytic cells, mainly neutrophils, and those eliminate tumor cells by a process called frustrated phagocytosis. During frustrated phagocytosis, neutrophils, in an attempt to ingest objects that are too big to be internalized, form clefts or pockets filled with enzymes and products of oxidative burst. These clefts and pockets, located in the space between the neutrophil and the target, lead to the destruction of the target [34,36]. Even though neutrophils were identified as key cells in this therapy, macrophages and NK cells are also able to recognize iC3b opsonized tumor cells (Fig. 1C) and participate in their elimination [33-35].

TLR ligands in the therapeutic mixture: The right combination and the right timing

Ligands stimulating phagocytosis (mannan) are not the only important component of presented immunotherapy. To stimulate massive tumor inflammatory infiltration, mannan must be combined with other PAMPs/TLR ligands. After extensive studies, we demonstrated that it was essential to use mannan with a mixture of several TLR ligands to achieve the best tumor infiltrating results, specifically a combination of resiquimod (R-848) (TLR7,8 ligand), polyinosinic:polycytidylic acid (poly(I:C)) (TLR3 ligand) and lipoteichoic acid (LTA) (TLR2 ligand) [35].

Moreover, TLR ligands require a specific application schedule to prevent the development of TLR resistance. Accordingly, we focused on the optimization of a precise delivery scheme, which resulted in a consensus of 5-day-long gaps between 3-day application pulses. Our findings regarding the application complexity of TLR ligands and the risk of resistance are consistent with Trinchieri and Sher's previous reports [41] as well as with the findings of Bourquin et al. [42]. We are confident that the correct timing of TLR ligands is necessary not only to ensure the innate immunity-based attack but also to initiate involvement of adaptive immunity. The application scheme mimics a vaccination scheme and can provide the required time and conditions for tumor antigen presentation and transition of the signal to adaptive immunity.

Adaptive immunity involvement as a second step of effective immunotherapy

Although this immunotherapy approach is based on the initial activation of innate immunity, there is undeniable evidence of adaptive immunity involvement. This can be explained by the interaction of multiple factors, which create ideal conditions for innate and adaptive immune cell communication. Phagocytic cells, involved in the initial stage of the therapy, present antigens to T cells in draining lymph nodes. Moreover, TLR ligands, besides their positive effect on tumor leukocyte infiltration, also promote maturation of DCs. DCs are known for their key role in antigen presentation and adaptive immunity activation.
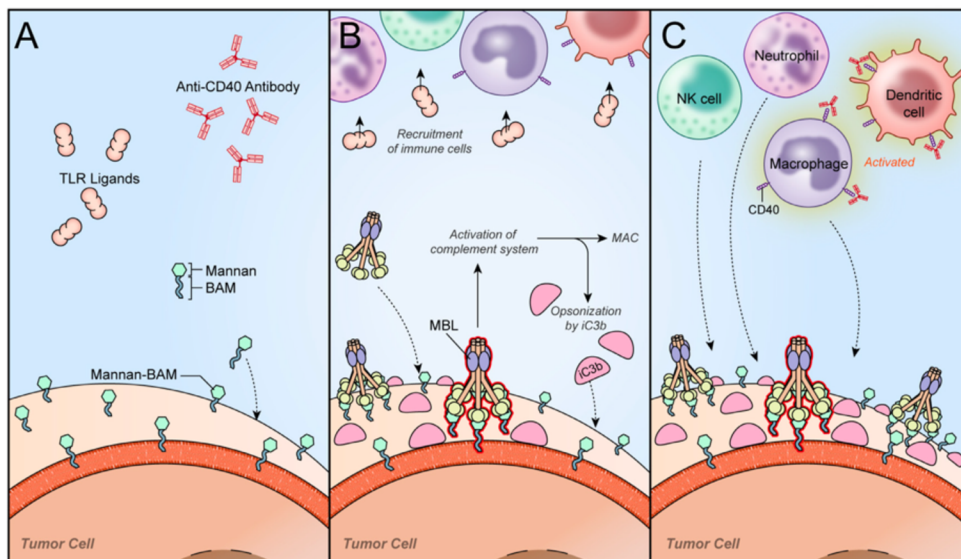
Fig. 1. The initial phase of immunotherapy based on the combination of TLR ligands, mannan–BAM, and anti-CD40 antibody. (A) After intratumoral application of the therapy (TLR ligands, mannan–BAM, anti-CD40 antibody), tumor cells are artificially opsonized by mannan anchored by biocompatible anchor for membrane BAM (mannan–BAM), where the terminal part of BAM is incorporated into the lipid bilayer of tumor cells. (B) Mannan–BAM is subsequently recognized by mannan binding lectin (MBL). This recognition results in the activation of the complement system followed by proteolytic cleavage of complement protein C3 and the production of the terminal membrane attack complex (MAC). During the proteolytic cleavage of C3 into C3a and C3b, inactive form of C3b (iC3b) opsonizes the tumor cells. Simultaneously, TLR ligands (R-848, poly(I:C), LTA) are recruiting immune cells into the tumor. (C) Tumor cells opsonized by iC3b are recognized by innate immune cells (NK cells, neutrophils, macrophages) previously recruited into the tumor. These innate immune cells use their effector mechanisms to kill the opsonized tumor cells. Anti-CD40 antibodies, as a part of the therapy, bind to CD40 receptors expressed mainly on antigen presenting cells (macrophages, dendritic cells) and initiate their activation. These activated antigen presenting cells further internalize tumor antigens and present them to T cells in lymph nodes.

Furthermore, we also observed strong IFN-gamma production and establishment of the type 1 T helper cells (Th1) immune response [34,36].

The involvement of adaptive immunity was verified both *in vitro* and *in vivo*. *In vitro* quantification assessed the response of CD4+ and CD8+ cells to antigenic stimulation [35]. *In vivo* verification focused on resistance to tumor cell re-challenging experiments [34,35] and measurement of anti-metastatic effects in mouse models [35,36].

Adaptive immune activation is dependent on the tumor environment and can be increased by modification of the therapeutic mixture

Our immunotherapy approach revealed excellent therapeutic results in murine melanoma B16-F10 and murine sarcoma S-180 models [33-35]. Subsequently, this approach was tested in a murine pancreatic adenocarcinoma model (Panc02) and pheochromocytoma model. In these models, we also observed a strong initial reduction of tumor growth; however, there was a decreased effect on survival when compared to previously tested murine models [35,36]. This result in the pancreatic adenocarcinoma model was expected, since this tumor is considered to be highly resistant against any kind of treatment [43]. Also, pheochromocytomas, specifically metastatic pheochromocytomas, are resistant against conventional treatments [44]. Moreover, there is very limited knowledge about the immunology of pheochromocytomas, with isolated reports describing a low neoepitope burden and low mutation burden, which may suggest a low immunogenicity of these tumors [45,46].

It can be concluded that the initial phase of the innate immune attack is not dependent on the tumor type; however, the subse-

quent activation of adaptive immunity and its effect on survival is dependent on the tumor environment, which is specific for each tumor type.

To address the effect of the tumor environment on adaptive immunity activation in pancreatic adenocarcinoma and subsequent partial resistance against tested immunotherapy, we decided to modulate this tumor environment by combining immunotherapy with immune checkpoint inhibitors or immune activators. Since the pancreatic adenocarcinoma model is known to have high levels of infiltrating Tregs [47], we used anti-CTLA-4 (cytotoxic T-lymphocyte-associated protein 4) for their depletion to see if this led to a significant difference in response to the tested immunotherapy. Although anti-CTLA-4 added to the therapeutic mixture improved the initial reduction of tumor growth, the survival of the tested mice was not affected.

In the second step, anti-PD-1 antibody was tested. Anti-PD-1 is a checkpoint inhibitor positively affecting T cell activation and function [48]. However, anti-PD-1 antibody did not have any effect on tumor growth or survival of the animals. This failure can be explained by a low expression of PD-L1 in pancreatic adenocarcinoma cells [49].

Subsequently, anti-CD40 (immunostimulant) was tested in pancreatic adenocarcinoma and pheochromocytoma murine models to improve the activation of the adaptive immunity. Anti-CD40 is an agonistic antibody that mimics CD40 ligands (CD40L, CD154) expressed on CD4+ cells. Anti-CD40 binds to CD40 receptor which are present on DCs and other myeloid cells [50]. Specifically, the ligation of CD40 with CD40 receptor on DCs leads to the upregulation of MHC molecules, CD80/CD86 costimulatory molecules, and the production of IL-12. This DC activation enhances antigen presentation and induces an effective T cell based anti-tumor response [51,52].
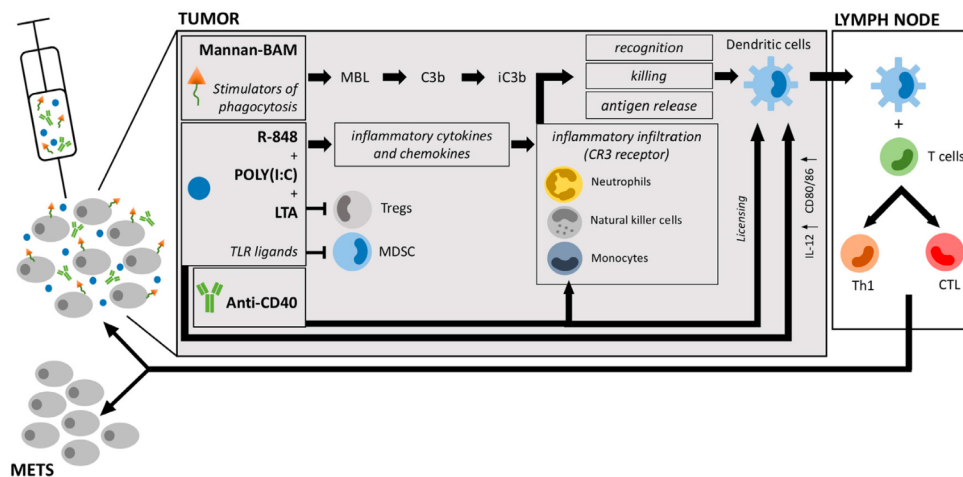
Fig. 2. The main mechanisms of the anti-cancer effect of the described immunotherapy. TLR ligands cause strong inflammatory infiltration of tumors via inflammatory cytokines and chemokines. Infiltrating cells kill artificially opsonized (iC3b) tumor cells. Liberated antigens are presented to the adaptive immune system in lymphatic nodes. TLR ligands stimulate the production of IL-12 and costimulatory molecules leading to support of antigen presentation and to the establishment of the anti-tumor Th1 immune response – Type 1 helper T cells (Th1) and cytotoxic T lymphocytes (CTL), respectively. The environment of acute inflammation suppresses regulatory T cells (Tregs) and myeloid-derived suppressor cells (MDSC). Anti-CD40 antibody activates phagocytes and takes part in the licensing of dendritic cells to induce an effective T cells-based anti-tumor response.

The enhancement of the therapeutic mixture with anti-CD40 resulted in 80% complete elimination of pancreatic adenocarcinoma tumors with resistance against tumor re-challenging after 120 days [35]. In the pheochromocytoma mouse model, anti-CD40 enhancement resulted in 62.5% complete elimination of subcutaneous tumors with complete resistance against tumor re-challenging. Additionally, the enhanced effect of mannan-BAM + TLR ligands + anti-CD40 therapy on activation of the specific part of immunity was also verified in metastatic pheochromocytoma. In metastatic pheochromocytoma, significant growth reduction and even complete elimination of distant liver lesions was observed and was dependent on the presence of CD8+ T cells [36]. The main mechanisms of the enhanced therapeutic mixture are shown in Fig. 2.

Overall, the combination of mannan-BAM + TLR ligands with checkpoint inhibitors (anti-CTLA-4, anti-PD-1) did not show improvement in the therapeutic outcome compared to anti-CD40. This can be explained by the fact that checkpoint inhibitors mainly target isolated steps in the adaptive immune response cascade with lack of innate immune system stimulation. On one hand, the therapeutic response to checkpoint inhibitors is dependent on previously activated innate immunity and on the presence of tumor immunosuppressive mechanisms. On the other hand, anti-CD40 acts simultaneously on the level of the innate and adaptive immunity, which supports the immune response in a more complex matter. Moreover, the synergy of anti-CD40 with R-848 and poly(I:C) that results in extensive expansion of APCs and CD8+ memory cells is another example of the advantage of anti-CD40 compared to checkpoint inhibitors [53].

Application of CD40 antibodies and FDA-approved TLR ligands in cancer therapy

Interestingly, several innate immunity-based immunotherapies including above mentioned TLR ligands and anti-CD40 antibodies are currently being tested in clinical trials or used in clinical practice.

Six anti-CD40 antibodies have been investigated in clinical trials: ADC-1013 (Janssen/Alligator), APX005M (Apexigen), CDX-1140

(Celldex), ChiLob7/4 (University of Southampton), SEA-CD40 (Seattle Genetics), and Selicrelumab (Roche) [54]. However, most of anti-CD40 antibodies alone have shown minimal rates of objective tumor response in patients. On the other hand, the combination of anti-CD40 with either chemotherapy (carboplatin, paclitaxel, gemcitabine) or immunotherapy (CTLA-4, PD-1, PD-L1 antibodies) has shown more promising results compared to anti-CD40 antibodies or chemotherapy alone [54].

In the case of TLR ligands, 3 types are already used in cancer therapy. Imiquimod, a TLR7 agonist, has been approved by Food and Drug Administration (FDA) as a therapeutic agent for basal cell carcinoma [55]. Bacillus Calmette-Guérin (BCG) has been shown to potently activate TLR2 and TLR4. This attenuated strain of *Mycobacterium bovis* is used as an immunotherapeutic agent against bladder carcinoma [56,57].

Monophosphoryl lipid A, a modified derivate of *Salmonella minnesota* endotoxin and a TLR4 agonist, has also been approved by FDA as an adjuvant for use in vaccines against human papillomavirus type 16 and 18 (Cervarix®) [58,59]. Moreover, many TLR ligands have been investigated in clinical trials and have been reviewed elsewhere [60-63].

Potential combination with other therapeutic approaches

Combination therapy is becoming the hallmark of successful cancer treatment. The complexity of this disease requires complex treatment solutions, especially in the case of enlarged inoperable tumors or multiple organ lesions (metastases). The described immunotherapy based on PAMPs-related artificial opsonization of tumor cells could potentially be combined with stereotactic radiotherapy, radiofrequency ablation, cryoablation, and/or chemotherapy with significant beneficial results.

The most important factor that has to be considered before the application of combination therapy is the right timing and order of the individual therapies. Even though, there are no conclusive data in this research area, it is clear that the mechanisms of action of each individual chemotherapeutic agents and immunotherapeutic modulators has to be considered prior their combination to ensure the ideal timing. Since chemotherapy and ra-

diotherapy may have significant negative impacts on the viability of immune cells [64,65]. We envisage that the application of the described immunotherapy prior to chemotherapy or radiotherapy will achieve the best therapeutic results. Prior application of immunotherapy based on artificial opsonization of tumor cells by PAMPs will vaccinate the organism against tumor antigens and support the development of memory cells specific to these antigens. Memory cells are known for their increased resistance against toxicity caused by radiotherapy [66] or chemotherapy [67,68] since they are in a quiescent G_0 state hidden in the body [69]. There are several studies conducted in humans or animal models which can possibly support this view. Based on the results from the clinical studies, patients initially treated with immunotherapy (antigen pulsed DCs) followed by chemotherapy had better clinical outcomes than patients who received chemotherapy alone [70,71]. In animal models, chemotherapy (gemcitabine + cisplatin) given after immunotherapy (adenoviral vector expressing IFN-alfa) had also better antitumor effect than either chemotherapy or immunotherapy alone [72].

On the other hand, when immunotherapy introduced by our group will be used in the opposite sequence (immunotherapy that comes after chemotherapy and radiotherapy), the immune system may be more or less impaired by physical or chemical attack, which prevents its effective activation and subsequent tumor cell elimination. Even though the white blood cell count can be normalized after chemotherapy or radiotherapy, the function of the immune system can be seriously affected in the long term. Moreover, most of the chemical or physical interventions can lead to a simultaneous massive release of tumor antigens, which can result in the establishment of high zone tolerance [73,74]. Furthermore, released adenosine and TGF-beta contribute to the suppressive effect on the immune system [75]. Under these circumstances, the chance of establishing a strong immune response may be very limited.

Even though the above-mentioned studies suggest the prior application of immunotherapy to be more beneficial, the timing of individual therapies still remains inconclusive and will need to be deeply investigated prior further clinical applications.

Perspective

Although the described immunotherapy can eliminate metastases and prolongate the survival of experimental animals, the size of the metastases is still a significant limitation for the therapeutic response. While small metastases can be completely eradicated with this therapy, advanced metastases are only slowed in growth. Therefore, future research has to be focused on the application of this immunotherapy in advanced metastatic disease and investigation of involved immune mechanisms in order to improve the therapeutic effect. Below we describe several approaches that can be studied for future improvement of this immunotherapy.

Intra-metastatic injection of the therapeutic mixture

In cases of metastatic disease presenting with a limited number of lesions, the individual lesions can be located and targeted with a dose of immunotherapy applied directly into the lesions involving interventional radiology techniques.

Adoptive transfer of innate immune cells into the metastases

Adoptive transfer of activated innate immune cells into the organ lesions can support the therapeutic response of uncontrolled metastases. This approach can represent a better option than the intra-metastatic injections of the therapeutic mixture mentioned above. With multiple injections of TLR ligands, the risk of side effects, such as fever or septic shock [76], can be increased. Since the main purpose of TLR ligands in this therapeutic mixture is to attract innate immune cells into the tumor and metastases, the direct adoptive transfer of innate immune cells into the metastases combined with mannan-BAM can overcome the challenges involved with multiple injections of TLR ligands.

Development of combination therapy with chemotherapy and/or radiotherapy involvement

Combination therapy is another possibility for improving the therapeutic response of advanced metastases. Specifically, immunotherapy applied in primary tumors with subsequent application of systemic chemotherapy or radiotherapy affecting distant tumors (metastases) may result in a synergistic effect and lead to complete elimination of advanced metastases.

Study of involved mechanisms

Acquiring a deeper understanding of the immune mechanisms involved in the eradication of tumors is one of the most important steps towards therapeutic improvement. Therefore, future studies should also focus on the investigation of innate and adaptive immune cell involvement and activation during immunotherapy application.

Conclusions

The immune system represents the most complex and effective tool which our bodies possess to fight cancer. Current cancer immunotherapies are manly focused on activation of adaptive immunity, and the complex activation initiated by innate immunity is missing. Here, we demonstrate that effective cancer immunotherapy requires phased activation of both immune parts, innate immunity and adaptive immunity, to achieve the complex immune response against tumors. Our proposed immunotherapy involves an initial attack of innate immunity with subsequent involvement of adaptive immunity, which was demonstrated in tumor mouse models. In the future, this unique concept of complex immune system activation can result in effective treatments for patients with inoperable tumors or can be used to shrink tumors prior to surgery. More importantly, this therapy can vaccinate organisms and result in elimination not only of primary tumors but also metastases, with future protection against recurrent disease. The proposed immunotherapy can be also potentially combined with other therapies such as chemotherapy or radiotherapy to yield an increased therapeutic effect. These qualities make this immunotherapeutic approach an outstanding candidate for the treatment of a broad range of tumors.

However, the main upcoming challenge will be to prove this therapeutic effect in clinical translation.

Support

Declaration of Competing Interest

The authors have nothing to disclose.

References

[1] Ribas A, Wolchok JD. Cancer immunotherapy using checkpoint blockade. Science 2018;359(6382):1350–5.

[2] Scott AM, Wolchok JD, Old LJ. Antibody therapy of cancer. Nat Rev Cancer 2012;12(4):278–87.

[3] Coley WB. The treatment of malignant tumors by repeated inoculations of erysipelas. With a report of ten original cases. 1893. Clin Orthop Relat Res. 1991(262):3–11.

[4] Akira S, Uematsu S, Takeuchi O. Pathogen recognition and innate immunity. Cell 2006;124(4):783–801.

[5] Wang RF. Tumor antigens discovery: perspectives for cancer therapy. Mol Med 1997;3(11):716–31.

[6] Kudrin A. Cancer vaccines: what do we need to measure in clinical trials? Hum Vaccin Immunother. 2014;10(11):3236–40.

[7] Jacobs JJ, Snackey C, Geldof AA, et al. Inefficacy of therapeutic cancer vaccines and proposed improvements. Casus of prostate cancer. Anticancer Res. 2014;34(6):2689–700.

[8] Hanahan D, Weinberg RA. Hallmarks of cancer: the next generation. Cell 2011;144(5):646–74.

[9] Russell M, Huang X, Vuzman D, et al. Characterization of biomarkers to immune checkpoint blockade therapy across solid tumors. J Clin Oncol 2018;36(5).

[10] Dempke WCM, Fenchel K, Uciechowski P, Dale SP. Second- and third-generation drugs for immuno- oncology treatment-The more the better? Eur J Cancer. 2017;74:55–72.

[11] Thallinger C, Fureder T, Preusser M, et al. Review of cancer treatment with immune checkpoint inhibitors: Current concepts, expectations, limitations and pitfalls. Wien Klin Wochenschr 2018;130(3–4):85–91.

[12] Kaiser J. Too much of a good thing? Science. 2018;359(6382):1346–7.

[13] Michot JM, Bigenwald C, Champiat S, et al. Immune-related adverse events with immune checkpoint blockade: a comprehensive review. Eur J Cancer 2016;54:139–48.

[14] Chaplin DD. Overview of the immune response. J Allergy Clin Immunol 2010;125(2 Suppl 2):S3–23.

[15] Dunn GP, Old LJ, Schreiber RD. The three Es of cancer immunoediting. Annu Rev Immunol 2004;22:329–60.

[16] Schreiber RD, Old LJ, Smyth MJ. Cancer immunoediting: integrating immunity's roles in cancer suppression and promotion. Science 2011;331(6024):1565–70.

[17] Smyth MJ, Godfrey DI, Trapani JA. A fresh look at tumor immunosurveillance and immunotherapy. Nat Immunol 2001;2(4):293–9.

[18] Reis ES, Mastellos DC, Ricklin D, Mantovani A, Lambris JD. Complement in cancer: untangling an intricate relationship. Nat Rev Immunol 2018;18(1):5–18.

[19] Kourtzelis I, Rafail S. The dual role of complement in cancer and its implication in anti-tumor therapy. Ann Transl Med 2016;4(14):265.

[20] Roumenina LT, Daugan MV, Noe R, et al. Tumor cells hijack macrophage-produced complement C1q to promote tumor growth. Cancer Immunol Res 2019;7(7):1091–105.

[21] Smyth MJ, Sullivan LC, Brooks AG, Andrews DM. Non-classical MHC Class I molecules regulating natural killer cell function. Oncoimmunology 2013;2(3):e23336.

[22] Waldhauer I, Steinle A. NK cells and cancer immunosurveillance. Oncogene 2008;27(45):5932–43.

[23] Wang X, Qiu L, Li Z, Wang XY, Yi H. Understanding the multifaceted role of neutrophils in cancer and autoimmune diseases. Front Immunol 2018;9:2456.

[24] Yan J, Kloecker G, Fleming C, et al. Human polymorphonuclear neutrophils specifically recognize and kill cancerous cells. Oncoimmunology 2014;3(7):e950163.

[25] Gardner A, Ruffell B. Dendritic cells and cancer immunity. Trends Immunol. 2016;37(12):855–65.

[26] Condeelis J, Pollard JW. Macrophages: obligate partners for tumor cell migration, invasion, and metastasis. Cell 2006;124(2):263–6.

[27] Balkwill F, Montfort A, Capasso M. B regulatory cells in cancer. Trends Immunol 2013;34(4):169–73.

[28] Ribas A. Adaptive immune resistance: how cancer protects from immune attack. Cancer Discov 2015;5(9):915–19.

[29] Zou W. Immunosuppressive networks in the tumour environment and their therapeutic relevance. Nat Rev Cancer 2005;5(4):263–74.

[30] Maia J, Caja S, Strano Moraes MC, Couto N, Costa-Silva B. Exosome-based cell-cell communication in the tumor microenvironment. Front Cell Dev Biol 2018;6:18.

[31] Seager RJ, Hajal C, Spill F, Kamm RD, Zaman MH. Dynamic interplay between tumour, stroma and immune system can drive or prevent tumour progression. Converg Sci Phys Oncol 2017:3.

[32] Cui Z, Willingham MC, Hicks AM, et al. Spontaneous regression of advanced cancer: identification of a unique genetically determined, age-dependent trait in mice. Proc Natl Acad Sci U S A 2003;100(11):6682–7.

[33] Janotova T, Jalovecka M, Auerova M, et al. The use of anchored agonists of phagocytic receptors for cancer immunotherapy: B16-F10 murine melanoma model. PLoS One 2014;9(1):e85222.

[34] Waldmannova E, Caisova V, Faberova J, et al. The use of Zymosan A and bacteria anchored to tumor cells for effective cancer immunotherapy: B16-F10 murine melanoma model. Int Immunopharmacol 2016;39:295–306.

[35] Caisova V, Uher O, Nedbalova P, et al. Effective cancer immunotherapy based on combination of TLR agonists with stimulation of phagocytosis. Int Immunopharmacol 2018;59:86–96.

[36] Caisova V, Li L, Gupta G, et al. The significant reduction or complete eradication of subcutaneous and metastatic lesions in a pheochromocytoma mouse model after immunotherapy using Mannan-BAM, TLR Ligands, and Anti-CD40. Cancers (Basel) 2019;11(5).

[37] Marabelle A, Kohrt H, Caux C, Levy R. Intratumoral immunization: a new paradigm for cancer therapy. Clin Cancer Res 2014;20(7):1747–56.

[38] Nelson D, Fisher S, Robinson B. The "Trojan Horse" approach to tumor immunotherapy: targeting the tumor microenvironment. J Immunol Res 2014;2014:789069.

[39] van den Boorn JG, Hartmann G. Turning tumors into vaccines: co-opting the innate immune system. Immunity 2013;39(1):27–37.

[40] Underhill DM, Gantner B. Integration of Toll-like receptor and phagocytic signaling for tailored immunity. Microbes Infect 2004;6(15):1368–73.

[41] Trinchieri G, Sher A. Cooperation of toll-like receptor signals in innate immune defence. Nat Rev Immunol 2007;7(3):179–90.

[42] Bourquin C, Hotz C, Noerenberg D, et al. Systemic cancer therapy with a small molecule agonist of toll-like receptor 7 can be improved by circumventing TLR tolerance. Cancer Res 2011;71(15):5123–33.

[43] Oberstein PE, Olive KP. Pancreatic cancer: why is it so hard to treat? Therap Adv Gastroenterol. 2013;6(4):321–37.

[44] Crona J, Taieb D, Pacak K. New perspectives on Pheochromocytoma and Paraganglioma: toward a molecular classification. Endocr Rev 2017;38(6):489–515.

[45] Wang X, Li M. Correlate tumor mutation burden with immune signatures in human cancers. BMC Immunol 2019;20(1):4.

[46] Wood MA, Paralkar M, Paralkar MP, et al. Population-level distribution and putative immunogenicity of cancer neoepitopes. BMC Cancer 2018;18(1):414.

[47] Liyanage UK, Goedegebuure PS, Moore TT, et al. Increased prevalence of regulatory T cells (Treg) is induced by pancreas adenocarcinoma. J Immunother 2006;29(4):416–24.

[48] Seidel JA, Otsuka A, Kabashima K. Anti-PD-1 and Anti-CTLA-4 Therapies in cancer: mechanisms of action, efficacy, and limitations. Front Oncol 2018;8:86.

[49] Soares KC, Rucki AA, Wu AA, et al. PD-1/PD-L1 blockade together with vaccine therapy facilitates effector T-cell infiltration into pancreatic tumors. J Immunother 2015;38(1):1–11.

[50] Rakhmilevich AL, Alderson KL, Sondel PM. T-cell-independent antitumor effects of CD40 ligation. Int Rev Immunol 2012;31(4):267–78.

[51] Khong A, Nelson DJ, Nowak AK, Lake RA, Robinson BWS. The use of agonistic Anti-CD40 therapy in treatments for cancer. Int Rev Immunol 2012;31(4):246–66.

[52] Vonderheide RH, Glennie MJ. Agonistic CD40 antibodies and cancer therapy. Clin Cancer Res 2013;19(5):1035–43.

[53] Ahonen CL, Doxsee CL, McGurran SM, et al. Combined TLR and CD40 triggering induces potent CD8+ T cell expansion with variable dependence on type I IFN. J Exp Med 2004;199(6):775–84.

[54] Vonderheide RH. CD40 agonist antibodies in cancer immunotherapy. Annu Rev Med 2019 [Epub ahead of print].

[55] Vacchelli E, Galluzzi L, Eggermont A, et al. Trial watch: FDA-approved Toll-like receptor agonists for cancer therapy. Oncoimmunology 2012;1(6):894–907.

[56] Fuge O, Vasdev N, Allchorne P, Green JS. Immunotherapy for bladder cancer. Res Rep Urol 2015;7:65–79.

[57] Gandhi NM, Morales A, Lamm DL. Bacillus Calmette-Guerin immunotherapy for genitourinary cancer. BJU Int 2013;112(3):288–97.

[58] Agosti JM, Goldie SJ. Introducing HPV vaccine in developing countries–key challenges and issues. N Engl J Med 2007;356(19):1908–10.

[59] Mata-Haro V, Cekic C, Martin M, et al. The vaccine adjuvant monophosphoryl lipid A as a TRIF-biased agonist of TLR4. Science 2007;316(5831):1628–32.

[60] Shi M, Chen X, Ye K, Yao Y, Li Y. Application potential of toll-like receptors in cancer immunotherapy: Systematic review. Medicine (Baltimore) 2016;95(25):e3951.

[61] Anwar MA, Shah M, Kim J, Choi S. Recent clinical trends in Toll-like receptor targeting therapeutics. Med Res Rev 2019;39(3):1053–90.

[62] Liu C, Han C, Liu J. The role of toll-like receptors in oncotherapy. Oncol Res 2019;27(8):965–78.

[63] Mikulandra M, Pavelic J, Glavan TM. Recent findings on the application of toll-like receptors agonists in cancer therapy. Curr Med Chem 2017;24(19):2011–32.

[64] Marsh JC. The effects of cancer chemotherapeutic agents on normal hematopoietic precursor cells: a review. Cancer Res 1976;36(6):1853–82.

[65] Mauch P, Constine L, Greenberger J, et al. Hematopoietic stem cell compartment: acute and late effects of radiation therapy and chemotherapy. Int J Radiat Oncol Biol Phys 1995;31(5):1319–39.

[66] Schaue D, McBride WH. T lymphocytes and normal tissue responses to radiation. Front Oncol 2012;2:119.

[67] Hanoteau A, Moser M. Chemotherapy and immunotherapy: a close interplay to fight cancer? Oncoimmunology. 2016;5(7):e1190061.

[68] Turtle CJ, Swanson HM, Fujii N, Estey EH, Riddell SR. A distinct subset of self-renewing human memory CD8+ T cells survives cytotoxic chemotherapy. Immunity 2009;31(5):834–44.

[69] Lea NC, Orr SJ, Stoeber K, et al. Commitment point during G0->G1 that controls entry into the cell cycle. Mol Cell Biol 2003;23(7):2351–61.

[70] Schlom J, Arlen PM, Gulley JL. Cancer vaccines: moving beyond current paradigms. Clin Cancer Res 2007;13(13):3776–82.

[71] Wheeler CJ, Das A, Liu G, Yu JS, Black KL. Clinical responsiveness of glioblastoma multiforme to chemotherapy after vaccination. Clin Cancer Res 2004;10(16):5316–26.

[72] Fridlender ZG, Sun J, Singhal S, et al. Chemotherapy delivered after viral immunogene therapy augments antitumor efficacy via multiple immune-mediated mechanisms. Mol Ther 2010;18(11):1947–59.

[73] Sabel MS. Cryo-immunology: a review of the literature and proposed mechanisms for stimulatory versus suppressive immune responses. Cryobiology 2009;58(1):1–11.

[74] Shi J, Li Y, Liang S, et al. Analysis of circulating tumor cells in colorectal cancer liver metastasis patients before and after cryosurgery. Cancer Biol Ther 2016;17(9):935–42.

[75] Wennerberg E, Lhuillier C, Vanpouille-Box C, et al. Barriers to radiation-induced in situ tumor vaccination. Front Immunol 2017;8:229.

[76] Engel AL, Holt GE, Lu H. The pharmacokinetics of toll-like receptor agonists and the impact on the immune system. Expert Rev Clin Pharmacol 2011;4(2):275–89.

Chapter IV

Mannan-BAM, TLR ligands, and Anti-CD40 Immunotherapy in Established Murine Pancreatic Adenocarcinoma: Understanding Therapeutic Potentials and Limitations

ORIGINAL ARTICLE

Mannan-BAM, TLR ligands, and anti-CD40 immunotherapy in established murine pancreatic adenocarcinoma: understanding therapeutic potentials and limitations

Ondrej Uher[1,2] · Veronika Caisova[2] · Lucie Padoukova[1] · Karolina Kvardova[1] · Kamila Masakova[1] · Radka Lencova[1] · Andrea Frejlachova[1] · Marketa Skalickova[1] · Anna Venhauerova[1] · Adela Chlastakova[1] · Per Hansen[3] · Jindrich Chmelar[1] · Jan Kopecky[1] · Zhengping Zhuang[4] · Karel Pacak[2] · Jan Zenka[1]

Abstract

Pancreatic adenocarcinoma is one of the leading causes of cancer-related deaths, and its therapy remains a challenge. Our proposed therapeutic approach is based on the intratumoral injections of mannan-BAM, toll-like receptor ligands, and anti-CD40 antibody (thus termed MBTA therapy), and has shown promising results in the elimination of subcutaneous murine melanoma, pheochromocytoma, colon carcinoma, and smaller pancreatic adenocarcinoma (Panc02). Here, we tested the short- and long-term effects of MBTA therapy in established subcutaneous Panc02 tumors two times larger than in previous study and bilateral Panc02 models as well as the roles of CD4^{+} and CD8^{+} T lymphocytes in this therapy. The MBTA therapy resulted in eradication of 67% of Panc02 tumors with the development of long-term memory as evidenced by the rejection of Panc02 cells after subcutaneous and intracranial transplantations. The initial Panc02 tumor elimination is not dependent on the presence of CD4^{+} T lymphocytes, although these cells seem to be important in long-term survival and resistance against tumor retransplantation. The resistance was revealed to be antigen-specific due to its inability to reject B16-F10 melanoma cells. In the bilateral Panc02 model, MBTA therapy manifested a lower therapeutic response. Despite numerous combinations of MBTA therapy with other therapeutic approaches, our results show that only simultaneous application of MBTA therapy into both tumors has potential for the treatment of the bilateral Panc02 model.

Keywords Pancreatic adenocarcinoma · TLR ligands · Mannan · Cancer immunotherapy · Metastases · Checkpoint inhibitors

Abbreviation

CTLA-4	Cytotoxic T-lymphocyte-associated antigen 4
HKLM	Heat-killed *Listeria monocytogenes*
MBT therapy	Mannan-BAM + TLR ligands
MBTA therapy	Mannan-BAM + TLR ligands + anti-CD40 antibody
RT	Radiotherapy
TLR	Toll-like receptor

Ondrej Uher and Veronika Caisova have contributed equally to this work.

✉ Jan Zenka
jzenka@gmail.com

1 Department of Medical Biology, Faculty of Science, University of South Bohemia, Ceske Budejovice 37005, Czech Republic

2 Section on Medical Neuroendocrinology, Eunice Kennedy Shriver National Institute of Child Health and Human Development, National Institutes of Health, Bethesda, MD 20814, USA

3 Immunoaction LLC, Charlotte, VT 05445, USA

4 Surgical Neurology Branch, National Institute of Neurological, Disorders and Stroke, National Institutes of Health, Bethesda, MD 20814, USA

Introduction

Pancreatic cancer is one of the leading causes of cancer-related deaths worldwide [1]. Patients with this type of cancer show a very limited response to currently available treatment approaches with only a 7% 5-year survival rate [2]. Its poor response and aggressivity can be explained by

⚛ Springer

low antigenicity and its unique desmoplastic tumor stroma [3]. Low antigenicity results in the inability of T cells to recognize malignant cells, whereas the unique desmoplastic stroma can act as a physical barrier and block the penetration of anti-cancer drugs. Therefore, the blockade of the two most studied checkpoint inhibitors, programmed death-1 (PD-1) and cytotoxic T-lymphocyte-associated antigen 4 (CTLA-4), in pancreatic cancer failed in phase I and II of clinical trials, respectively [4, 5]. Lower effectiveness of these checkpoint inhibitors and their combinations has also been observed in other cancer patients, except those with non-small cell lung cancer, melanoma, renal cell carcinoma, etc. [6, 7]. We thus speculate certain immunotherapy limitations in the narrow effect of the checkpoint inhibitors on the immune system. Checkpoint inhibitors are particularly involved in the last steps of an immune response, which represents the feedback of control mechanisms. This suggests that effective cancer immunotherapy has to be more complex and has to affect the immune system particularly during the initial activation of innate immunity and subsequent activation of adaptive immunity.

Previously, we studied cancer immunotherapy in murine models directed on the activation of the natural mechanisms of immune response and thereby involving both arms of the immune response, i.e., innate and adaptive immunity [8]. This novel approach combines toll-like receptor (TLR) ligands and a phagocytosis-activating ligand and exhibits promising results in the murine melanoma B16-F10 model. Here, TLR ligands support the infiltration of immune cells into a tumor and activation of immune cells [9–11]. The combination of resiquimod (R-848), polyinosinic–polycytidylic acid (poly(I:C)), and lipoteichoic acid (LTA) was assessed as the most potent. Mannan, a phagocytosis-activating ligand, artificially binds to tumor cell surfaces via a biocompatible anchor for cell membrane (BAM) and labels them for the infiltrated immune cells [9–12]. For the pancreatic adenocarcinoma (Panc02), pheochromocytoma (MTT), and colon carcinoma (CT26) mouse model, the combined application of mannan-BAM, R-848, poly(I:C), and LTA together with anti-CD40 antibody (called MBTA therapy) improved the survival of experimental mice [11–13].

The aim of this present study was to evaluate the effect of MBTA therapy in subcutaneous Panc02 tumors with a higher burden to more mimic the real situation of patients with pancreatic adenocarcinoma often during initial diagnosis. Specifically, mice with established pancreatic adenocarcinoma larger than so far studied and mice with two tumors, i.e., a bilateral Panc02 model, which enables to better study a systemic response to therapies, were used. Our results strongly indicate that MBTA therapy is effective for the treatment of established Panc02 tumors. Additionally, tumor rechallenge experiments revealed antigen-specific memory and rejection of Panc02 cells after subcutaneous

and intracranial reinjections. CD4$^+$ T lymphocytes had a minimal role during initial tumor reduction, but they were important in the survival of treated mice. In the bilateral Panc02 model, MBTA therapy only led to a decrease in the progression of both tumors. Therefore, to improve its applicability, we focused on its combination with checkpoint inhibitors, modification of tumor desmoplasia, chemoablation, or radiotherapy (RT) of the parallel tumor. Only simultaneous application of MBTA therapy into both tumors achieved effective therapeutic response in this challenging tumor model.

Materials and methods

Materials

Tissue culture media, media supplements, mannan from *Saccharomyces cerevisiae,* lipoteichoic acid (LTA) from *Bacillus subtilis*, polyinosinic–polycytidylic acid, sodium salt (poly (I:C)), and hyaluronidase (Type I-S) were purchased from Sigma-Aldrich (St. Louis, MO, USA). Resiquimod (R-848) was obtained from Tocris Bioscience (Bristol, UK). Biocompatible anchor for cell membrane (BAM, Mw 4000) was purchased from NOF EUROPE (Grobbendonk, Belgium). Monoclonal anti-CD40 antibody (rat IgG2a, clone FGK4.5/FGK45), anti-CTLA-4 antibody (hamster IgG, clone (9H10), and anti-PD-L1 antibody (rat IgG2b, clone 10F.9G2) were purchased from BioXCell (West Lebanon, NH, USA). Heat-killed *Listeria monocytogenes* (HKLM) was purchased from InvivoGen (Toulouse, France).

Cell lines and mice

The murine pancreatic adenocarcinoma cell line Panc02 was obtained from Prof. Lars Ivo Partecke (Greifswald, Germany). Cells were maintained in Dulbecco's modified eagle media (DMEM) supplemented with 10% heat-inactivated fetal bovine serum and antibiotics (PAA, Pasching, Austria). Murine melanoma B16-F10 cells were purchased from the American Type Culture Collection (ATCC, Manassas, VA, USA) and maintained in RPMI 1640 media supplemented with 10% heat-inactivated fetal bovine serum and antibiotics (PAA, Pasching, Australia). Both cell lines were cultured at 37 °C in humidified air with 5% carbon dioxide.

SPF C57BL/6 mice were purchased from Charles River Laboratories (Sulzfeld, Germany). B6.129S2-Cd4^{tm1Mak}/J mice (CD4$^{-/-}$ mice) and B6.129S2-Cd8a^{tm1Mak}/J mice (CD8$^{-/-}$ mice) were purchased from The Jackson Laboratory (Bar Harbor, ME, USA). All mice weighing between 18 g and 20 g were housed in specific pathogen-free barrier facilities with free access to sterile food and water; the photoperiod was 12/12.

Synthesis of mannan-BAM

Mannan-BAM was synthesized as previously described [10].

Tumor transplantation

Subcutaneous transplantation

Mice were subcutaneously injected with 4×10^5 Panc02 cells in 0.1 ml of DMEM or 4×10^5 B16-F10 cells in 0.1 ml of RPMI 1640 without additives into the previously shaved lower dorsal site (right or both right and left).

Intracranial transplantation

Mice were intraperitoneally injected with a mixture of ketamine (Narkamon, Bioveta, Czech Republic, 100 mg/kg) and xylazine (Rometar, Bioveta, Czech Republic, 5 mg/kg). Subsequently, the mice were intracranially injected with 1×10^5 Panc02 cells in 0.03 ml of DMEM without additives.

Treatment and its evaluation

MBTA therapy

50 µl of the therapeutic mixture consisting of 0.5 mg R-848 (HCl form), 0.5 mg poly(I:C), 0.5 mg LTA, and 0.4 mg

Hyaluronidase and hyaluronidase + anti-CD40 antibody therapy

Hyaluronidase (40,000 U/ml of PBS), anti-CD40 antibody (0.8 mg/ml of PBS), or their combination was injected intratumorally (50 µl/mouse) on following days: 1, 7, 14, 21, and 28.

Radiotherapy (RT)

RT was applied using a TrueBeam linear electron accelerator system (Varian Medical System, Palo Alto, California, USA). For anesthesia, the mice were intraperitoneally injected with a mixture of ketamine (100 mg/kg) and xylazine (5 mg/kg). Subsequently, the mice received a single fraction of 12-Gray on days 0, 14, and 28 (focused on relevant tumors only).

Anti-PD-L1 therapy

Anti-PD-L1 antibody (0.4 mg/ml of PBS) was injected intratumorally (50 µl/mouse) on the following days: 15, 18, 21, 24, 29, and 32.

All mice were housed individually. Tumor size was measured every other day using a caliper. The formula $V = (\pi/6) AB^2$, where A is the largest dimension of the tumor and B is the smallest dimension, was used to calculate tumor volume [14]. The reduction in tumor growth (%) as compared with control was calculated on day 14 using the following equation:

$$\frac{(\text{mean tumor volume in the control group} - \text{mean tumor volume in the treated group}) \times 100}{\text{mean tumor volume in the control group}}.$$

anti-CD40 per ml of 0.2 mM mannan-BAM in PBS was injected intratumorally on the following days: 0, 1, 2, 8, 9, 10, 16, 17, 18, 24, 25, and 26.

MBT therapy

Anti-CD40 was not included.

Anti-CTLA-4, HKLM, and EtOH therapy

Anti-CTLA-4 antibody (1 mg/ml of PBS), HKLM (10^9/ml of PBS), and EtOH (ethanol absolute) were injected intratumorally (50 µl/mouse) on the following days: 20, 27, and 34.

Statistical analysis

For analyses involving multiple groups and times, the area under the curve (AUC) was calculated, and statistical analysis was performed on AUC values using one-way ANOVA with Tukey's post hoc test. Kaplan–Meier survival curves were compared using a log-rank test. Data were analyzed using STATISTICA 12 (StatSoft, Inc., Tulsa, OK, USA). Error bars indicate the standard error of the mean (SEM).
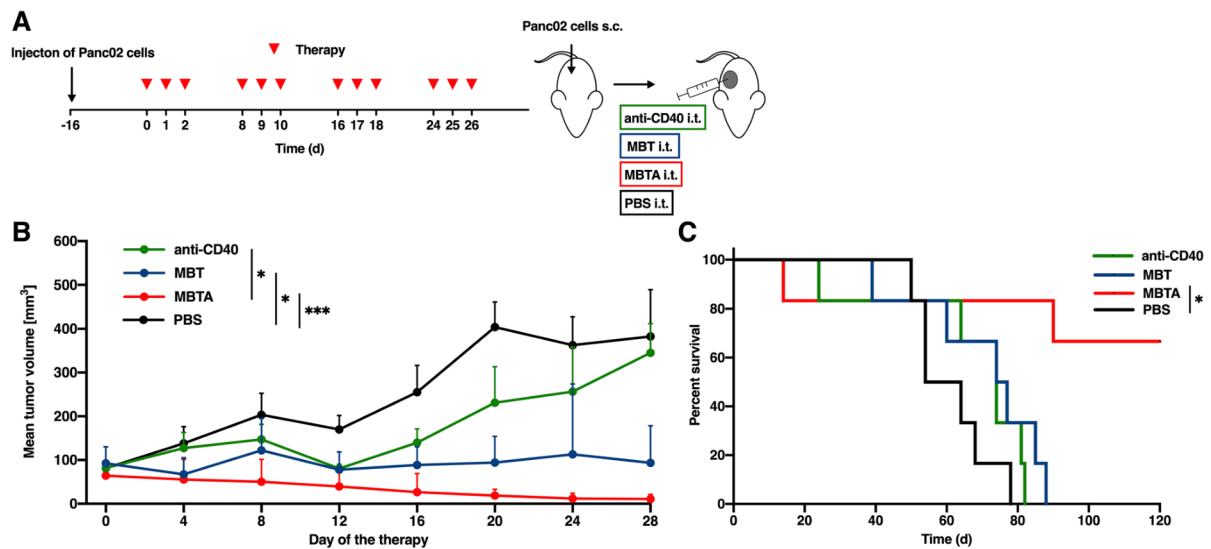
Fig. 1 MBTA therapy in established Panc02 tumors. **a** C57BL/6 mice were subcutaneously injected with Panc02 cells in the right flank. After 16 days, mice were randomized into 4 groups (n=6/group): the group treated with anti-CD40 antibody; the group treated with MBT therapy; the group treated with MBTA therapy; the group treated with PBS. Therapy was given intratumorally on days 0, 1, 2, 8, 9, 10, 16, 17, 18, 24, 25, and 26. The tumor volume was measured with a caliper. **b** The tumor volume growth is presented as a growth curve (*$p < 0.05$, ***$p < 0.005$). **c** The survival analysis is presented as a Kaplan–Meier curve (*$p < 0.05$)

Results

Eradication of established Panc02 tumors using MBTA therapy

In our previous study [11], MBTA therapy eradicated 80% of smaller Panc02 tumors with an average tumor volume of 44.1 ± 9.9 mm³ (at the beginning of the therapy, i.e., 12 days after Panc02 cells transplantation) and volume range of 19.5–78.9 mm³. Here, we applied MBTA therapy to established Panc02 tumors larger than in the previous study, averaging 79.7 ± 30.7 mm³ (at the beginning of the therapy, i.e., 16 days after Panc02 cells transplantation) and ranging from 32.8 to 136.5 mm³ in tumor volume. Despite the degree of tumor size, MBTA therapy achieved 67% complete eradication (Fig. 1). The experiment was repeated four times with different tumor sizes. It was confirmed that the complete elimination is dependent on initial size of the tumor (Fig. S1, Supplementary materials). We also confirmed the crucial role of anti-CD40 antibody in MBTA therapy for the effective treatment of Panc02 tumors. Although MBT therapy (without anti-CD40 antibody) only led to partial elimination of tumor growth, mice survival was comparable to that of the control group.

Additionally, MBTA-treated mice with complete tumor elimination (4 out of 6) were rechallenged on day 120 (day 0 as the start of therapy) with 1×10^6 Panc02 cells per mouse and revealed complete resistance against Panc02 retransplantation. The rechallenged mice initially developed small tumors in the first days after the transplantation, but subsequently, all tumors were eradicated (data not shown).

Underlying mechanisms of MBTA therapy in Panc02 tumors

In the first experiment, we used mice lacking CD4+ T lymphocytes (CD4$^{-/-}$ mice) or CD8+ T lymphocytes (CD8$^{-/-}$ mice). MBTA therapy used in these immunodeficient mice revealed a reduction in tumor growth in both groups (Fig. 2). In CD4$^{-/-}$ mice, growth reduction was only temporary, and tumor regrowth followed 45 days after the start of the therapy. Meanwhile, in CD8$^{-/-}$ mice, eradication of tumors was observed in 4 out of 6 mice. Subsequently, 3 out of these 4 cured mice were resistant to subcutaneous retransplantation of Panc02 cells (4×10^5 cells/mouse) performed on day 120 (day 0 as the start of the therapy) (data not shown). Our findings suggest a strong initial effect of innate immunity and the important role of adaptive immunity (mainly CD4+ T lymphocytes) in complete eradication of tumor and resistance to its recurrence.
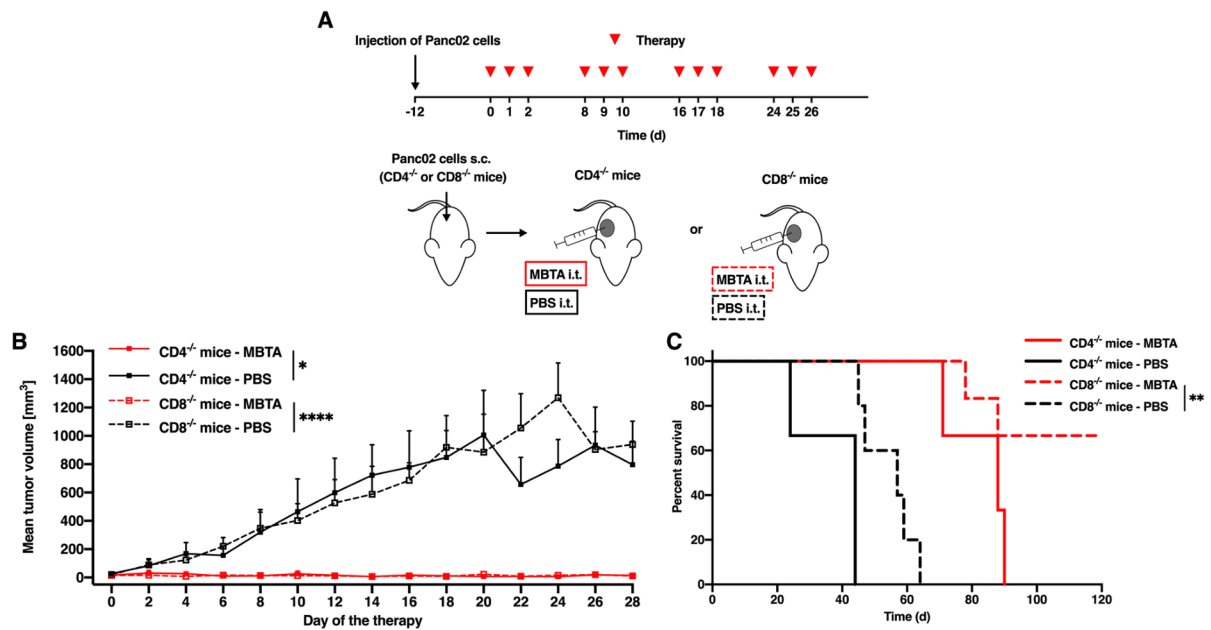
Fig. 2 MBTA therapy of Panc02 tumors and the role of CD4$^+$ T lymphocytes. **a** The CD4$^{-/-}$ and CD8$^{-/-}$ mice were subcutaneously injected with Panc02 cells in the right flank. After 12 days, both CD4$^{-/-}$ and CD8$^{-/-}$ mice were randomized into 4 groups (i) the CD4$^{-/-}$ mice treated with MBTA therapy (n=3); (ii) CD4$^{-/-}$ mice treated with PBS (n=3) (iii) the CD8$^{-/-}$ mice treated with MBTA therapy (n=6); (iv) the CD8$^{-/-}$ mice treated with PBS (n=5). Therapy was given intratumorally on days 0, 1, 2, 8, 9, 10, 16, 17, 18, 24, 25, and 26. The tumor volume was measured with a caliper. **b** The tumor volume growth is presented as a growth curve (*$p < 0.05$, ****$p < 0.001$). **c** The survival analysis is presented as a Kaplan–Meier curve (**$p < 0.01$)

Antigen specificity of immune memory induced by MBTA therapy

Mice-bearing Panc02 tumors were treated using MBTA therapy as described in Fig. 1. MBTA-treated mice with complete tumor elimination (4 out of 6 mice) were rechallenged with 4×10^5 Panc02 cells per mouse on day 120. All the mice were fully resistant and did not manifest subsequent tumor growth (data not shown). The rechallenge experiment was repeated on day 164 with 4×10^5 B16-F10 melanoma cells per mouse and resulted in rapid tumor growth (Fig. S2, Supplementary materials). Subsequent euthanization of these mice on day 203 followed due to the tumor growth. These results confirmed that the memory induced by MBTA therapy may be antigen specific.

Immune memory protects mice against intracranial Panc02 cells retransplantation

For this experiment, mice-bearing Panc02 tumors were also treated by MBTA therapy as described in Fig. 1 and 6 mice with complete tumor elimination (data not shown) were retransplanted with 1×10^5 Panc02 cells per mouse intracranially on day 120. For the control group, 8 healthy mice of the same age were used. Interestingly, MBTA-treated mice

showing complete tumor elimination were fully resistant to Panc02 intracranial transplantation. In contrast, all mice in the control group died 11–14 days after the Panc02 intracranial transplantation (Fig. S3, Supplementary materials). Dissection of these mice revealed intracranial Panc02 tumors averaging 17.1 ± 15.5 mm^3 in volume with a range of 2.1 – 32.8 mm^3.

MBTA therapy of metastatic Panc02: the bilateral tumor model

Metastatic disease is the biggest challenge of cancer therapy. As previously described [11], MBTA therapy can effectively suppress micrometastases in murine melanoma. However, for clinical purposes, more robust therapy is necessary to effectively eliminate advanced metastatic disease often caused by high-burden tumors. Therefore, we used the bilateral Panc02 model in our study. MBTA therapy was injected into the right tumor, and the left parallel (non-treated) tumor was observed for changes in its size (Fig. 3). The growth of the right MBTA-treated tumors was significantly reduced compared to that of the control (Fig. 3b), and tumor growth reduction was also observed in the left parallel (non-treated) tumors. The growth of the left parallel (non-treated) tumors was twice slower compared to that of the control (Fig. 3c).
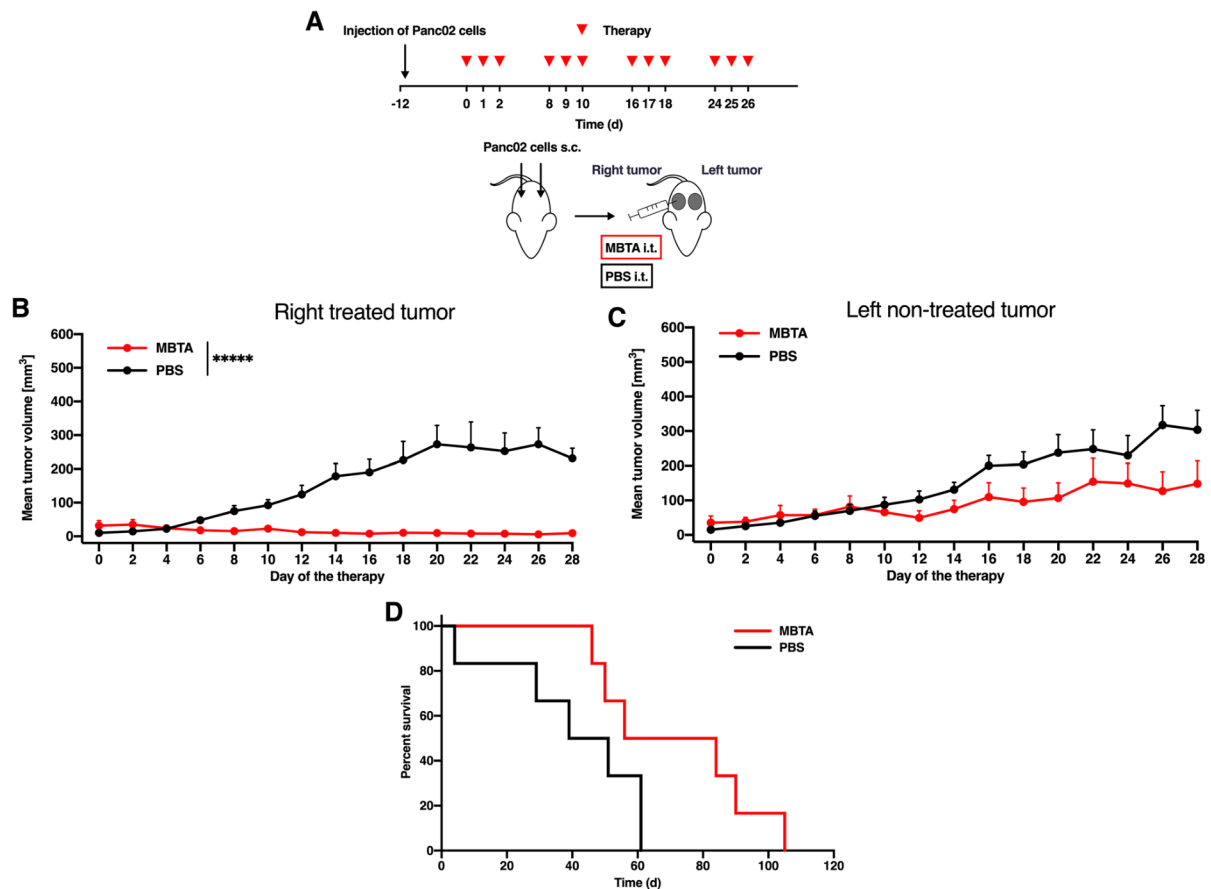
Fig. 3 MBTA therapy of the bilateral Panc02 model. **a** C57BL/6 mice were subcutaneously injected with Panc02 cells in both right and left flanks. After 12 days, mice were randomized into 2 groups (n = 6/group): (i) the group treated with MBTA therapy; (ii) the group treated with PBS. Therapy was given intratumorally into the right tumor on days 0, 1, 2, 8, 9, 10, 16, 17, 18, 24, 25, and 26. The tumor volume of both tumors was measured with a caliper. **b** The tumor volume growth of the right MBTA-treated and (**c**) the left parallel (non-treated) tumors is presented as a growth curve (*****$p < 0.0005$). **d** The survival analysis is presented as a Kaplan–Meier curve

Interestingly, we observed that the presence of the left parallel (non-treated) tumor negatively affected the efficacy of MBTA therapy in the right tumor. In one tumor model, the reduction in tumor size caused by MBTA therapy led to the complete elimination of tumors in the majority of the treated mice [11, 12]. In contrast, in the bilateral Panc02 tumor model, the initial reduction in size of right MBTA-treated tumors relapsed, and the Panc02 tumors grew in half of the experimental animals.

## Combination of MBTA therapy with other therapeutic approaches

Our results from the bilateral Panc02 tumor model suggested that MBTA therapy of only one tumor (the right MBTA-treated tumor) is not sufficient to eliminate the left parallel (non-treated) tumor. To boost the therapeutic effect of our proposed MBTA therapy, we simultaneously applied other therapeutic approaches on the left parallel tumor.

We first tested the intratumoral applications of anti-CTLA-4 antibody, heat-killed *Listeria monocytogenes*, and EtOH into the left parallel tumor with simultaneous application of MBTA therapy into the right tumor. Interestingly, we did not observe any augmentation on the therapeutic effect (Fig. S4, Supplementary materials).

Next, we focused on the manipulation of the Panc02 microenvironment, specifically on the reduction in extensive desmoplasia represented by the abundant presence of collagens, fibronectin, and hyaluronan in the intracellular space of Panc02 tumors. Desmoplasia limits the penetration of immune cells into the tumor, thus potentially
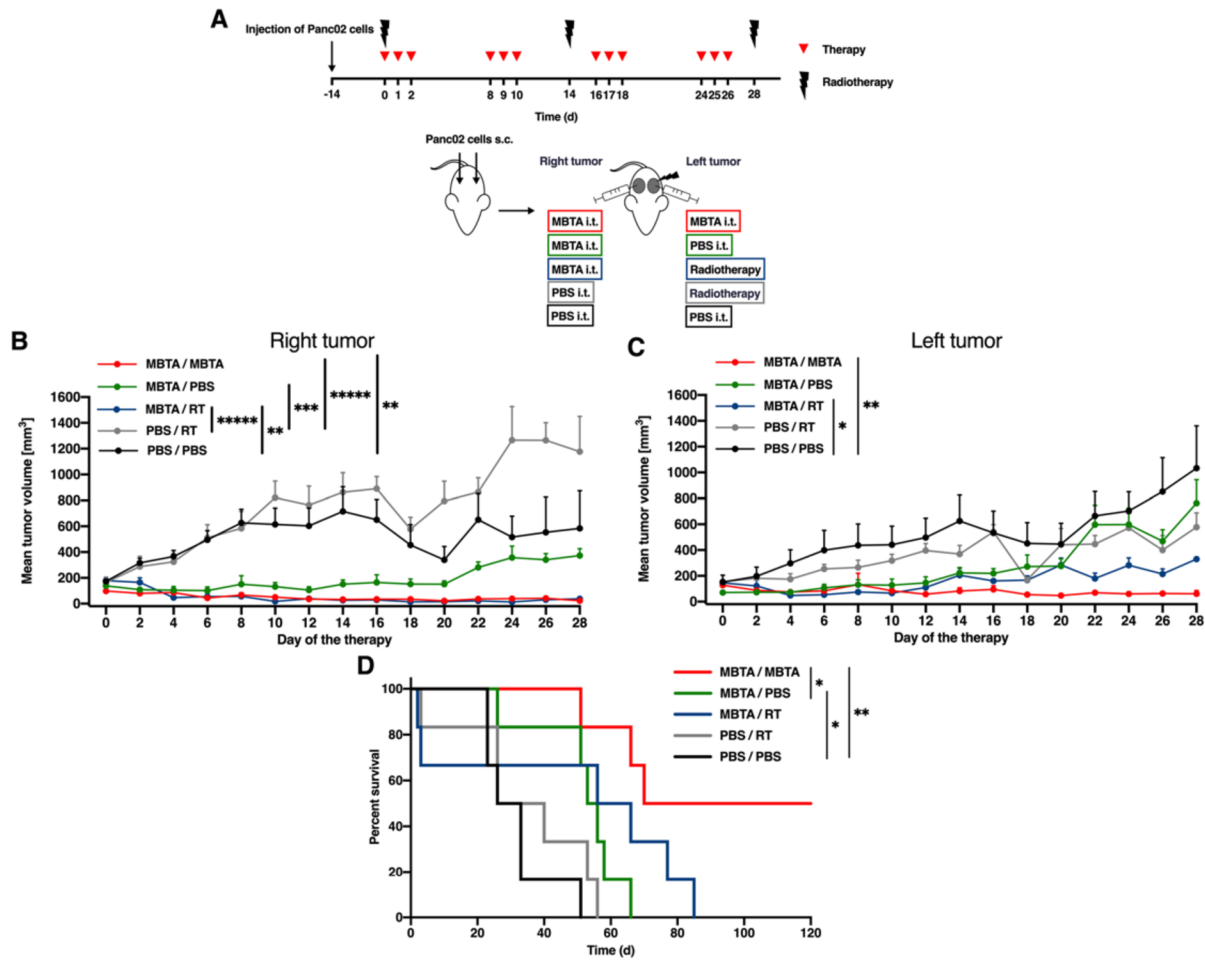
Fig. 4 Simultaneous MBTA therapy in the right and left parallel Panc02 tumors and irradiation of the left parallel tumor. **a** C57BL/6 mice were subcutaneously injected with Panc02 cells in both right and left flanks. After 12 days, mice were randomized into 5 groups (n=6/group): the group treated with MBTA therapy (right and left tumor); the group treated with MBTA therapy (right tumor) and PBS (left tumor); the group treated with MBTA therapy (right tumor) and radiotherapy (RT) (left tumor); the group treated with PBS (right tumor) and RT (left tumor); the group treated with PBS (right tumor) and RT (left tumor); the group treated with PBS (both tumors). Therapy was given intratumorally into the right or parallel tumor on days 0, 1, 2, 8, 9, 10, 16, 17, 18, 24, 25, and 26. The left parallel tumors were irradiated on days 0, 14, and 28. The tumor volume of both tumors was measured with a caliper. **b** The tumor volume growth of the right MBTA-treated and (**c**) the left parallel-treated tumors is presented as a growth curve (*$p < 0.05$, **$p < 0.01$, ***$p < 0.005$, *****$p < 0.0005$). **d** The survival analysis is presented as a Kaplan–Meier curve (*$p < 0.05$, **$p < 0.01$)

suppressing immunotherapeutic outcomes [15]. The right tumors were treated by MBTA therapy, whereas the left parallel tumors were injected with anti-CD40 and hyaluronidase to decrease the density of protein fraction and to degrade hyaluronan, respectively [16, 17]. Interestingly, the effects of anti-CD40 antibody, hyaluronidase, and their combination were negligible (Fig. S5, Supplementary materials).

Simultaneous MBTA therapy and its combination with radiotherapy in the bilateral Panc02 model

Lastly, we tested the simultaneous application of MBTA therapy into both right and left tumors and combined MBTA therapy of the right tumor with RT of the left parallel tumor in the bilateral Panc02 model. Panc02 tumors were utilized with the right tumors averaging 150.5 ± 62.9 mm^3 with a range of 72.3–247.0 mm^3, whereas the left parallel tumors averaged 129.9 ± 76.5 mm^3 and ranged from 55.1 to 398.8 mm^3.

Simultaneous application of MBTA therapy resulted in 96% reduction in right tumor volume and 87% reduction in left tumor volume as compared to that of the control (Fig. 4b, c). The reduction in tumor volume was accompanied by a significant prolongation of survival (Fig. 4d). Meanwhile, combined MBTA therapy with RT exhibited a therapeutic effect, as manifested by 67% growth reduction of left parallel tumors compared to that of the control group (Fig. 4c) with slight prolongation of survival (Fig. 4d). Because RT results in elevated expression of PD-L1 expression in tumors [18], we additionally tested the intratumoral application of anti-PD-L1 antibodies into the left parallel irradiated tumors. However, no additional therapeutic effects were observed (data not shown).

Moreover, we observed that the presence of the left parallel (non-treated) tumors negatively affected the efficacy of MBTA therapy in the right tumors (Fig. 4b, c, green curves), which corresponds with the aforementioned observation discussed in "MBTA therapy of metastatic Panc02: the bilateral tumor model."

Discussion

We showed that MBTA therapy had a significant therapeutic effect not only in smaller but also in larger murine Panc02 tumors, as evidenced by the significant tumor growth reduction and tumor eradication in 67% of the treated animals and subsequent resistance against tumor rechallenge. Focusing on the underlying immune mechanisms involved in MBTA therapy, we observed that the presence of $CD4^+$ T lymphocytes was not critical for significant tumor growth reduction. However, $CD4^+$ T lymphocytes seem to be essential for delayed tumor response, long survival, and resistance against tumor rechallenge. When MBTA therapy was applied to subcutaneous murine bilateral Panc02 model, we observed a partial therapeutic effect on the left parallel (non-treated) tumor. To boost its therapeutic effect, we combined MBTA therapy with several different therapeutic approaches, such as intratumoral applications of anti-CTLA-4 antibody, heat-killed *Listeria monocytogenes* (HKLM), and EtOH (chemoablation), targeting the Panc02 microenvironment (reduction in extensive desmoplasia), simultaneous application of MBTA therapy into the distant tumor, and its combination with RT. Among these, only simultaneous application of MBTA therapy on the primary and distant tumors showed the most promising therapeutic outcomes in murine bilateral Panc02 model.

Tumor size is an important factor for successful cancer treatment. Although small tumors show better response to various therapeutic options, high-burden tumors remain a major challenge [19]. In a previous study, we successfully applied MBTA therapy in smaller subcutaneous Panc02

tumors (± 44.1 mm^3). In the present study, we investigated its therapeutic effect on larger established Panc02 tumors (± 79.7 mm^3) because they more closely mimic the real situation in patients during initial diagnosis and present a great challenge in cancer therapy. Interestingly, we achieved 67% complete eradication of Panc02 tumors using MBTA therapy, which was slightly less than the 80% complete eradication of smaller Panc02 from our previous study [11]. We also verified the importance of the presence of anti-CD40 antibodies in MBTA therapy, ensuring long-lasting survival of treated mice and tumor resistance during retransplantation. This is consistent with previously published Panc02 and murine pheochromocytoma data where the addition of anti-CD40 to MBT therapy also resulted in an increase in the overall survival of treated mice. Interestingly, the addition of anti-CD40 does not have any significant effect on reduction of tumor growth [11, 12].

We then focused on the underlying mechanisms of MBTA therapy in the Panc02 tumor model. Surprisingly, MBTA therapy fully suppressed tumor growth in the absence of either $CD4^+$ T lymphocytes ($CD4^{-/-}$ mice) or $CD8^+$ T lymphocytes ($CD8^{-/-}$ mice). However, the presence of $CD4^+$ T lymphocytes seems to be important for long-lasting survival of mice and for resistance against tumor retransplantation. Resistance against retransplantation (75%) in $CD8^{-/-}$ mice could be interpreted based on the $CD4^+$ T lymphocyte-driven macrophage activity [20–22]. However, a further study focused on the role of $CD4^+$ in immune memory after MBTA therapy must be performed.

Subsequently, we also studied the antigen specificity involved in the mechanism of immune memory induced by MBTA therapy. MBTA therapy has shown 100% resistance against retransplantation of Panc02 tumor cells [11]. However, it remains unknown if this resistance is antigen specific. Therefore, mice with MBTA-therapy-eradicated Panc02 tumors were rechallenged with Panc02 tumor cells and B16-F10 murine melanoma cells. Interestingly, all mice manifested resistance against Panc02, but resistance against B16-F10 was not observed, suggesting that the immunological memory induced by MBTA therapy is antigen specific for each type of tumor.

To further investigate the immune memory induced by MBTA therapy, we retransplanted Panc02 cells into the immune-privileged site—the central nervous system (intracranial tumor cell retransplantation). All mice previously treated by MBTA therapy showed resistance as compared to the control group, in which all animals died 11–14 days after Panc02 injection. These data are consistent with MBTA therapy of CT26, where all mice were protected against subcutaneous and intracranial retransplantation with the same tumor cells [13]. This revealed the ability of the immune memory induced by MBTA therapy to cross over

the blood–brain barrier, confirming its potential applicability in metastatic brain tumors.

The eradication of metastases is an important aspect of successful cancer treatment. Previously, we observed that MBTA therapy of the primary tumor is associated with growth reduction or elimination of small metastases [11, 12]. However, in larger distant Panc02 metastases, particularly in the bilateral Panc02 model, only limited anti-tumor effect was observed, and we, therefore, focused on the enhancement of this distant therapeutic effect. In the first set of experiments, we tested the application of anti-CTLA-4 antibody, heat-killed *Listeria monocytogenes* (HKLM), and EtOH (chemoablation) into the left tumor with simultaneous application of MBTA therapy into the right tumor. Anti-CTLA-4 antibody was expected to enhance the immune attack through depletion of Tregs [23]. HKLM was supposed to stimulate acute inflammation in the tumor [24] and change the pro-tumor environment into an anti-tumor one. Chemoablation is known to lead to cell membrane lysis, protein denaturation, vascular occlusion, and eventually tumor cell death [25]. Despite their proven individual anti-tumorigenic effects, no therapeutic improvement was detected when combined with MBTA therapy.

In the second set of experiments, we focused on the manipulation of Panc02 environment, specifically on the reduction in desmoplasia. Anti-CD40 antibody and hyaluronidase were applied into the left tumor with the simultaneous application of MBTA therapy into the right tumor. Anti-CD40 antibody was used to decrease the density of protein fraction (collagen I, fibronectin) [17], whereas hyaluronidase was used to degrade hyaluronan [16]. Neither of these substances nor their combination increased the therapeutic effect of MBTA therapy on distant tumors. As previously mentioned, advanced tumors possess protection against immune attack on many different levels; therefore, targeting just one of these levels is insufficient.

To improve the MBTA therapy's outcome on distant tumors, we also tested its simultaneous application into the primary tumor (right tumor) and distant metastases (left tumor), resulting in 87% left tumor growth reduction and complete eradication of both tumors in 50% of the mice. These results suggest that the targeted application of MBTA therapy into primary tumors with simultaneous application into metastases can result in successful treatment of metastatic disease. The combination of MBTA therapy and RT showed promising results in tumor growth reduction but did not show a significant difference in survival of treated mice.

Panc02 tumors with higher tumor burden remain a challenge for modern cancer treatment. Even though the proposed MBTA therapy showed promising results in established murine Panc02 tumors and bilateral Panc02 tumors, we are still far away from completely curing these challenging tumors. Nevertheless, our study showed that only

simultaneous application of MBTA therapy into the primary tumor and distant metastases improved the outcomes of large established and metastatic Panc02 tumors. As we discussed previously [8], this combination of TLR ligands, mannan-BAM, and anti-CD40 antibody has the potential to result ineffective treatments for patients with inoperable tumors or as a neoadjuvant therapy before surgery. Moreover, several TLR ligands and anti-CD40 antibodies are already in clinical trials or FDA-approved which can significantly speed up the potential application of MBTA therapy in the clinic [26, 27].

Declarations

Conflict of interest The authors declare that they have no conflict of interest.

Ethical approval and ethical standards All experimental procedures involving mice were performed in accordance with the laws of the Czech Republic. The experimental Project was approved by the Ministry of Education, Youth, and Sports of the Czech Republic (Protocol No. 12098/2016-2).

References

1. Rawla P, Sunkara T, Gaduputi V (2019) Epidemiology of pancreatic cancer: global trends, etiology and risk factors. World J Oncol 10(1):10–27. https://doi.org/10.14740/wjon1166
2. Kleeff J, Korc M, Apte M, La Vecchia C, Johnson CD, Biankin AV, Neale RE, Tempero M, Tuveson DA, Hruban RH, Neoptolemos JP (2016) Pancreatic cancer. Nat Rev Dis Primers 2:16022. https://doi.org/10.1038/nrdp.2016.22
3. Neesse A, Bauer CA, Ohlund D, Lauth M, Buchholz M, Michl P, Tuveson DA, Gress TM (2019) Stromal biology and therapy in pancreatic cancer: ready for clinical translation? Gut 68(1):159–171. https://doi.org/10.1136/gutjnl-2018-316451
4. Royal RE, Levy C, Turner K, Mathur A, Hughes M, Kammula US, Sherry RM, Topalian SL, Yang JC, Lowy I, Rosenberg SA (2010) Phase 2 trial of single agent Ipilimumab (anti-CTLA-4) for locally advanced or metastatic pancreatic adenocarcinoma. J Immunother 33(8):828–833. https://doi.org/10.1097/CJI.0b013e3181eec14c
5. Brahmer JR, Tykodi SS, Chow LQ, Hwu WJ, Topalian SL, Hwu P, Drake CG, Camacho LH, Kauh J, Odunsi K, Pitot HC, Hamid O, Bhatia S, Martins R, Eaton K, Chen S, Salay TM, Alaparthy S, Grosso JF, Korman AJ, Parker SM, Agrawal S, Goldberg SM, Pardoll DM, Gupta A, Wigginton JM (2012) Safety and activity

of anti-PD-L1 antibody in patients with advanced cancer. N Engl J Med 366(26):2455–2465. https://doi.org/10.1056/NEJMoa1200694

6. Darvin P, Toor SM, Sasidharan Nair V, Elkord E (2018) Immune checkpoint inhibitors: recent progress and potential biomarkers. Exp Mol Med 50(12):165. https://doi.org/10.1038/s12276-018-0191-1

7. Hargadon KM, Johnson CE, Williams CJ (2018) Immune checkpoint blockade therapy for cancer: an overview of FDA-approved immune checkpoint inhibitors. Int Immunopharmacol 62:29–39. https://doi.org/10.1016/j.intimp.2018.06.001

8. Uher O, Caisova V, Hansen P, Kopecky J, Chmelar J, Zhuang Z, Zenka J, Pacak K (2019) Coley's immunotherapy revived: innate immunity as a link in priming cancer cells for an attack by adaptive immunity. Semin Oncol. https://doi.org/10.1053/j.seminoncol.2019.10.004

9. Janotova T, Jalovecka M, Auerova M, Svecova I, Bruzlova P, Maierova V, Kumzakova Z, Cunatova S, Vlckova Z, Caisova V, Rozsypalova P, Lukacova K, Vacova N, Wachtlova M, Salat J, Lieskovska J, Kopecky J, Zenka J (2014) The use of anchored agonists of phagocytic receptors for cancer immunotherapy: B16-F10 murine melanoma model. PLoS ONE 9(1): https://doi.org/10.1371/journal.pone.0085222

10. Waldmannova E, Caisova V, Faberova J, Svackova P, Kovarova M, Svackova D, Kumzakova Z, Jackova A, Vacova N, Nedbalova P, Horka M, Kopecky J, Zenka J (2016) The use of Zymosan A and bacteria anchored to tumor cells for effective cancer immunotherapy: B16-F10 murine melanoma model. Int Immunopharmacol 39:295–306. https://doi.org/10.1016/j.intimp.2016.08.004

11. Caisova V, Uher O, Nedbalova P, Jochmanova I, Kvardova K, Masakova K, Krejcova G, Padoukova L, Chmelar J, Kopecky J, Zenka J (2018) Effective cancer immunotherapy based on combination of TLR agonists with stimulation of phagocytosis. Int Immunopharmacol 59:86–96. https://doi.org/10.1016/j.intimp.2018.03.038

12. Caisova V, Li L, Gupta G, Jochmanova I, Jha A, Uher O, Huynh TT, Miettinen M, Pang Y, Abunimer L, Niu G, Chen X, Ghayee HK, Taieb D, Zhuang Z, Zenka J, Pacak K (2019) The significant reduction or complete eradication of subcutaneous and metastatic lesions in a pheochromocytoma mouse model after immunotherapy using mannan-BAM, TLR ligands, and anti-CD40. Cancers (Basel). https://doi.org/10.3390/cancers11050654

13. Medina R, Wang HR, Caisova V, Cui J, Indig IH, Uher O, Ye J, Nwankwo A, Sanchez V, Wu TX, Nduom E, Heiss J, Gilbert MR, Terabe M, Ho W, Zenka J, Pacak K, Zhuang ZP (2020) Induction of immune response against metastatic tumors via vaccination of mannan-BAM, TLR ligands, and anti-CD40 antibody (MBTA). Adv Ther Germany. https://doi.org/10.1002/adtp.202000044

14. Li J, Piao YF, Jiang Z, Chen L, Sun HB (2009) Silencing of signal transducer and activator of transcription 3 expression by RNA interference suppresses growth of human hepatocellular carcinoma in tumor-bearing nude mice. World J Gastroenterol 15(21):2602–2608. https://doi.org/10.3748/wjg.15.2602

15. Kunk PR, Bauer TW, Slingluff CL, Rahma OE (2016) From bench to bedside a comprehensive review of pancreatic cancer immunotherapy. J Immunother Cancer 4:14. https://doi.org/10.1186/s40425-016-0119-z

16. Kultti A, Li X, Jiang P, Thompson CB, Frost GI, Shepard HM (2012) Therapeutic targeting of hyaluronan in the tumor stroma. Cancers (Basel) 4(3):873–903. https://doi.org/10.3390/cancers4030873

17. Long KB, Gladney WL, Tooker GM, Graham K, Fraietta JA, Beatty GL (2016) IFNgamma and CCL2 cooperate to redirect tumor-infiltrating monocytes to degrade fibrosis and enhance chemotherapy efficacy in pancreatic carcinoma. Cancer Discov 6(4):400–413. https://doi.org/10.1158/2159-8290.CD-15-1032

18. Azad A, Yin Lim S, D'Costa Z, Jones K, Diana A, Sansom OJ, Kruger P, Liu S, McKenna WG, Dushek O, Muschel RJ, Fokas E (2017) PD-L1 blockade enhances response of pancreatic ductal adenocarcinoma to radiotherapy. EMBO Mol Med 9(2):167–180. https://doi.org/10.15252/emmm.201606674

19. Jackaman C, Bundell CS, Kinnear BF, Smith AM, Filion P, van Hagen D, Robinson BW, Nelson DJ (2003) IL-2 intratumoral immunotherapy enhances CD8 + T cells that mediate destruction of tumor cells and tumor-associated vasculature: a novel mechanism for IL-2. J Immunol 171(10):5051–5063. https://doi.org/10.4049/jimmunol.171.10.5051

20. Haabeth OA, Tveita AA, Fauskanger M, Schjesvold F, Lorvik KB, Hofgaard PO, Omholt H, Munthe LA, Dembic Z, Corthay A, Bogen B (2014) How do CD4(+) T cells detect and eliminate tumor cells that either lack or express MHC class II molecules? Front Immunol 5:174. https://doi.org/10.3389/fimmu.2014.00174

21. Bogen B, Fauskanger M, Haabeth OA, Tveita A (2019) CD4(+) T cells indirectly kill tumor cells via induction of cytotoxic macrophages in mouse models. Cancer Immunol Immunother. https://doi.org/10.1007/s00262-019-02374-0

22. Eisel D, Das K, Dickes E, Konig R, Osen W, Eichmuller SB (2019) Cognate interaction with CD4(+) T cells instructs tumor-associated macrophages to acquire M1-like phenotype. Front Immunol 10:219. https://doi.org/10.3389/fimmu.2019.00219

23. Tang F, Du X, Liu M, Zheng P, Liu Y (2018) Anti-CTLA-4 antibodies in cancer immunotherapy: selective depletion of intratumoral regulatory T cells or checkpoint blockade? Cell Biosci 8:30. https://doi.org/10.1186/s13578-018-0229-z

24. Park DW, Kim JS, Chin BR, Baek SH (2012) Resveratrol inhibits inflammation induced by heat-killed Listeria monocytogenes. J Med Food 15(9):788–794. https://doi.org/10.1089/jmf.2012.2194

25. Mathers BW, Harvey HA, Dye CE, Dougherty-Hamod B, Moyer MT (2014) Endoscopic ultrasound-guided ethanol ablation of a large metastatic carcinoid tumor: success with a note of caution. Endosc Int Open 2(4):E256–E258. https://doi.org/10.1055/s-0034-1377612

26. Anwar MA, Shah M, Kim J, Choi S (2019) Recent clinical trends in Toll-like receptor targeting therapeutics. Med Res Rev 39(3):1053–1090. https://doi.org/10.1002/med.21553

27. Vonderheide RH (2020) CD40 agonist antibodies in cancer immunotherapy. Annu Rev Med 71:47–58. https://doi.org/10.1146/annurev-med-062518-045435-045435

Chapter V

Identification of Immune Cell Infiltration in Murine Pheochromocytoma
During Combined Mannan-BAM, TLR Ligand, and Anti-CD40 Antibody-Based
Immunotherapy

Article

Identification of Immune Cell Infiltration in Murine Pheochromocytoma during Combined Mannan-BAM, TLR Ligand, and Anti-CD40 Antibody-Based Immunotherapy

Ondrej Uher [1,2], Thanh-Truc Huynh [1], Boqun Zhu [1,3], Lucas A. Horn [4], Veronika Caisova [1], Katerina Hadrava Vanova [1], Rogelio Medina [5], Herui Wang [5], Claudia Palena [4], Jindrich Chmelar [2], Zhengping Zhuang [5], Jan Zenka [2] and Karel Pacak [1,*]

[1] Section on Medical Neuroendocrinology, *Eunice Kennedy Shriver* National Institute of Child Health and Human Development, NIH, Bethesda, MD 20892, USA; ondrej.uher@nih.gov (O.U.); huynht@mail.nih.gov (T.-T.H.); zhu.boqun@zs-hospital.sh.cn (B.Z.); vcaisova@childrensnational.org (V.C.); katerina.hadravavanova@nih.gov (K.H.V.)
[2] Department of Medical Biology, Faculty of Science, University of South Bohemia, 37005 Ceske Budejovice, Czech Republic; chmelar@prf.jcu.cz (J.C.); jzenka@prf.jcu.cz (J.Z.)
[3] Endoscopy Center and Endoscopy Research Institute, Zhongshan Hospital, Fudan University, Shanghai 200032, China
[4] Laboratory of Tumor Immunology and Biology, Center for Cancer Research, National Cancer Institute, NIH, Bethesda, MD 20892, USA; lucas.horn@nih.gov (L.A.H.); palenac@mail.nih.gov (C.P.)
[5] Neuro-Oncology Branch, National Cancer Institute, NIH, Bethesda, MD 20892, USA; rogelio.medina@nih.gov (R.M.); herui.wang@nih.gov (H.W.); zhengping.zhuang@nih.gov (Z.Z.)
* Correspondence: karel@mail.nih.gov; Tel.: +1-301-402-4594

Simple Summary: Multiple types of primary tumors and metastases that present with very little if any immune cell infiltration (so-called immunologically "cold" tumors) do not respond to current immunotherapies. In this study, we show that recently developed intratumoral application-based immunotherapy using mannan-BAM, TLR ligands, and anti-CD40 antibody (MBTA therapy) efficiently suppresses tumor growth in a murine bilateral pheochromocytoma model. Moreover, MBTA therapy increases the recruitment of innate immune cells followed by adaptive immune cells not only to primary (injected) tumors but also distal (non-injected) tumors. We also demonstrated that after successful MBTA therapy of subcutaneous pheochromocytoma, long-term immunological memory is driven by CD4^{+} T cells. Taken together, this study helps to better understand the systemic effect of MBTA therapy and its use for tumor and metastasis reduction or even elimination.

Abstract: Immunotherapy has become an essential component in cancer treatment. However, the majority of solid metastatic cancers, such as pheochromocytoma, are resistant to this approach. Therefore, understanding immune cell composition in primary and distant metastatic tumors is important for therapeutic intervention and diagnostics. Combined mannan-BAM, TLR ligand, and anti-CD40 antibody-based intratumoral immunotherapy (MBTA therapy) previously resulted in the complete eradication of murine subcutaneous pheochromocytoma and demonstrated a systemic antitumor immune response in a metastatic model. Here, we further evaluated this systemic effect using a bilateral pheochromocytoma model, performing MBTA therapy through injection into the primary tumor and using distant (non-injected) tumors to monitor size changes and detailed immune cell infiltration. MBTA therapy suppressed the growth of not only injected but also distal tumors and prolonged MBTA-treated mice survival. Our flow cytometry analysis showed that MBTA therapy led to increased recruitment of innate and adaptive immune cells in both tumors and the spleen. Moreover, adoptive CD4^{+} T cell transfer from successfully MBTA-treated mice (i.e., subcutaneous pheochromocytoma) demonstrates the importance of these cells in long-term immunological memory. In summary, this study unravels further details on the systemic effect of MBTA therapy and its use for tumor and metastasis reduction or even elimination.

1. Introduction

The currently increased interest in cancer immunotherapy is based on numerous clinical benefits in the treatment of different tumor types [1]. Nevertheless, systemic delivery of immunotherapeutic drugs, especially various checkpoint inhibitors, might cause severe off-target toxicities, reportedly exhibiting a dose-related effect [2]. Moreover, these therapies are quite expensive, and in some tumors, the therapeutic outcomes are suboptimal. In contrast, intratumoral therapies result in high drug concentration within the tumor microenvironment, while small amounts of drugs are used, leading to lower systemic drug concentration, reduced side effects, and substantial cost reduction [3]. Furthermore, several recent studies have shown that intratumoral drug administration could induce a systemic immune response even in distal non-treated tumors, followed by their successful growth inhibition or even elimination [3,4].

Pheochromocytoma (PHEO) and paraganglioma (PGL) are rare neuroendocrine tumors derived from neural crest cells [5]. Up to 30% of all PHEO/PGL cases develop metastases for which therapeutic options are still very limited [6]. PHEO/PGL can also be considered as immunologically "cold" tumors due to their low amounts of neoantigens, low somatic mutation burden, and lack of leukocyte infiltration [7–9]. Currently, there are only two clinical trials that include immunotherapy in metastatic/inoperable PHEO/PGL, specifically, systemic application of different checkpoint inhibitors nivolumab + ipilimumab and pembrolizumab (identifiers: NCT02834013 and NCT02721732) [10].

The basics of the immunotherapeutic approach used here were published previously by our group and are based on the intratumoral injection of mannan anchored to the tumor cell surface via a biocompatible anchor for cell membrane (BAM), a mixture of toll-like receptor (TLR) ligands, and agonistic anti-CD40 monoclonal antibody (MBTA therapy). Mannan is a *Saccharomyces cerevisiae*-derived polysaccharide that serves as a ligand stimulating phagocytosis via the activation of the complement lectin pathway and resulting in iC3b production and subsequent tumor cell opsonization [11–13]. TLR ligands support the infiltration of immune cells into tumors, as well as their activation. The combination of TLR ligands (resiquimod, polyinosinic-polycytidylic acid, and lipoteichoic acid) has been previously assessed as the most potent approach. Resiquimod (R-848) is an imidazoquinolinamine and synthetic analog of viral ssRNA that activates immune cells via the TLR7/8 and TLR7 pathways in humans and mice, respectively [14]. Polyinosinic-polycytidylic acid (poly(I:C)) is a synthetic analog of dsRNA that activates immune cells via the TLR3 pathway [15]. Finally, lipoteichoic acid (LTA) is a constituent of the *Bacillus subtilis* cell wall, activating the immune cells via the TLR2 pathway [16]. Anti-CD40 is an agonistic antibody that mimics the CD40 ligand expressed on helper (CD4$^+$) T cells. The ligation of CD40 on macrophages, dendritic cells, and B cells leads to activation of these cells, enhances antigen presentation, and induces an effective T cell anti-tumor response [17–19]. Previous research publications, leading to the current components of MBTA therapy, have been published here [12,20,21] and summarized in this review [22].

MBTA therapy has been previously tested in various subcutaneous murine models. In the melanoma B16-F10 model, MBTA therapy, even without anti-CD40, demonstrated the eradication of tumors in 83% of treated animals. In the aggressive pancreatic adenocarcinoma model (Panc02), the efficacy of therapy was observed in 80% of the treated animals [20]. When tested in primary and bilateral tumor models of colon carcinoma (CT26), MBTA therapy resulted in the slower progression and prolonged survival of the treated animals [23]. Finally, in the murine subcutaneous PHEO model, MBTA therapy resulted in the complete elimination of tumors in 62.5% of mice, significantly decreased the

bioluminescence signal intensity of metastatic organ lesions, and prolonged the survival of MBTA-treated mice when tested on metastatic PHEO [24].

All the aforementioned studies have focused heavily on local immune responses in MBTA-injected tumors. Therefore, in the present study, we assessed immune responses induced by intratumoral MBTA therapy using a bilateral PHEO tumor model that mimics the presence of both primary and distal tumors and enables the real-time analysis of both tumor types, including the assessment of immune cell trafficking into these tumors [25,26]. First, we established a bilateral PHEO model and studied the systemic immune response during intratumoral MBTA therapy in primary (injected) and distal (non-injected) tumors. We demonstrate that MBTA therapy could suppress the growth of not only injected but also distal tumors. Second, we describe the detailed infiltration of innate and adaptive cells in injected and distal tumors, as well as the changes in the spleen during MBTA therapy. Flow cytometry analysis showed the ability of MBTA therapy to increase the recruitment of innate and adaptive immune cells in both tumors and the spleen. Finally, we demonstrated the importance of CD4$^+$ cells in immunological memory after successful MBTA therapy. The results of this study are essential for a better understanding of how MBTA therapy contributes to tumor growth reduction or even elimination, including metastases. Such an understanding would further help optimize this therapeutic approach with future vision using it in clinical trials to fight metastatic cancers.

2. Materials and Methods

2.1. Mannan-BAM Synthesis and MBTA Therapy

Mannan from *Saccharomyces cerevisiae*; lipoteichoic acid (LTA) from *Bacillus subtilis*; polyinosinic-polycytidylic acid, sodium salt (poly(I:C)); ammonium acetate, and natrium cyanoborohydride were obtained from Sigma-Aldrich (St. Louis, MO, USA). BAM was obtained from NOF Corporation (White Plains, NY, USA). Resiquimod (R-848) was obtained from Tocris Bioscience (Minneapolis, MN, USA). Monoclonal anti-CD40 (clone FGK4.5/FGK45) was obtained from BioXCell (West Lebanon, NH, USA). Aminated mannan was prepared by reductive amination. Mannan solution in an environment of ammonium acetate (300 mg/mL) was reduced by 0.2 M natrium cyanoborohydride at pH 7.5 and 50 °C for five days. The solution was further dialyzed using a MWCO 3500 dialysis tube (Serva, Heildelberg, Germany) against PBS at 4 °C overnight. Binding of BAM on the amino group of mannan was performed at pH 7.3 according to the methodology described by Kato et al. [27]. For 1 h at room temperature, the N-hydroxysuccinimide (NHS) group of BAM was allowed to react with the amino group of mannan. Solution of mannan-BAM was obtained after dialysis, as described above, and stored frozen at −20 °C. Mice were treated intratumorally on days 0, 1, 2, 8, 9, 10, 16, 17, 18, 24, 25, and 26 with 50 µL of MBTA therapeutic mixture consisting of 0.5 mg R-848 (HCl form), 0.5 mg poly(I:C), 0.5 mg LTA, and 0.4 mg anti-CD40 per mL of 0.2 mM mannan-BAM in PBS. MBTA therapy was always only applied to the right tumor.

2.2. Cell Lines, Mice, and Tumor Establishment

The MTT-luc cells (mouse tumor tissue–luciferase cells) used in this study are rapidly growing cells derived from liver metastases of MPC (mouse pheochromocytoma cells) and transfected with a luciferase plasmid [28,29]. The cells were maintained in Dulbecco's modified Eagle medium (DMEM) (Sigma-Aldrich) supplemented with 10% of heat-inactivated fetal bovine serum (Gemini, West Sacramento, CA, USA), 100 U/mL of penicillin/streptomycin (Gemini), and 750 µg/mL of geneticin (Thermo Fisher Scientific, Waltham, MA, USA) for stable cell line selection. Cells were cultured at 37 °C in humidified air with 5% CO$_2$. The cell lines were tested for mycoplasma using a MycoAlert™ detection kit purchased from Lonza (Walkersville, MD, USA).

Female B6(Cg)- *Tyr*$^{c-2J}$/J (B6 albino) mice were purchased from the Jackson Laboratory (Bar Harbor, ME, USA). Mice were housed in specific pathogen-free barrier facilities with free access to sterile food and water, with a photoperiod of 12/12.

For the subcutaneous PHEO model, mice were subcutaneously injected in the previously shaved right flank with 3×10^6 MTT-luc cells in DMEM (0.2 mL) without additives. For the bilateral PHEO model, mice were subcutaneously injected in both the previously shaved right and left flank with 3×10^6 MTT-luc cells in 0.2 mL of DMEM without additives (each site).

2.3. Antibodies for Flow Cytometry

Antibodies purchased from BioLegend (San Diego, CA, USA) included PerCP-Cy5.5 anti-mouse/human CD44 (clone IM7), Alexa Fluor® 700 anti-mouse CD3ε (clone 500A2), APC/Cy7 anti-mouse CD45 (clone 30-F11), Brilliant Violet 785™ anti-mouse CD8a (clone 53-6.7), Brilliant Violet 711™ anti-mouse CD4 (clone RM4-5), Brilliant Violet 785™ anti-mouse CD19 (clone 6D5), APC anti-mouse/human CD11b (clone M1/70), PeCP-Cy5.5 anti-mouse Ly-6C (clone HK1.4), FITC anti-mouse Ly-6G (clone 1A8), Brilliant Violet 711™ anti-mouse F4/80 (clone BM8), Alexa Fluor® 700 anti-mouse I-A/I-E (clone M5/114.15.2), Brilliant Violet 605™ anti-mouse CD335 (NKp46) (clone 29A1.4), Brilliant Violet 421™ anti-mouse CD62L (clone MEL-14), APC anti-mouse CD366 (Tim-3) (clone B8.2C12), PE anti-mouse CD279 (PD-1) (clone 29F.1A12), and Brilliant Violet 421™ anti-mouse CD38 (clone 90). BV605 anti-mouse CD11c (clone HL3) was purchased from BD Biosciences (San Jose, CA, USA).

2.4. Isolation of Cells Infiltrating the Tumors and Spleen and Flow Cytometry Analysis

Tumor-bearing mice were euthanized by cervical dislocation, followed by the collection of blood samples, spleens, and tumors. Spleens were processed into single-cell suspensions via mechanical dissociation, filtration (70 μm), and erythrocyte lysis. Tumors were weighed, mechanically dissociated, and digested using a digestion cocktail composed of collagenase types I and IV (both 1 mg/mL) (Thermo Fisher Scientific) and deoxyribonuclease I (40 U/mL) (Invitrogen, Carlsbad, CA, USA). After an incubation of 1 h at 37 °C with constant agitation, the samples were centrifuged and the supernatants were collected and used for ELISA-based cytokine detection. Cell pellets were passed through 70 μm filters, then tumor-infiltrating cells were isolated by density gradient centrifugation. Briefly, each pellet was resuspended in 40% Percoll™ PLUS (GE Healthcare, Chicago, IL, USA)/Hanks' balanced salt solution, overlaid with a 70% Percoll™ PLUS/HBSS, and the interface was isolated after 30 min of centrifugation ($800\times g$). Subsequently, the cells were incubated for 30–45 min with the antibodies. Dead cells were excluded using the LIVE/DEAD™ Fixable Aqua Dead Cell Stain Kit (Thermo Fisher Scientific). CountBright™ absolute counting beads (Invitrogen) were used to count the absolute numbers of individual CD45$^+$ cells. All analyses were performed using an Attune NxT Flow Cytometer (Thermo Fisher Scientific) and interpreted using the FlowJo™ software (version 10.6.1, Beckon Dickinson, Ashland, OR, USA). The flow cytometry analysis of immune cell subsets was defined as follows: CD4$^+$ T cells = CD45$^+$ CD3$^+$ CD4$^+$; CD8$^+$ T cells = CD45$^+$ CD3$^+$ CD8$^+$; TCM = CD45$^+$ CD3$^+$ CD44$^+$ CD62L$^+$; TE/EM = CD45$^+$ CD3$^+$ CD44$^+$ CD62L$^-$; neutrophil = CD45$^+$ CD11b$^+$ F4/80$^-$ Ly6G$^+$ Ly6C^{lo}; monocyte = CD45$^+$ CD11b$^+$ F4/80$^-$ Ly6G$^-$ Ly6C^{hi}; dendritic cell = CD45$^+$ CD11b$^-$ F4/80$^-$ CD11c$^+$; NK cell = CD45$^+$ CD3$^+$ CD335$^+$; macrophage = CD45$^+$ CD11b$^+$ F4/80$^+$, M1-like macrophage = CD45$^+$ CD11b$^+$ F4/80$^+$ CD279$^-$ CD38^{hi}; M2-like macrophage = CD45$^+$ CD11b$^+$ F4/80$^+$ CD279$^{+/-}$ CD38^{lo}. A representative gating strategy could be found in the Supplementary Materials (Figures S2 and S3). The M1/M2 ratios were calculated as percentages of M1-like macrophages divided by M2-like macrophages.

2.5. Adoptive CD4$^+$ and CD8$^+$ T Cell Transfer

Splenocytes were isolated from cured MBTA-treated donor mice previously bearing subcutaneous PHEO (MTT-luc cells) and untouched control donor mice of the same age ($n = 5$ per group). CD4$^+$ or CD8$^+$ T cells were isolated from a single-cell suspension of splenocytes after ACK lysis using a MACS negative selection kit (Miltenyi Biotec, Auburn,

CA, USA). The procedures were performed according to the manufacturer's instructions. Subsequently, cells were diluted in PBS and 2.5×10^6 cells (CD4$^+$ or CD8$^+$ T cells) in a volume of 0.2 mL were intraperitoneally injected into recipient mice (n = 5 per group). The purity of the preparations was 94 and 93% for the CD4$^+$ and CD8$^+$ T cells, respectively. After 7 days, recipient mice received a subcutaneous injection of MTT-luc cells as described above.

2.6. Cytokine Assay

Tumor supernatants and plasma collected during the analysis of tumor-infiltrating cells were used to measure IFN-γ and IL-10 levels, using the IFN-γ ELISA Kit, Extra Sensitive (Thermo Fisher Scientific, Waltham, MA, USA), and IL-10 (LSBio, Seattle, WA, USA) for detection.

2.7. Data and Statistical Analysis

The tumor volume was measured with a caliper and calculated as $V = (\pi/6)AB^2$ (where A and B stand for the largest and the smallest dimensions of the tumor, respectively). For the tumor growth analysis, the area under the curve (AUC) was calculated until treatment day 20. Statistical analysis was performed on these AUC values using *t*-test (Mann–Whitney test). Reduction of tumor growth (%) was determined as follows: $\frac{(AUC\ value\ in\ control\ group - AUC\ value\ in\ treated\ group) \times 100}{AUC\ value\ in\ control\ group}$. Kaplan–Meier survival curves were compared using a log-rank test. For the flow cytometry and ELISA test data analysis, multiple *t*-tests were used. Data were analyzed using the GraphPad Prism software version 8 for Mac OS (GraphPad Software, La Jolla, CA, USA). The error bars indicate the standard errors of the mean (SEM). The pictures were created using BioRender.com.

3. Results

3.1. Effect of MBTA Therapy on the Bilateral PHEO Model

To better understand the systemic immune response generated by the intratumoral MBTA therapy and immune cell trafficking into injected (primary) and non-injected (distal) tumors, we first established a bilateral PHEO model. Mice were subcutaneously injected with MTT-luc cells in both the right and left flanks. After 35 days, the average tumor volume on the right and left sites were 59.5 and 22.0 mm^3, ranging between 6.9–118.0 and 6.0–34.9 mm^3. MBTA therapy was applied to the primary tumor, and both the primary and distal tumors were observed for size changes (Figure 1A). The growth of the MBTA-injected (Figure 1B) and distal tumors (Figure 1C) got reduced during MBTA therapy, although it was not completely eliminated. Until day 20 from the start of the treatment, the reduction of tumor growth of the MBTA-injected tumors and the distal tumors was 76.8% and 72.7%, respectively. However, both the MBTA-injected and distal tumors started to grow after day 20, despite ongoing MBTA therapy (last treatment cycle was given at days 24–26). Non-injected (distal) tumors showed a strong increase in tumor volume, whereas MBTA-injected tumors showed only a moderate increase. Nevertheless, we observed the prolonged survival of MBTA-treated mice compared to the control (Figure 1D). These results confirmed that the intratumoral application of MBTA therapy in primary tumors induced systemic effects on distal tumors, resulting in significantly improved survival of the MBTA-treated mice.
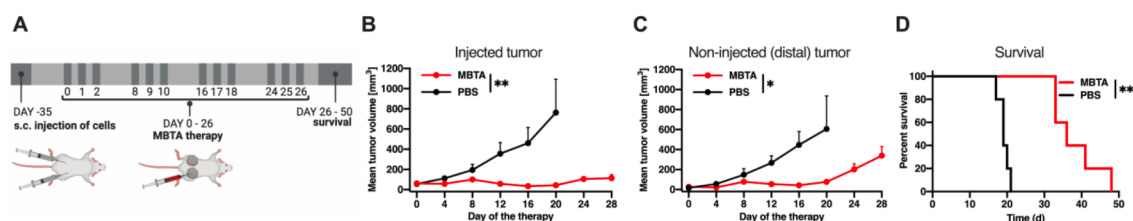
Figure 1. Bilateral subcutaneous PHEO mouse model. (**A**) Experimental design diagram of MBTA therapy in the bilateral subcutaneous PHEO mouse model. (**B**) The tumor volume growth of the injected and (**C**) the distal tumors presented as growth curves (*n* = 5 per group) (* *p* < 0.05, ** *p* < 0.01). (**D**) The survival analysis presented as a Kaplan–Meier curve (** *p* < 0.01).

3.2. Characterization of Tumor Infiltrating and Splenic Leukocytes, as Well as Innate Immune Cells during MBTA Therapy

First, flow cytometry analyses of tumor-infiltrating leukocytes were performed to assess the detailed immune profiles of injected (primary) and non-injected (distal) tumors, as well as those of spleens during MBTA or PBS therapy (Figure 2A). The results from these analyses revealed that intratumoral MBTA therapy significantly increased the number of leukocytes ($CD45^+$ cells) in both the injected and distal tumors compared to the control (Figure 2B). The number of splenic leukocytes significantly increased only on day 5 after the first MBTA injection cycle (Figure 2B). Further assessment of innate leukocyte subpopulations revealed striking and site-specific inflammatory responses in the MBTA-treated mice. Neutrophils were significantly increased in the injected but almost absent in the distal tumors during MBTA therapy, while in the spleen, neutrophils were elevated after the third therapeutic cycle (day 21) (Figure 2C). The number of monocytes was elevated in both tumor types of MBTA-treated mice during the entire therapy and increased in the spleen from day 13 (Figure 2D). The number of dendritic cells (DCs) was significantly elevated in the injected and distal tumors after the second MBTA therapeutic cycle (day 13). Interestingly, the number of DCs in the spleen consistently increased during the therapy (Figure 2E). The number of natural killer (NK) cells in the MBTA-injected tumors were significantly increased 5 days after the start of the treatment, while distal tumors demonstrated such an increase 13 days after the start of the treatment (Figure 2F).

We also focused on two major phenotypes of macrophages, M1-like and M2-like macrophages. The overall macrophage number significantly increased directly after the first MBTA therapeutic cycle (day 5) in the injected tumors. Such an increase was observed in distal tumors and in the spleen after the second therapeutic cycle (day 13) (Figure 2G). In both injected and distal tumors, the percentage of classically activated M1-like macrophages significantly increased only on day 5 (Figure 2H). Of note, the percentage of alternatively activated M2-like macrophages significantly decreased in injected and distal tumors as well as in the spleens of MBTA-treated mice when compared to the control group throughout the treatment course (Figure 2I). Thus, the ratio of M1-like to M2-like macrophages (M1/M2) in both tumors and spleens was significantly higher in the MBTA-treated group than in the control group (Figure 2J), suggesting the ability of MBTA therapy to systematically activate macrophages, increase trafficking into tumors, and decrease the induction of immunosuppressive M2-like phenotype.

When MBTA-injected tumors were compared with distal tumors, all types of innate cells, except DCs, were significantly elevated only in MBTA-injected tumors and not in distal tumors after the first cycle of treatment (day 5), underscoring MBTA's ability to induce an immune response first in injected tumors and subsequently in distal tumors (Figure S1).

In summary, these results demonstrate that intratumoral injection of MBTA therapy significantly augmented the trafficking of innate immune cells not only within distal non-treated tumors and within the spleen.
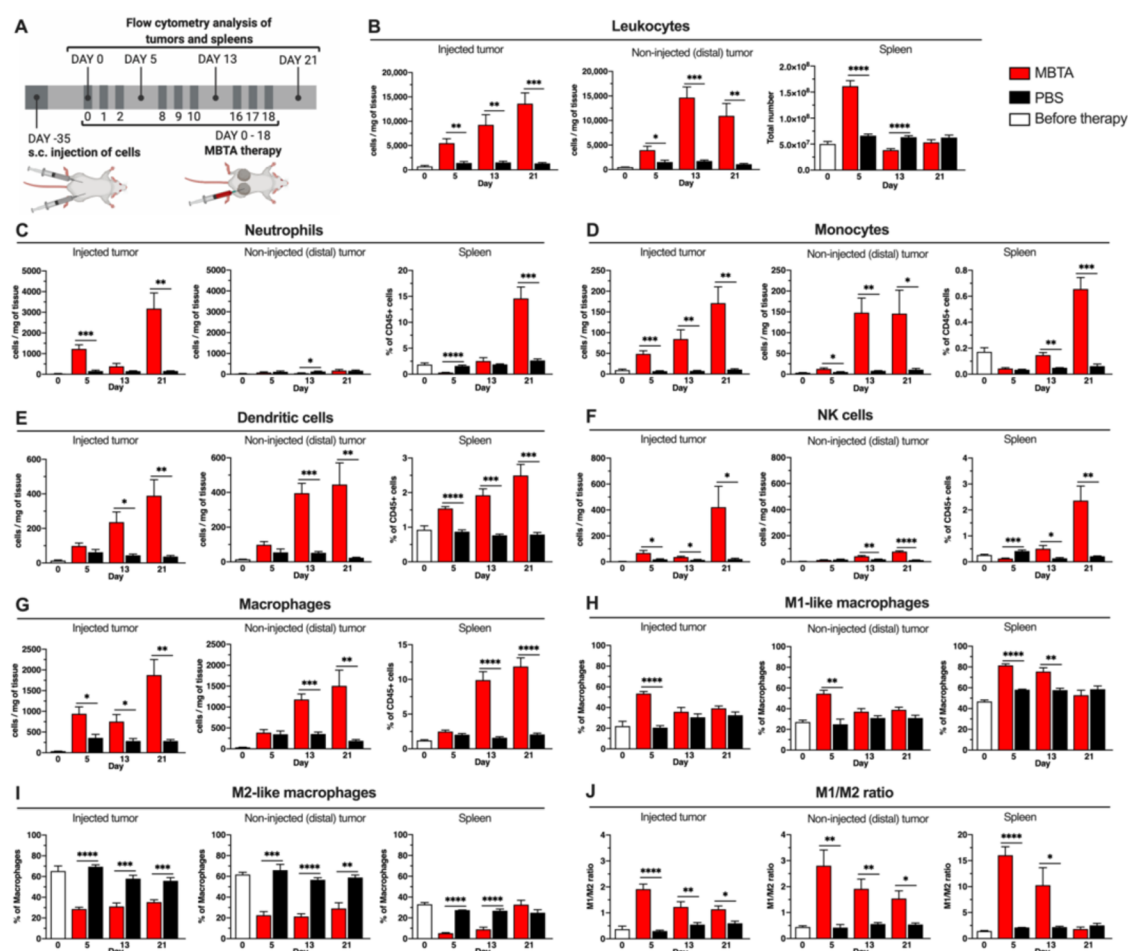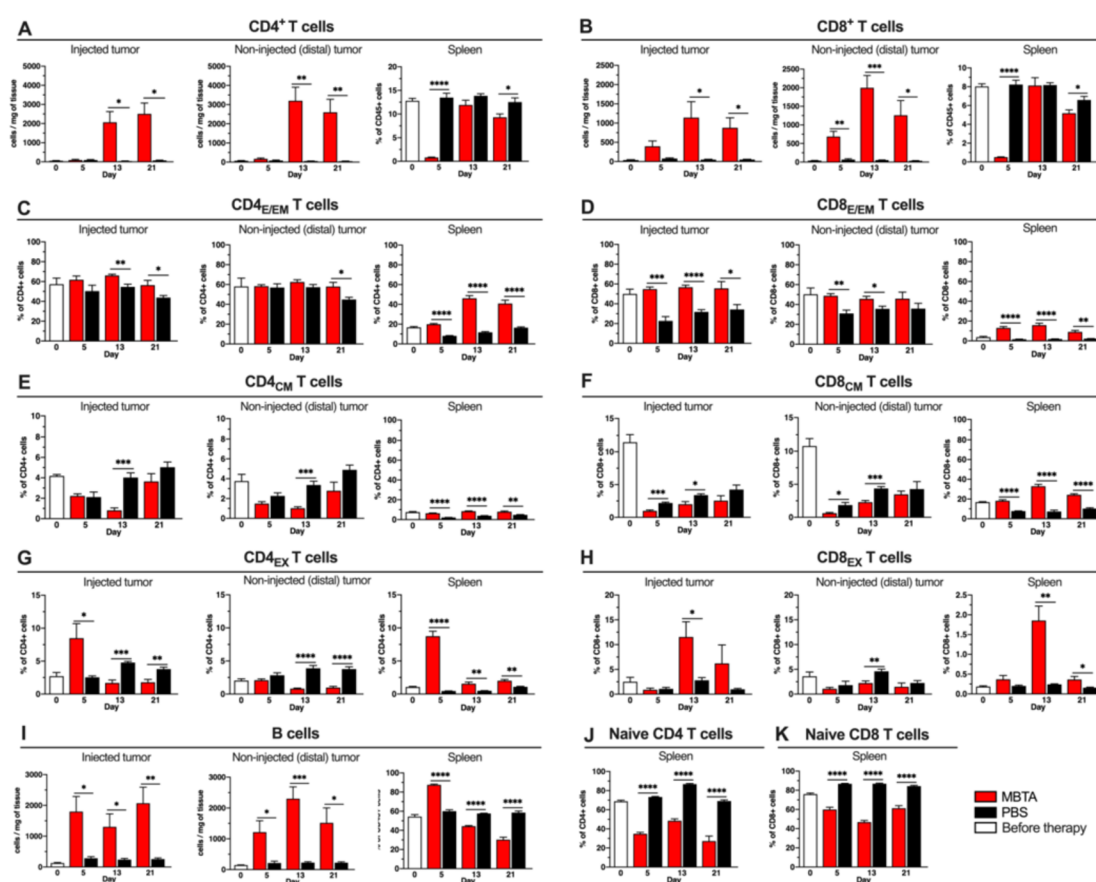
Figure 2. Flow cytometry analysis of tumor infiltrating leukocytes and innate immune cells. (**A**) Experimental design diagram of the flow cytometry analysis. The results from the analysis of injected and distal tumors and spleens: (**B**) leukocytes (CD45$^+$), (**C**) neutrophils (CD45$^+$ CD11b$^+$ F4/80$^-$ Ly6G$^+$ Ly6C^{lo}), (**D**) monocytes (CD45$^+$ CD11b$^+$ F4/80$^-$ Ly6G$^-$ Ly6C^{hi}), (**E**) DCs (CD45$^+$ CD11b$^-$ F4/80$^-$CD11c$^+$), (**F**) NK cells (CD45$^+$ CD3$^+$ CD335$^+$), (**G**) Macrophages (CD45$^+$ CD11b$^+$ F4/80$^+$), (**H**) M1-like macrophages (CD45$^+$ CD11b$^+$ F4/80$^+$ CD279$^-$ CD38^{hi}), (**I**) M2-like macrophages (CD45$^+$ CD11b$^+$ F4/80$^+$ CD279$^{+/-}$ CD38^{lo}), (**J**) M1/M2 ratio ($n = 5$ per group/day) (* $p < 0.05$, ** $p < 0.01$, *** $p < 0.001$, **** $p < 0.0001$).

3.3. Characterization of Tumor Infiltrating and Splenic Lymphocytes during MBTA Therapy

Tumor-infiltrating lymphocytes (TILs) and their subpopulations were similarly explored using flow cytometry. TIL analyses showed strong infiltration of helper CD4$^+$ and cytotoxic CD8$^+$ T cells in both the injected and distal tumors (Figure 3A,B). The CD4$^+$ T cells significantly increased after the second MBTA therapeutic cycle (day 13). In contrast, in both tumors, CD8$^+$ T cells were already elevated after the first therapeutic cycle but statistical significance could be observed only in distal tumors. The analysis of the splenic T cells revealed a strong decrease in CD4$^+$ and CD8$^+$ T cells directly after the first therapeutic cycle compared to the control. A higher increase in the proportion of effector/effector memory T cells (E/EM, CD44$^+$ CD62L$^-$) in the tumors of MBTA-treated mice during the entire therapy was observed in CD8$_{E/EM}$ and less so in CD4$_{E/EM}$. The proportion of splenic CD4$_{E/EM}$ and CD8$_{E/EM}$ T cells was significantly elevated during the entire MBTA therapy

compared to that in the control (Figure 3C,D). The assessment of the central memory (CM, CD44$^+$ CD62L$^+$) CD4$^+$ or CD8$^+$ T cells in the tumors did not show a significantly higher percentage of these cells in the MBTA-treated group. In contrast, a significant increase in the percentage of both CD4$_{CM}$ and CD8$_{CM}$ T cells could be observed in the spleens of MBTA-treated mice compared to the control (Figure 3E,F). We could observe differences in the exhausted T cells (EX, PD1$^+$ TIM3$^+$) in the tumors in CD4$_{EX}$, where MBTA-injected tumors displayed a higher proportion of these cells on day 5 compared to the control. However, at the end of the analysis, a significantly higher CD4$_{EX}$ T cell percentage proportion could be observed in the tumors of the control group than in those of the MBTA-treated group. The splenic CD4$_{EX}$ T cells in the MBTA-treated mice were significantly higher during the entire therapy than in the control. We could observe significant increases in the CD8$_{EX}$ T cells of the MBTA-treated mice only in the injected tumor and spleen on day 13 (Figure 3G,H).


Figure 3. Flow cytometry analysis of tumor infiltrating lymphocytes and their subpopulations in injected and distal tumors. B6(Cg)- *Tyr*$^{c-2J}$/J mice were treated and flow cytometry analysis was performed as described in Figure 2. (**A**) CD4$^+$ T cells (CD45$^+$ CD3$^+$ CD4$^+$), (**B**) CD8$^+$ T cells (CD45$^+$ CD3$^+$ CD8$^+$), (**C**) CD4$_{E/EM}$ T cells (CD45$^+$ CD3$^+$ CD4$^+$ CD44$^+$ CD62L$^-$), (**D**) CD8$_{E/EM}$ T cells (CD45$^+$ CD3$^+$ CD8$^+$ CD44$^+$ CD62L$^-$), (**E**) CD4$_{CM}$ T cells (CD45$^+$ CD3$^+$ CD4$^+$ CD44$^+$ CD62L$^+$), (**F**) CD8$_{CM}$ T cells (CD45$^+$ CD3$^+$ CD8$^+$ CD44$^+$ CD62L$^+$), (**G**) CD4$_{EX}$ T cells (CD45$^+$ CD3$^+$ CD4$^+$ PD1$^+$ TIM3$^+$), (**H**) CD8$_{EX}$ T cells (CD45$^+$ CD3$^+$ CD8$^+$ PD1$^+$ TIM3$^+$), (**I**) B cells (CD45$^+$ CD19$^+$), (**J**) Naïve CD4 T cells (CD45$^+$ CD3$^+$ CD4$^+$ CD44$^-$ CD62L$^+$), (**K**) Naïve CD8 T cells (CD45$^+$ CD3$^+$ CD8$^+$ CD44$^-$ CD62L$^+$) (*n* = 5 per group/day) (* *p* < 0.05, ** *p* < 0.01, *** *p* < 0.001, **** *p* < 0.0001).

Splenic naïve CD4$^+$ and CD8$^+$ T cells were significantly lower in the MBTA-treated mice than in the control during the entire therapy (Figure 3J,K). The B cell analysis showed strong infiltration in both tumors of the MBTA-treated mice. Interestingly, the number of splenic B cells was highest after the first therapeutic, and 90% of all leukocytes in the spleen were B cells. However, after day 5, the number of B cells in the spleen constantly decreased (Figure 3I).

In summary, CD4$^+$ T cells were the most abundant T lymphocytes in both the injected and distal tumors. The highest changes in the TIL subpopulation percentage proportions were observed in the CD8$_{E/EM}$ T cells in both the injected and distal tumors of the MBTA-treated mice. All T lymphocyte splenic subpopulations, except for the naïve T cells, were elevated during MBTA therapy compared to those in the control, suggesting strong T cell activation upon MBTA therapy.

3.4. IFN-γ and IL-10 Level Detection in the Bilateral PHEO Model

To characterize whether the immune response in the injected and distal tumors is pro- or anti-inflammatory, we measured the IFN-γ and IL-10 levels. The ELISA assays revealed significantly elevated pro-inflammatory IFN-γ levels in both tumors, mostly after the second MBTA therapeutic cycle on day 13 (Figure 4A). The level of anti-inflammatory IL-10 in the MTBA tumors were 8-fold lower (~0.05 pg/mg) than the level of IFN-γ (~0.4 pg/mg). More precisely, a significant IL-10 level difference could be observed in MBTA-injected tumors on day 5 and in distal tumors on day 13 (Figure 4B). The IFN-γ plasma levels in MBTA-treated mice were 200-fold higher (~2000 pg/mL) than in the control (~10 pg/mL), whereas the IL-10 plasma levels were below the detection limit. When we calculated the IFN-γ/IL-10 ratio, we detected significant differences in the injected tumors on day 21 and in distal tumors on days 13 and 21, underscoring the pro-inflammatory microenvironment that was established by the MBTA therapy (Figure 4C).
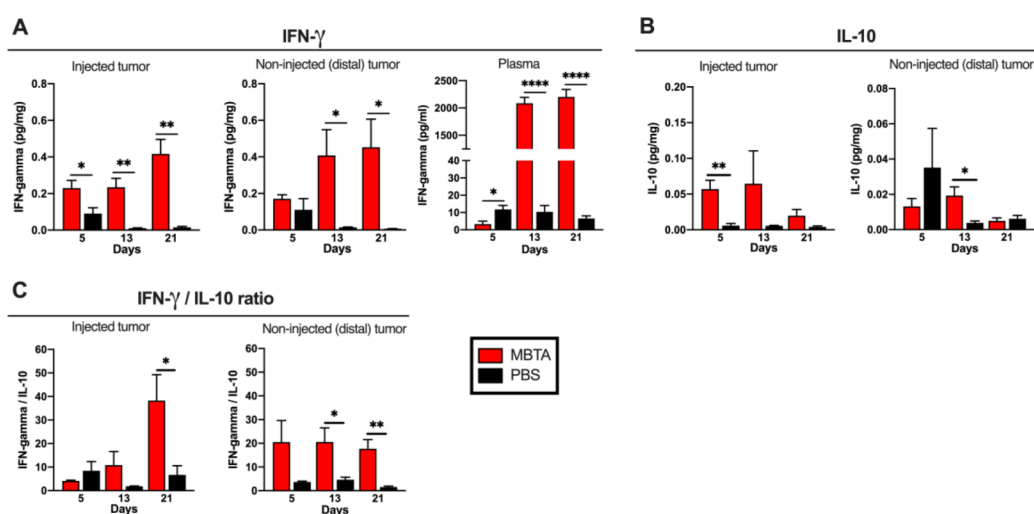
Figure 4. IFN-γ and IL-10 levels in the injected and distal tumors. (**A**) IFN-γ levels and (**B**) IL-10 levels from tumor samples measured by ELISA. (**C**) IFN-γ/IL-10 ratio in tumors (*n* = 5 per group/day) (* *p* < 0.05, ** *p* < 0.01, **** *p* < 0.0001).

3.5. The Immune Memory after MBTA Therapy Is CD4$^+$ T Cell-Dependent

To determine whether immunological memory against PHEO following MBTA therapy could be generated by CD4$^+$ or CD8$^+$ T cells, we performed their adoptive transfer. Mice were injected with MTT-luc cells in the right flank (subcutaneous PHEO), and after tumor development, they were treated with MBTA therapeutic mixture as described above.

Mice that remained tumor-free for 120 days after the start of MBTA therapy were used as donor mice. Seven days after adoptive transfer of CD4+ or CD8+ T cells, recipient mice were subcutaneously injected with MTT-luc cells in the right flank and were monitored for PHEO tumor development (Figure 5A).
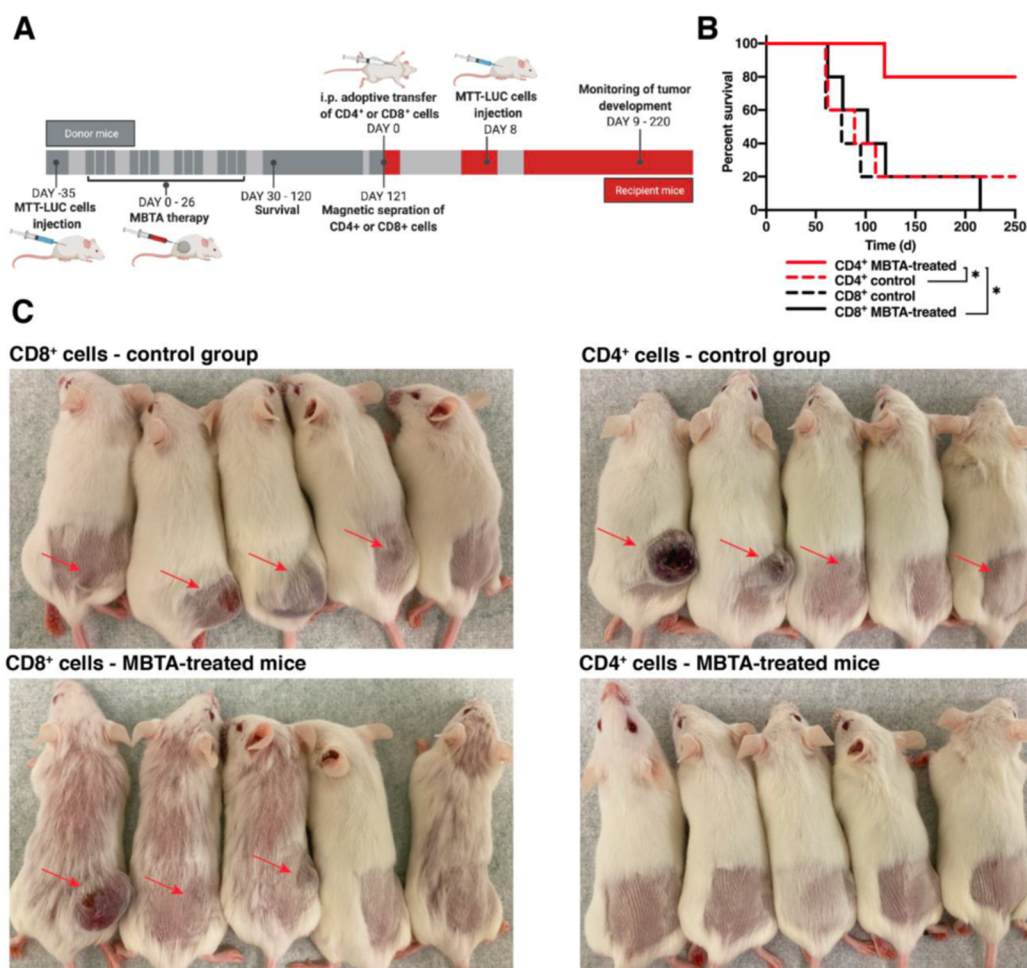
Figure 5. Adoptive transfer of CD4+ or CD8+ T cells. (**A**) Experimental design diagram of adoptive transfer. (**B**) The survival analysis is presented as a Kaplan-Meier curve (*n* = 5 per group) (* *p* < 0.05). (**C**) Pictures of recipient mice taken after 60 days from the MTT-luc inoculation.

Interestingly, flow cytometry analysis, performed 120 days after the start of treatment, revealed no significant changes in the numbers of leukocytes, CD4+, and CD8+ T cells, and their effector/effector memory, central memory, and exhausted subpopulations in spleens of MBTA-treated mice when compared to the same age control mice.

On day 60 after the adoptive transfer, tumor rejection was observed in 40% of recipient mice with CD8+ T cells from MBTA-treated mice (2 from 6 mice), 100% of recipient mice with CD4+ T cells from MBTA-treated mice, and in 20% of both control groups with CD4+ or CD8+ T cells (Figure 5C). Mice were observed for tumor development for 250 days after adoptive transfer and by the end of this observation period, all mice that received donor CD8+ T cells from MBTA treated mice developed tumor, whereas 80% of mice that

received donor CD4$^+$ T cells from MBTA treated mice were protected against the tumor development (Figure 5B). Collectively, these data suggest the importance of CD4$^+$ T cells in the rejection of tumor cells after successful MBTA therapy.

4. Discussion

In the present study, we focused on MBTA therapy-induced systemic immune responses. First, we used a bilateral PHEO model, in which one tumor was injected with MBTA therapeutic mixture and it was observed along with non-injected (distal) tumors for their size changes. The growth of MBTA-injected and distal tumors decreased during the first 20 days of therapy, followed by the subsequent growth of both tumors. In line with a significantly reduced tumor growth rate, MBTA-treated mice also demonstrated significantly prolonged survival compared to the control, underscoring MBTA therapeutic efficacy against representative primary and distal tumors. To analyze which immune cells were involved in this disease model and its response to MBTA therapy, we focused on characterizing innate and adaptive immune cell trafficking and infiltration in MBTA-injected and distal tumors, as well as in the spleen. Our data demonstrated that MBTA therapy displays a unique potential to increase innate immune cell infiltration not only in injected but also in distal tumors. MBTA therapy increased the M1/M2 ratio in both the tumors and the spleen. The adaptive immune cell assessment revealed very effective CD4$^+$ and CD8$^+$ T cell infiltration in both tumor types in MBTA-treated mice, with the highest-level changes observed in the CD8$_{E/EM}$ T cells. Finally, we also demonstrated the importance of CD4$^+$ T cells in long-lasting immune memory after MBTA therapy of subcutaneous PHEO. Taken together, these data suggest that the MBTA therapy-induced PHEO growth inhibition could be initiated by a strong innate immune response followed by an adaptive immune response with CD4$^+$ T cells preserving long-lasting immune memory after successful treatment.

Systemic immune response during MBTA therapy has been previously observed by Caisova et al. during the therapy of murine metastatic PHEO, where the therapy resulted in slower progression of metastatic lesions and their higher infiltration of CD3$^+$ T cells [24]. Medina et al. also described the systemic immune response in a murine bilateral colon carcinoma (CT26) model, in which approximately 30% of the MBTA-treated mice achieved complete tumor regression of both tumors [23]. In this study, similar to murine metastatic PHEO, MBTA therapy did not result in complete tumor elimination, although it contributed to the significant prolongation of the overall survival of treated mice.

These findings led us to focus on the microenvironment in MBTA-injected and distal tumors and analyzed immune cell infiltration during MTBA therapy. The detailed trafficking and infiltration of innate and adaptive immune cells following the treatment showed that MBTA therapy could lead to the conversion of immunologically "cold" to "hot" tumor microenvironments. Taken together, not only were adaptive immune cells elevated in tumors of MBTA-treated mice but also innate immune cells were able to infiltrate the non-injected (distal) tumors. The assessment of innate leukocyte subpopulations indicated higher infiltration of NK cells, monocytes, macrophages, and DCs in both injected and distant tumors. These data are consistent with the previous data from MBTA therapy of the bilateral CT26 model, where DC and monocyte increase also observed in distal tumors [23]. Surprisingly, neutrophils were the only immune cell type elevated solely in the injected tumors. This could be explained by the role of complement receptor 3 and mannan-BAM. After the intratumoral MBTA injection, mannan-BAM anchors into the lipid bilayer of the tumor cells via the hydrophobic properties of BAM, while mannan is recognized by the mannan-binding lectin complement cascade. The resulting activation of the complement cascade induces the proteolytic cleavage of the complement protein C3 into C3a and C3b. Subsequently, the inactive C3b (iC3b) form opsonizes the mannan-BAM-labeled tumor cells. Neutrophils express the receptor CR3, which recognizes iC3b and enables their activation and the frustrated phagocytosis of opsonized tumor cells [30,31]. The lack of neutrophils in non-injected (distal) tumors could also explain the lower response in these tumors during

MBTA therapy. However, detailed studies focused on lower response in distal tumors as well as the regrowth of tumors after MBTA therapy are needed.

Classically activated M1-like macrophages exhibit immunostimulatory functions. They are associated with the production of high levels of proinflammatory cytokines and chemokines and the presentation of antigens in the lymphatic nodes. In contrast, alternatively activated M2-like macrophages can reduce inflammation through anti-inflammatory cytokines and promote tumor progression and metastasis [32]. Our data indicate that MBTA therapy triggers macrophage infiltration in the tumors and the spleen while reducing the M2-like phenotype, resulting in a systematically higher M1/M2 macrophage ratio. These findings are consistent with those of other studies where the use of TLR ligands was also associated with a systematically increased M1/M2 ratio [33,34]. In addition, since the anti-CD40 antibody is a component of MBTA therapy, antigen-presenting cells (APCs) that express CD40 receptors, including macrophages, are activated. In the spleen of MBTA-treated mice, we observed a gradual APC increase, namely that of DCs and macrophages, during the entire course of MBTA therapy, suggesting a boosting effect after each cycle of therapy and possibly higher presentation of tumor antigens to the adaptive immune system after each cycle.

It has been established that CD4$^+$ T cells also play an important role in developing and sustaining effective antitumor responses, even in cancer immunotherapies primarily designed to activate CD8$^+$ T cell responses. The flow cytometry analysis of T cells during MBTA therapy revealed systemic T cell infiltration in the tumors of treated mice, where CD4$^+$ T cells became the predominant T cell type. We also show the importance of the CD4$^+$ T cells in immune memory after MBTA therapy, using the adoptive transfer of splenic CD4$^+$ T cells from previously treated mice. The therapeutic efficacy of CD4$^+$ T cells could be attributed to their ability to produce proinflammatory chemo- and cytokines that recruit and activate CD8$^+$ T cells and innate immune cells, such as macrophages, to the site of the infection [35,36]. This complex activation of both arms of the immune system could result in a better effector response, for example, after the retransplantation of mice with tumor cells. We have previously shown the role of CD8$^+$ T cells in the inhibition of metastatic PHEO lesions during MBTA therapy using T cell depletion antibodies [24]. When CD8$^+$ T cells were depleted, metastatic lesion growth in the MBTA-treated group was comparable to that in the control group. These results suggest that CD8$^+$ T cells are involved in the eradication of PHEO tumors during MBTA therapy, but CD4$^+$ T cells are important for the long-term memory after MBTA therapy of murine PHEO. Similarly, previous results from MBTA therapy of murine pancreatic adenocarcinoma (Panc02) have shown that CD4$^+$ T cells are important for the complete eradication of tumor growth and resistance to its recurrence in CD8$^{-/-}$ knockout mice, suggesting that CD4$^+$ T cells might play diverse anti-tumor roles in different types of murine tumor models [37]. During the assessment of T cells in bilateral PHEO tumors, only CD8$^+$ T cells and their subpopulation of CD8$_{E/EM}$ T cells were elevated in both tumors directly after the first MBTA injection cycle, suggesting a faster acute response in tumors compared to CD4$^+$ T cells. Among both the CD4$^+$ and CD8$^+$ T cells, the effector/effector memory phenotype (CD44$^+$) was the most common T cell type not only in the tumors of treated mice but also in the spleen. Previous studies have described the higher proliferation of T cell memory phenotype (CD44^{high}) and its antitumor effect during cancer therapies based on a combination of TLR agonists, agonist antibodies, or cytokines [38,39].

B cells play an important role in regulating the immune response to cancer. However, they can produce antibodies against tumor antigens, act as APCs, and produce a variety of immunomodulatory cytokines, thereby activating other cells. Moreover, they can suppress cytolytic responses by acting as regulatory cells and producing immunoregulatory cytokines, such as IL-10 and TGF-β [40]. The exact role of B cells during MBTA therapy is questionable. Previously, we did not observe any B cell increase in tumors during MBT therapy (therapy without anti-CD40) [24]. Since MBTA therapy incorporates anti-CD40 (which polarizes B cells towards an anti-tumor role), it is reasonable to suggest that B cells

drive an anti-tumor immune response through their antigen presentation capacity and also the production of anti-tumor antibodies. B cell depletion studies would be certainly required to shed light on this topic, which could be a potential future direction of MBTA immunotherapy.

Understanding the underlying mechanisms that contribute to tumor elimination during MBTA therapy in murine PHEO and other tumor types is indispensable. Here, we present a detailed explanation of immune cell trafficking during intratumoral MBTA therapy to better understand these mechanisms. Despite the potential of this therapy to systematically change the tumor microenvironment into immunologically "hot," reduce tumor growth, and prolong the survival of treated animals, we could not achieve the complete eradication of murine PHEO tumors with high tumor burden. Our previous study demonstrated that only simultaneous MBTA therapeutic injections into both tumors could potentially treat the bilateral Panc02 model [37]. Therefore, an optimal therapeutic approach, along with MBTA therapy, to increase the antitumor effect in metastatic murine PHEO tumors, is yet to be investigated.

5. Conclusions

In conclusion, we showed that intratumoral immunotherapy based on the application of mannan-BAM, TLR ligands, and anti-CD40 antibody (MBTA therapy) exhibits the potential to suppress tumor growth in a murine bilateral pheochromocytoma model. The MBTA therapy could increase the recruitment of innate followed by adaptive immune cells not only into primary (injected) but also into distal (non-injected) tumors. Furthermore, we demonstrated that after successful MBTA therapy of subcutaneous pheochromocytoma, the long-term immunological memory is driven by $CD4^+$ T cells. In summary, this study helps to better understand the systemic effect of MBTA therapy and its use for tumor reduction or even elimination, including metastasis.

References

1. Ventola, C.L. Cancer Immunotherapy, Part 2: Efficacy, Safety, and Other Clinical Considerations. *Pharm. Ther.* **2017**, *42*, 452–463.
2. Ascierto, P.A.; Del Vecchio, M.; Robert, C.; Mackiewicz, A.; Chiarion-Sileni, V.; Arance, A.; Lebbe, C.; Bastholt, L.; Hamid, O.; Rutkowski, P.; et al. Ipilimumab 10 mg/kg versus ipilimumab 3 mg/kg in patients with unresectable or metastatic melanoma: A randomised, double-blind, multicentre, phase 3 trial. *Lancet Oncol.* **2017**, *18*, 611–622. [CrossRef]
3. Marabelle, A.; Tselikas, L.; de Baere, T.; Houot, R. Intratumoral immunotherapy: Using the tumor as the remedy. *Ann. Oncol.* **2017**, *28*, xii33–xii43. [CrossRef] [PubMed]

4. Hamid, O.; Ismail, R.; Puzanov, I. Intratumoral Immunotherapy-Update 2019. *Oncologist* **2020**, *25*, e423–e438. [CrossRef] [PubMed]

5. Lenders, J.W.; Eisenhofer, G.; Mannelli, M.; Pacak, K. Phaeochromocytoma. *Lancet* **2005**, *366*, 665–675. [CrossRef]

6. Crona, J.; Taieb, D.; Pacak, K. New Perspectives on Pheochromocytoma and Paraganglioma: Toward a Molecular Classification. *Endocr. Rev.* **2017**, *38*, 489–515. [CrossRef] [PubMed]

7. Fishbein, L.; Leshchiner, I.; Walter, V.; Danilova, L.; Robertson, A.G.; Johnson, A.R.; Lichtenberg, T.M.; Murray, B.A.; Ghayee, H.K.; Else, T.; et al. Comprehensive Molecular Characterization of Pheochromocytoma and Paraganglioma. *Cancer Cell* **2017**, *31*, 181–193. [CrossRef]

8. Wood, M.A.; Paralkar, M.; Paralkar, M.P.; Nguyen, A.; Struck, A.J.; Ellrott, K.; Margolin, A.; Nellore, A.; Thompson, R.F. Population-level distribution and putative immunogenicity of cancer neoepitopes. *BMC Cancer* **2018**, *18*, 414. [CrossRef]

9. Thorsson, V.; Gibbs, D.L.; Brown, S.D.; Wolf, D.; Bortone, D.S.; Ou Yang, T.H.; Porta-Pardo, E.; Gao, G.F.; Plaisier, C.L.; Eddy, J.A.; et al. The Immune Landscape of Cancer. *Immunity* **2018**, *48*, 812–830. [CrossRef]

10. Nolting, S.; Ullrich, M.; Pietzsch, J.; Ziegler, C.G.; Eisenhofer, G.; Grossman, A.; Pacak, K. Current Management of Pheochromocytoma/Paraganglioma: A Guide for the Practicing Clinician in the Era of Precision Medicine. *Cancers* **2019**, *11*, 1505. [CrossRef]

11. Figueiredo, R.T.; Carneiro, L.A.; Bozza, M.T. Fungal surface and innate immune recognition of filamentous fungi. *Front. Microbiol.* **2011**, *2*, 248. [CrossRef] [PubMed]

12. Janotova, T.; Jalovecka, M.; Auerova, M.; Svecova, I.; Bruzlova, P.; Maierova, V.; Kumzakova, Z.; Cunatova, S.; Vlckova, Z.; Caisova, V.; et al. The use of anchored agonists of phagocytic receptors for cancer immunotherapy: B16-F10 murine melanoma model. *PLoS ONE* **2014**, *9*, e85222. [CrossRef]

13. Garred, P.; Genster, N.; Pilely, K.; Bayarri-Olmos, R.; Rosbjerg, A.; Ma, Y.J.; Skjoedt, M.O. A journey through the lectin pathway of complement-MBL and beyond. *Immunol. Rev.* **2016**, *274*, 74–97. [CrossRef] [PubMed]

14. Wu, J.J.; Huang, D.B.; Tyring, S.K. Resiquimod: A new immune response modifier with potential as a vaccine adjuvant for Th1 immune responses. *Antiviral Res.* **2004**, *64*, 79–83. [CrossRef]

15. Matsumoto, M.; Seya, T. TLR3: Interferon induction by double-stranded RNA including poly(I:C). *Adv. Drug Deliv. Rev.* **2008**, *60*, 805–812. [CrossRef]

16. Seo, H.S.; Michalek, S.M.; Nahm, M.H. Lipoteichoic acid is important in innate immune responses to gram-positive bacteria. *Infect. Immun.* **2008**, *76*, 206–213. [CrossRef]

17. Khong, A.; Nelson, D.J.; Nowak, A.K.; Lake, R.A.; Robinson, B.W.S. The Use of Agonistic Anti-CD40 Therapy in Treatments for Cancer. *Int. Rev. Immunol.* **2012**, *31*, 246–266. [CrossRef]

18. Rakhmilevich, A.L.; Alderson, K.L.; Sondel, P.M. T-cell-independent antitumor effects of CD40 ligation. *Int. Rev. Immunol.* **2012**, *31*, 267–278. [CrossRef] [PubMed]

19. Vonderheide, R.H.; Glennie, M.J. Agonistic CD40 antibodies and cancer therapy. *Clin. Cancer Res.* **2013**, *19*, 1035–1043. [CrossRef]

20. Caisova, V.; Uher, O.; Nedbalova, P.; Jochmanova, I.; Kvardova, K.; Masakova, K.; Krejcova, G.; Padoukova, L.; Chmelar, J.; Kopecky, J.; et al. Effective cancer immunotherapy based on combination of TLR agonists with stimulation of phagocytosis. *Int. Immunopharmacol.* **2018**, *59*, 86–96. [CrossRef]

21. Caisova, V.; Vieru, A.; Kumzakova, Z.; Glaserova, S.; Husnikova, H.; Vacova, N.; Krejcova, G.; Padoukova, L.; Jochmanova, I.; Wolf, K.I.; et al. Innate immunity based cancer immunotherapy: B16-F10 murine melanoma model. *BMC Cancer* **2016**, *16*, 940. [CrossRef] [PubMed]

22. Uher, O.; Caisova, V.; Hansen, P.; Kopecky, J.; Chmelar, J.; Zhuang, Z.; Zenka, J.; Pacak, K. Coley's immunotherapy revived: Innate immunity as a link in priming cancer cells for an attack by adaptive immunity. *Semin. Oncol.* **2019**. [CrossRef] [PubMed]

23. Medina, R.; Wang, H.R.; Caisova, V.; Cui, J.; Indig, I.H.; Uher, O.; Ye, J.; Nwankwo, A.; Sanchez, V.; Wu, T.X.; et al. Induction of Immune Response against Metastatic Tumors via Vaccination of Mannan-BAM, TLR Ligands, and Anti-CD40 Antibody (MBTA). *Adv. Ther. Ger.* **2020**. [CrossRef] [PubMed]

24. Caisova, V.; Li, L.; Gupta, G.; Jochmanova, I.; Jha, A.; Uher, O.; Huynh, T.T.; Miettinen, M.; Pang, Y.; Abunimer, L.; et al. The Significant Reduction or Complete Eradication of Subcutaneous and Metastatic Lesions in a Pheochromocytoma Mouse Model after Immunotherapy Using Mannan-BAM, TLR Ligands, and Anti-CD40. *Cancers* **2019**, *11*, 654. [CrossRef]

25. Haabeth, O.A.W.; Blake, T.R.; McKinlay, C.J.; Tveita, A.A.; Sallets, A.; Waymouth, R.M.; Wender, P.A.; Levy, R. Local Delivery of Ox40l, Cd80, and Cd86 mRNA Kindles Global Anticancer Immunity. *Cancer Res.* **2019**, *79*, 1624–1634. [CrossRef]

26. Zemek, R.M.; Fear, V.S.; Forbes, C.; de Jong, E.; Casey, T.H.; Boon, L.; Lassmann, T.; Bosco, A.; Millward, M.J.; Nowak, A.K.; et al. Bilateral murine tumor models for characterizing the response to immune checkpoint blockade. *Nat. Protoc.* **2020**, *15*, 1628–1648. [CrossRef]

27. Kato, K.; Itoh, C.; Yasukouchi, T.; Nagamune, T. Rapid protein anchoring into the membranes of Mammalian cells using oleyl chain and poly(ethylene glycol) derivatives. *Biotechnol. Prog.* **2004**, *20*, 897–904. [CrossRef]

28. Korpershoek, E.; Pacak, K.; Martiniova, L. Murine models and cell lines for the investigation of pheochromocytoma: Applications for future therapies? *Endocr. Pathol.* **2012**, *23*, 43–54. [CrossRef] [PubMed]

29. Martiniova, L.; Lai, E.W.; Elkahloun, A.G.; Abu-Asab, M.; Wickremasinghe, A.; Solis, D.C.; Perera, S.M.; Huynh, T.T.; Lubensky, I.A.; Tischler, A.S.; et al. Characterization of an animal model of aggressive metastatic pheochromocytoma linked to a specific gene signature. *Clin. Exp. Metastasis* **2009**, *26*, 239–250. [CrossRef]

30. Gordon, D.L.; Rice, J.L.; McDonald, P.J. Regulation of human neutrophil type 3 complement receptor (iC3b receptor) expression during phagocytosis of Staphylococcus aureus and Escherichia coli. *Immunology* **1989**, *67*, 460–465.

31. Holers, V.M. Complement and its receptors: New insights into human disease. *Annu. Rev. Immunol.* **2014**, *32*, 433–459. [CrossRef]

32. Lin, Y.; Xu, J.; Lan, H. Tumor-associated macrophages in tumor metastasis: Biological roles and clinical therapeutic applications. *J. Hematol. Oncol.* **2019**, *12*, 76. [CrossRef] [PubMed]

33. Sato-Kaneko, F.; Yao, S.; Ahmadi, A.; Zhang, S.S.; Hosoya, T.; Kaneda, M.M.; Varner, J.A.; Pu, M.; Messer, K.S.; Guiducci, C.; et al. Combination immunotherapy with TLR agonists and checkpoint inhibitors suppresses head and neck cancer. *JCI Insight* **2017**, *2*, e93397. [CrossRef]

34. Lu, C.H.; Lai, C.Y.; Yeh, D.W.; Liu, Y.L.; Su, Y.W.; Hsu, L.C.; Chang, C.H.; Catherine Jin, S.L.; Chuang, T.H. Involvement of M1 Macrophage Polarization in Endosomal Toll-Like Receptors Activated Psoriatic Inflammation. *Mediat. Inflamm.* **2018**, *2018*, 3523642. [CrossRef]

35. Lin, A.A.; Tripathi, P.K.; Sholl, A.; Jordan, M.B.; Hildeman, D.A. Gamma interferon signaling in macrophage lineage cells regulates central nervous system inflammation and chemokine production. *J. Virol.* **2009**, *83*, 8604–8615. [CrossRef]

36. Bogen, B.; Fauskanger, M.; Haabeth, O.A.; Tveita, A. CD4(+) T cells indirectly kill tumor cells via induction of cytotoxic macrophages in mouse models. *Cancer Immunol. Immunother.* **2019**, *68*, 1865–1873. [CrossRef] [PubMed]

37. Uher, O.; Caisova, V.; Padoukova, L.; Kvardova, K.; Masakova, K.; Lencova, R.; Frejlachova, A.; Skalickova, M.; Venhauerova, A.; Chlastakova, A.; et al. Mannan-BAM, TLR ligands, and anti-CD40 immunotherapy in established murine pancreatic adenocarcinoma: Understanding therapeutic potentials and limitations. *Cancer Immunol. Immunother.* **2021**. [CrossRef]

38. Sprent, J.; Zhang, X.; Sun, S.; Tough, D. T-cell proliferation in vivo and the role of cytokines. *Philos. Trans. R. Soc. Lond. B Biol. Sci.* **2000**, *355*, 317–322. [CrossRef] [PubMed]

39. Berner, V.; Liu, H.; Zhou, Q.; Alderson, K.L.; Sun, K.; Weiss, J.M.; Back, T.C.; Longo, D.L.; Blazar, B.R.; Wiltrout, R.H.; et al. IFN-gamma mediates CD4+ T-cell loss and impairs secondary antitumor responses after successful initial immunotherapy. *Nat. Med.* **2007**, *13*, 354–360. [CrossRef] [PubMed]

40. Yuen, G.J.; Demissie, E.; Pillai, S. B lymphocytes and cancer: A love-hate relationship. *Trends Cancer* **2016**, *2*, 747–757. [CrossRef]

Chapter VI

Intratumoral Immunotherapy of Murine Pheochromocytoma Shows No Age-Dependent Differences in Its Efficacy - manuscript

Intratumoral Immunotherapy of Murine Pheochromocytoma Shows No Age-Dependent Differences in Its Efficacy

Ondrej Uher[1,2], Katerina Hadrava Vanova[1], Herui Wang[3], Zhengping Zhuang[3], Jan Zenka[2], and Karel Pacak[1]

[1]Section on Medical Neuroendocrinology, *Eunice Kennedy Shriver* National Institute of Child Health and Human Development, NIH, Bethesda, Maryland, USA
[2]Department of Medical Biology, Faculty of Science, University of South Bohemia, Ceske Budejovice, Czech Republic
[3]Neuro-Oncology Branch, National Cancer Institute, NIH, Bethesda, Maryland, USA

Corresponding author: Karel Pacak, MD, PhD, DSc, FACE,
Senior Investigator
Chief, Section on Medical Neuroendocrinology
Head, Development Endocrine Oncology and Genetics Affinity Group
Professor of Medicine
Eunice Kennedy Shriver NICHD, NIH
Building 10, CRC, Room 1E-3140
10 Center Drive MSC-1109
Bethesda, Maryland 20892-1109 USA
E-mail: karel@mail.nih.gov
Phone: (301) 402-4594
FAX: (301) 402-4712

Keywords: intratumoral immunotherapy, aging, pheochromocytoma

Abstract

Cancer immunotherapy has shown remarkable clinical progress in recent years. Although age is one of the biggest leading risk factors for cancer development and older adults represent a majority of cancer patients, only a few new cancer immunotherapeutic interventions have been preclinically tested in aged animals. Thus, the lack of preclinical studies focused on age-dependent effect during cancer immunotherapy could led to different therapeutic outcomes in young and aged animals and future modifications of human clinical trials. Here, we compare the efficacy of previously developed and tested intratumoral immunotherapy, based on the combination of polysaccharide mannan, TLR ligands, and anti-CD40 antibody

(MBTA immunotherapy), in young (6 weeks) and aged (71 weeks) mice bearing pheochromocytoma. The presented results point out that despite faster growth of pheochromocytoma in aged mice MBTA intratumoral immunotherapy is effective approach without age dependence and could be one of the possible therapeutic interventions to enhance immune response to pheochromocytoma and perhaps other neuroendocrine tumors also in aged host.

Summary

The primary aim of this dissertation was to study and describe the mechanisms of intratumoral immunotherapy using the combination of phagocytosis ligands and Toll-like receptor ligands in murine pancreatic adenocarcinoma (Panc02) and pheochromocytoma (PHEO) models.

Chapter I focuses on the optimization of intratumoral immunotherapy based on the combination of mannan-BAM, the TLR ligand resiquimod, poly(I:C), and inactivated *L. monocytogenes* in the murine B16-F10 melanoma model.

L. monocytogenes (TLR2 agonist) was replaced by a well-defined TLR2 agonist – lipoteichoic acid (LTA). The combination of mannan-BAM, resiquimod, poly(I:C), and LTA (MBT therapy) and its optimized timing resulted in the eradication of B16-F10 melanoma in 83% of tested cases.

When we investigated potential underlying mechanisms, our flow cytometry analysis of tumor-infiltrating CD45+ leukocytes and their subpopulations showed elevated leukocyte (CD45+) infiltration where granulocytes (Gr1+) were the most abundant cells. Increased numbers of NK cells (NK1.1+) were also detected during MBT therapy. Furthermore, we found that the activation of innate immunity is followed by the activation of adaptive immunity, represented as long-lasting resistance to subcutaneous retransplantation of B16-F10 cells in MBT-treated mice with previous completely eradicated B16-F10 tumors. The involvement of the adaptive immune system was further verified by MBT therapy in SCID mice bearing B16-F10 cells, in which the absence of functional T and B cells resulted in partial inhibition of melanoma growth without any survival prolongation. MBT therapy also showed a potential antimetastatic effect.

To investigate the effect of MBT therapy in other tumor types, MBT therapy was tested in a murine Panc02 model. However, MBT therapy of Panc02 mice resulted in lower inhibition of tumor growth than treatment in the B16-F10 melanoma model, and none of the mice were successfully treated. Therefore, we decided to test whether blocking immune checkpoints (checkpoint inhibitors PD-1 and CTLA-4, and checkpoint stimulator CD40) could increase the efficacy of MBT therapy in the Panc02 model. Our results (80% effectively treated mice) indicated that the combination of agonistic anti-CD40 antibody with MBT therapy (MBTA therapy) is a better treatment option for Panc02 tumors.

Chapter II focuses on MBT and MBTA therapies in murine subcutaneous and metastatic PHEO models.

Similar to the Panc02 model discussed in the previous chapter, MBT therapy significantly stabilized the growth of subcutaneous MTT PHEO and prolonged the survival of MBT-treated mice compared with that observed in the control group. Experiments with SCID mice bearing PHEO confirmed the role of both the innate and adaptive immune systems during tumor growth stabilization. Immunohistochemistry (IHC) staining showed higher levels of CD45+ leukocytes in the MBT-treated group than in the control group. These results were also confirmed by flow cytometry analysis of tumor-infiltrating CD45+ leukocytes and their subpopulations, where these cells were increased compared with the corresponding cell populations in the control. T cells (CD3+) are the most common leukocytes in MBT-treated tumors. IHC staining localized CD45+ leukocytes, CD3+ T cells, and neutrophils (Ly6G/Ly6C) within the tumors and showed that immune cells can infiltrate the entire tumor microenvironment. Moreover, *in vitro* analysis of neutrophil cytotoxicity in murine MTT PHEO cells and human pheochromocytoma (hPheo1) cells labeled with mannan-BAM showed increased cytotoxicity toward labeled cells than toward non-labeled cells. Macroscopic evaluation revealed frustrated phagocytosis and neutrophil rosette formation in the mannan-BAM group. These results confirmed the important role of neutrophils in MBT therapy.

To increase the therapeutic effect of MBT therapy in the murine PHEO model, we tested the combination of agonistic anti-CD40 antibody and MBT therapy (MBTA therapy). The results showed that MBTA therapy had the same efficacy in tumor stabilization as MBT therapy; however, MBTA therapy increased mouse survival when compared with MBT therapy. Five of eight MBTA-treated mice manifested complete elimination of subcutaneous PHEO tumors compared to two of eight mice from the MBT-treated group. A rechallenge experiment on these mice confirmed the involvement of the adaptive immune system and its long-term immune memory. Successful therapy presented as the resistance of these mice to developing PHEO tumors after subcutaneous retransplantation.

We also evaluated the systemic effect of MBTA therapy on the metastases observed in previous experiments. We established a murine metastatic PHEO model through subcutaneous injection of MTT cells into the right flank and an intravenous injection of MTT-luciferase cells into the lateral vein. MBTA therapy of

subcutaneous tumors confirmed the systemic effect of the therapy on metastatic organ lesions, which presented as lower bioluminescence signal intensity of these lesions compared with the signal intensity for lesions within the control group. Moreover, MBTA therapy significantly prolonged the survival of treated mice. IHC staining also showed an increased number of CD3+ cells in metastases. Finally, we evaluated the role of CD4+ and CD8+ T cells in the metastatic PHEO mouse model by *in vivo* depleting these cells. The results showed the importance of CD8+ cells in the stabilization of metastatic growth.

In **Chapter III**, we discuss the importance of the initial activation of the innate immune system, followed by activation of the adaptive immune system in cancer treatment. We briefly describe the role of the immune system in cancer pathogenesis and its history, which led our team to use the combination of ligands stimulating phagocytosis and TLR ligands for treatment. Subsequently, we discuss the potential combination of this therapy with other therapeutic approaches for the treatment of metastatic cancer, as well as certain potential future directions for the improvement of this therapy.

Chapter IV focuses on some of the potential combinations of MBTA therapy with other therapeutic approaches in treating tumors with a high tumor burden, as mentioned in Chapter III.

We evaluated the efficacy of MBTA therapy in larger Panc02 tumors compared with smaller tumors from a previous study (Chapter I). We confirmed that complete elimination of tumors during MBTA therapy is dependent on the initial tumor size. In an experiment focusing on the role of CD4+ and CD8+ cells during MBTA therapy in Panc02 tumors using CD4-/- and CD8-/- knockout mice, we observed that the presence of CD4+ T cells was not critical for tumor growth reduction, but essential for delayed tumor response, prolonged survival, and resistance against retransplantation. We also examined whether immune memory after MBTA therapy is antigen-specific. We re-challenged mice with MBTA-eradicated Panc02 tumors with Panc02 and B16-F10 tumor cells. All mice were tumor-free when re-challenged with Panc02 cells, but not with B16-F10 cells, suggesting that the memory induced by MBTA therapy is antigen-specific for each tumor type. We also confirmed the ability of immune memory to cross the blood–brain barrier by intracranial retransplantation of Panc02 cells; all MBTA treated mice demonstrated

a resistance against tumor cell retransplantation unlike the control group mice, which developed tumors.

To study the potential enhancement of MBTA therapy with other therapeutic approaches in animals with high tumor burden and distant large metastases, we established a bilateral Panc02 murine model. We first confirmed that the application of MBTA to one tumor reduced tumor growth in both the treated and distal non-treated tumors and prolonged the survival of treated mice identically as it did in metastatic PHEO mice (Chapter II). Interestingly, we did not observe any completely cured mice after MBTA therapy. Next, we tested the combination of MBTA therapy with the following treatments: inhibition of the CTLA-4 checkpoint inhibitor, application of heat-killed *L. monocytogenes*, and chemoablation. However, we did not observe any enhancement in the efficacy of MBTA therapy. Additionally, we attempted to change the desmoplasia of Panc02 tumors by applying anti-CD40 and hyaluronidase to the left tumor with simultaneous application of MBTA therapy to the right tumor; however, no improvement was observed. Finally, we tested using radiotherapy on the distal tumor and the simultaneous application of MBTA therapy to both tumors. However, only the simultaneous application of MBTA therapy to both tumors resulted in the reduction of both tumors and subsequent survival of 50% of mice.

In **Chapter V**, we analyzed the tumor microenvironment of the bilateral PHEO tumor model during MBTA therapy and determined which cells are important for immune memory. We first established a bilateral PHEO model and confirmed the decreased efficacy of MBTA therapy in this model with a higher tumor burden. In subsequent flow cytometry analyses, we captured detailed immune profiles of injected and non-injected (distal) tumors, as well as the profiles of different spleens, treating with MBTA therapy or PBS at different time points. The analyses showed that both the adaptive and innate immune cells were able to infiltrate non-injected (distal) tumors. With only one exception, we found that neutrophils increased in the MBTA-injected group but were almost absent in the distal tumors. Innate immune cell profiling in the spleen showed an increasing number of cells, such as neutrophils, dendritic cells, monocytes, and macrophages, during the entire course of therapy. Phenotyping the macrophages present, we identified a high ratio of classically activated or immunostimulatory M1-like macrophages and alternatively activated or immunosuppressive M2-like macrophages (M1/M2 ratio) in the tumors

and spleens of MBTA-treated mice, suggesting that the MBTA therapy can systematically activate M-1 macrophages and decrease the induction of immunosuppressive M2-like macrophages. Analyses of tumor-infiltrating lymphocytes showed strong infiltration of helper CD4+ and cytotoxic CD8+ T cells in both MBTA-injected and distal tumors, with CD4+ being the most abundant T lymphocyte in the tumors. However, we observed a greater increase in the proportion of effector/effector memory CD8+ T cells (CD44+CD62L-) and affected effector memory CD4+ T cells. Assessment of the central memory (CD44+CD62L+) T cells showed a significant increase only in the spleen and not in the tumors. We also observed a decrease in the percentage of naïve T cells in the spleen during the entire therapy period, confirming the activation of T cells. Finally, the analysis of B cells showed strong infiltration in both tumors and a continuous decrease in the spleen. We also measured IFN-γ and IL-10 levels in tumors and confirmed the pro-inflammatory response in tumors and plasma of MBTA-treated mice.

The last experiment included in this chapter focused on immune memory following MBTA therapy. We performed adoptive transfer of CD4+ and CD8+ from previously treated MBTA mice to naïve mice and confirmed that the long-term immune memory, shown previously as the resistance against PHEO tumor cell retransplantation, is executed by CD4+ T cells.

In **Chapter VI**, we compare the efficacy of MBTA therapy in young (6 weeks) and aged (71 weeks) mice. We showed that the growth of PHEO tumors is faster, and the incidence of tumors is higher in aged mice than in young mice. MBTA therapy of these tumors demonstrated that despite the faster growth of tumors in aged mice, the efficacy of the therapy is the same in both young and aged mice.

In summary, this dissertation provides unique insights into the complex relationship between various tumors and the immune system. We have shown that the intratumoral therapy based on a combination of phagocytosis ligand and Toll-like ligands and anti-CD40 antibody is a feasible approach for therapy of diverse and aggressive murine tumor models, including colon carcinoma [23] and as described here, melanoma, pancreatic adenocarcinoma, and pheochromocytoma. Our findings demonstrate that this therapy can activate the innate immune system with subsequent activation of the adaptive immune system, not only locally in

treated tumors but also systematically in non-treated distal tumors. These results are promising and have narrowed the questions that must be answered before future clinical trials.

Futures perspectives

Our future next step will be to find the right combination of intratumoral MBTA therapy with other therapeutic approaches to treat large primary tumors and/or numerous (large) metastases with a high tumor burden. As described in the case of murine pancreatic adenocarcinoma (Chapter IV), we have tried several approaches, such as checkpoint blocking, manipulation of the tumor environment, and radiotherapy, but without any further improvements to the MBTA scheme. Our preliminary experiments have shown that one promising modality may be targeting the metabolism of the tumor cells. In the case of PHEO, we tried combinations of MBTA therapy with other approaches, but without any additional effect. Therefore, future research should also focus on anticancer agents that inhibit hypoxia-inducible factors (HIFs) since most hereditary PHEOs/PGLs are related to the hypoxia signaling pathway, mainly through mutations within many genes, which leads to increased stability of HIFs [24]. We hypothesized that the use of HIF inhibitors combined with MBTA therapy may be a treatment for aggressive and metastatic murine pheochromocytoma tumors.

Additionally, our future studies will use intratumoral MBTA therapy as neoadjuvant therapy. Neoadjuvant therapy is usually used as a first step to shrink the tumor before the main treatment (surgery). We would like to confirm our hypothesis that intratumoral application of MBTA therapy before surgery can protect organisms against recurrences and the future development of metastases.

Next, our future studies will use MBTA therapy as a subcutaneous tumor vaccine. Intratumoral application of MBTA therapy could be considered a limitation, particularly for metastatic pheochromocytomas and paragangliomas, because metastases can be found in deep organs, lymph nodes, and bones. Therefore, we tested the subcutaneous application of irradiated whole tumor cells pulsed with MBTA therapy *in vitro*. We have already attempted this vaccination approach in mice bearing colon carcinoma (CT26), resulting in the generation of antitumor immune responses in distal tumors, improved tumor growth control, and prolonged survival of treated mice [23]. Another promising use of this MBTA vaccination approach may be the treatment of glioblastomas, as discussed in a previous review [25]. This MBTA vaccination approach may also be used as adjuvant therapy after intratumoral MBTA neoadjuvant therapy and surgery to prolong the systemic antitumor effect of MBTA after surgery.

Finally, we will focus on optimizing MBTA therapy, particularly in determining the optimal injected intratumoral volume, optimal concentration, and the most

efficient time schedule for therapy. It is still unclear whether the volume/concentration of intratumoral immunotherapies should be fixed or adjusted to the size of the injected lesions. A limited number of studies have focused on these issues [26]. In the case of pheochromocytoma, our preliminary results indicate that MBTA therapy can be given as a reduced number of injections, but the time of MBTA therapy must be prolonged to achieve the same efficacy as the "normal" scheme – four pulses of 3 injections with a five-day gap (unpublished results).

We believe that our presented results and proposed future steps will help optimize this therapeutic approach for future use in clinical trials.

List of abbreviations

B16-F10	murine melanoma tumor cells
CTLA-4	cytotoxic T-lymphocyte-associated protein 4
HIF	hypoxia-inducible factor
iC3b	inactivated protein fragment of C3b
LTA	lipoteichoic acid
MBT therapy	R-848 + poly(I:C) + LTA + mannan-BAM
MBTA therapy	R-848 + poly(I:C) + LTA + mannan-BAM + anti-CD40
MTT	mouse tumor tissue-derived pheochromocytoma cells
NK cells	natural killer cells
Panc02	murine pancreatic adenocarcinoma
PD-1	programmed cell death protein 1
PD-L1	programmed death-ligand 1
PGLs	paragangliomas
PHEOs	pheochromocytomas
Poly(I:C)	polyinosinic-polycytidylic acid
R-848	resiquimod
SCID	severe combined immunodeficiency
SMCC	anchor, succinimidyl-4-(N-maleimidomethyl)cyclohexane-1-carboxylate
TLR	Toll-Like receptor

References

1. Robert, C., *A decade of immune-checkpoint inhibitors in cancer therapy.* Nat Commun, 2020. **11**(1): p. 3801.
2. Coley, W.B., *The treatment of malignant tumors by repeated inoculations of erysipelas. With a report of ten original cases. 1893.* Clin Orthop Relat Res, 1991(262): p. 3-11.
3. Kaiser, J., *Too much of a good thing?* Science, 2018. **359**(6382): p. 1346-1347.
4. Melero, I., et al., *Intratumoural administration and tumour tissue targeting of cancer immunotherapies.* Nat Rev Clin Oncol, 2021. **18**(9): p. 558-576.
5. Ascierto, P.A., et al., *Ipilimumab 10 mg/kg versus ipilimumab 3 mg/kg in patients with unresectable or metastatic melanoma: a randomised, double-blind, multicentre, phase 3 trial.* Lancet Oncol, 2017. **18**(5): p. 611-622.
6. Marabelle, A., et al., *Intratumoral immunotherapy: using the tumor as the remedy.* Ann Oncol, 2017. **28**(suppl_12): p. xii33-xii43.
7. Caisova, V., et al., *Innate immunity based cancer immunotherapy: B16-F10 murine melanoma model.* BMC Cancer, 2016. **16**(1): p. 940.
8. Wu, J.J., D.B. Huang, and S.K. Tyring, *Resiquimod: a new immune response modifier with potential as a vaccine adjuvant for Th1 immune responses.* Antiviral Res, 2004. **64**(2): p. 79-83.
9. Matsumoto, M. and T. Seya, *TLR3: interferon induction by double-stranded RNA including poly(I:C).* Adv Drug Deliv Rev, 2008. **60**(7): p. 805-12.
10. Kilpatrick, D.C., *Mannan-binding lectin and its role in innate immunity.* Transfus Med, 2002. **12**(6): p. 335-52.
11. Apostolopoulos, V. and I.F. McKenzie, *Role of the mannose receptor in the immune response.* Curr Mol Med, 2001. **1**(4): p. 469-74.
12. Caisova, V., et al., *Effective cancer immunotherapy based on combination of TLR agonists with stimulation of phagocytosis.* International Immunopharmacology, 2018. **59**: p. 86-96.
13. Caisova, V., et al., *Effective cancer immunotherapy based on combination of TLR agonists with stimulation of phagocytosis.* Int Immunopharmacol, 2018. **59**: p. 86-96.
14. Caisova, V., et al., *The Significant Reduction or Complete Eradication of Subcutaneous and Metastatic Lesions in a Pheochromocytoma Mouse Model after Immunotherapy Using Mannan-BAM, TLR Ligands, and Anti-CD40.* Cancers (Basel), 2019. **11**(5).
15. Garbe, C., et al., *Diagnosis and treatment of melanoma: European consensus-based interdisciplinary guideline.* Eur J Cancer, 2010. **46**(2): p. 270-83.
16. Giavazzi, R. and A. Decio, *Syngeneic murine metastasis models: B16 melanoma.* Methods Mol Biol, 2014. **1070**: p. 131-40.

17.   Partecke, L.I., et al., *A syngeneic orthotopic murine model of pancreatic adenocarcinoma in the C57/BL6 mouse using the Panc02 and 6606PDA cell lines.* Eur Surg Res, 2011. **47**(2): p. 98-107.

18.   Lenders, J.W., et al., *Phaeochromocytoma.* Lancet, 2005. **366**(9486): p. 665-75.

19.   Crona, J., D. Taieb, and K. Pacak, *New Perspectives on Pheochromocytoma and Paraganglioma: Toward a Molecular Classification.* Endocr Rev, 2017. **38**(6): p. 489-515.

20.   Vonderheide, R.H. and M.J. Glennie, *Agonistic CD40 antibodies and cancer therapy.* Clin Cancer Res, 2013. **19**(5): p. 1035-43.

21.   Uher, O., et al., *Identification of Immune Cell Infiltration in Murine Pheochromocytoma during Combined Mannan-BAM, TLR Ligand, and Anti-CD40 Antibody-Based Immunotherapy.* Cancers (Basel), 2021. **13**(16).

22.   Uher, O., et al., *Mannan-BAM, TLR ligands, and anti-CD40 immunotherapy in established murine pancreatic adenocarcinoma: understanding therapeutic potentials and limitations.* Cancer Immunol Immunother, 2021.

23.   Medina, R., et al., *Induction of Immune Response against Metastatic Tumors via Vaccination of Mannan-BAM, TLR Ligands, and Anti-CD40 Antibody (MBTA).* Advanced Therapeutics, 2020.

24.   Jochmanova, I., et al., *HIF signaling pathway in pheochromocytoma and other neuroendocrine tumors.* Physiol Res, 2014. **63 Suppl 2**: p. S251-62.

25.   Lookian, P.P., et al., *Mannan-BAM, TLR Ligands, Anti-CD40 Antibody (MBTA) Vaccine Immunotherapy: A Review of Current Evidence and Applications in Glioblastoma.* Int J Mol Sci, 2021. **22**(7).

26.   Champiat, S., et al., *Intratumoral Immunotherapy: From Trial Design to Clinical Practice.* Clin Cancer Res, 2021. **27**(3): p. 665-679.

Curriculum vitae

Mgr. Ondřej Uher

+1 (240) 885-1778; +420 732 143 829   uher.ond@gmail.com   Oráčov 27, 270 32
https://orcid.org/ 0000-0003-3978-9822

Education and Research Experiences

2018 – PRESENT	**NATIONAL INSTITUTES OF HEALTH**
	Eunice Kennedy Shriver National Institute of Child Health and Human Development, Dr. Karel Pacak – supervisor Visiting fellow Intratumoral Immunotherapy of Murine Pheochromocytoma
2018 – PRESENT	**UNIVERSITY OF SOUTH BOHEMIA IN CESKE BUDEJOVICE**
	Faculty of Science, Department of Medical Biology Infection Biology - PhD program
2016 – 2018	**UNIVERSITY OF SOUTH BOHEMIA IN CESKE BUDEJOVICE**
	Faculty of Science, Department of Medical Biology Clinical Biology - Master's program Thesis theme: The analysis of immune processes during cancer immunotherapy based on synergy between TLR agonists and phagocytosis stimulating ligands.
2012 - 2016	**UNIVERSITY OF SOUTH BOHEMIA IN CESKE BUDEJOVICE**
	Faculty of Science, Department of Medical Biology Biomedical Laboratory Techniques - Bachelor's program Thesis theme: Cancer immunotherapy based on the combination of TLR ligands and ligands of phagocytic receptors.

Work Experience

2016 – 2018	**LABORATORY ASSISTANT**
	Strongwest, a.s., Ceske Budejovice
	Developing of *in vitro* cultivation of *Chlamydia pneumoniae*. Testing the sensitivity of *Chlamydia pneumoniae* to various antimicrobial drugs. Work with cell lines (Hep-2, HeLa) and with *Chlamydia pneumonia* strain.

Partnerships program, Courses, and Conferences

06/2021	**MICROBIOME AND CANCER SYMPOSIUM, NCI, NIH**
05/2021	**16th ANNUAL RETREAT NICHD – poster session**
03/2021	**ENDO 2021 (conference) – poster session**
11/2018	**IMPACT MEETING, PRAGUE (conference)**
10/2017	**MEET IN ITALY FOR LIFE SCIENCE, TURIN (conference)**
09/2015 - 11/2015	**INTERNSHIP**
	Department of Immunology, 2nd Medical School Charles University and University Hospital Motol, Prague

Immunotherapy based on the activation of dendritic cells

11/2014   **RECEPTOR NEUROPHYSIOLOGY - COURSE**

Institute of Physiology of the Czech Academy of Sciences, Prague

Memberships

1/2021 – PRESENT   **Member of Endocrine Society**

1/2022 – PRESENT   **Member of Society for Immunotherapy of Cancer**

Publications

Hadrava Vanova, K., Pang, Y., Krobova, L., Kraus, M., Nahacka, Z, Boukalova, S., Pack, S. D., Zobalova, R., Zhu, J., Huynh, T. T., Jochmanova, I., **Uher, O.**, … & Pacak. K. (2021). Germline *SUCLG2* Variants in Patients with Pheochromocytoma and Paraganglioma. JNCI: *Journal of the National Cancer Institute*. *114*(1) 130-138.

Uher, O., Huynh, T. T., Zhu, B., Horn, L. A., Caisova, V., Hadrava Vanova, K., ... & Pacak, K. (2021). Identification of Immune Cell Infiltration in Murine Pheochromocytoma during Combined Mannan-BAM, TLR Ligand, and Anti-CD40 Antibody-Based Immunotherapy. *Cancers*, *13*(16), 3942.

Uher, O., Caisova, V., Padoukova, L., Kvardova, K., Masakova, K., Lencova, R., … & Zenka, J. (2021). Mannan-BAM, TLR ligands, and anti-CD40 immunotherapy in established murine pancreatic adenocarcinoma: understanding therapeutic potentials and limitation. *Cancer Immunology, Immunotherapy*, 1-10.

Medina, R., Wang, H., Caisová, V., Cui, J., Indig, I. H., **Uher, O.**, ... & Zhuang, Z. (2020). Induction of Immune Response against Metastatic Tumors via Vaccination of Mannan-BAM, TLR Ligands, and Anti-CD40 Antibody (MBTA). *Advanced Therapeutics*, *3*(9), 2000044.

Liu, Y., Pang, Y., Zhu, B., **Uher, O.**, Caisova, V., Huynh, T. T., ... & Pacak, K. (2020). Therapeutic targeting of SDHB-mutated pheochromocytoma/paraganglioma with pharmacologic ascorbic acid. *Clinical Cancer Research*, *26*(14), 3868-3880.

Uher, O., Caisova, V., Hansen, P., Kopecky, J., Chmelar, J., Zhuang, Z., ... & Pacak, K. (2019). Coley's immunotherapy revived: Innate immunity as a link in priming cancer cells for an attack by adaptive immunity. *Seminars in oncology*, 46(4-5), 385.

Caisova, V., Li, L., Gupta, G., Jochmanova, I., Jha, A., **Uher, O.**, ... & Pacak, K. (2019). The significant reduction or complete eradication of subcutaneous and metastatic lesions in a pheochromocytoma mouse model after immunotherapy using mannan-BAM, TLR ligands, and anti-CD40. *Cancers*, *11*(5), 654.

Caisová, V., **Uher, O.**, Nedbalová, P., Jochmanová, I., Kvardová, K., Masáková, K., ... & Ženka, J. (2018). Effective cancer immunotherapy based on combination of TLR agonists with stimulation of phagocytosis. *International immunopharmacology*, *59*, 86-96.

Study of Cancer Immunotherapy Mechanisms in Pancreatic Adenocarcinoma and
Pheochromocytoma Murine Models

Ph.D. Thesis Series, 2022, No.4